# Spatial Water Quality Monitoring and Assessment in Malewa River and Lake Naivasha, Kenya

Lyssette Elena Muñoz Villers

March, 2002

# Spatial Water Quality Monitoring and Assessment in Malewa River and Lake Naivasha, Kenya

by

**Lyssette Elena Muñoz Villers**

Thesis submitted to the International Institute for Geo-Information Science and Earth Observation in partial fulfilment of the requirements for the degree of Master of Science in Water Resources and Environmental Management.

**Degree Assessment Board**

| | |
|---|---|
| Chairman: | Prof. Dr. A.M.J. Meijerink (Head WRES, ITC) |
| External Examiner: | Dr. Ir. E.O. Seyhan (Free University Amsterdam) |
| Primary Supervisor: | Dr. Ir. C.M.M. Mannaerts (WRES, ITC) |
| Member: | Dr. Zoltan Vekerdy (WRES, ITC) |


**INTERNATIONAL INSTITUTE FOR GEO-INFORMATION SCIENCE AND EARTH OBSERVATION**

**ENSCHEDE, THE NETHERLANDS**

## Disclaimer

This document describes work undertaken as part of a program of study at the International Institute for Geo-Information Science and Earth Observation. All views and opinions expressed therein remain the sole responsibility of the author, and do not necessarily represent those of the Institute.

*To my mother, father, sister and brother.*
*To my fiancé, Juan.*

*You are all special to me...*

## Acknowledgements

I wish to express my sincere gratitude to Dr. Ir. Chris Mannaerts, my supervisor, for the time, comments, valuable ideas, support and guidance throughout the research study. I wish to thank Prof. Meijerink (head of WRES, ITC) Dr. Zoltan Vekerdy and Dr. Seyhan for their time to read my thesis and comments.

Special thanks to Ing. Remco Dost for his so important support during fieldwork in Kenya.

I appreciate very much the personal assistance of the Water Resources Ministry of Nakuru, Kenya, particularly from Alex and Dominique Wambua for their knowledge and extraordinary advises in the field. I would like to thank the personal from the technical laboratory of Sulmac, Ltd., for their contribution and confidence to work with all of us. I thank Simon and Isaac for their efforts and assistance during the field surveys.

I am grateful to Barbara Casentini for the assistance in the ITC laboratory and along with Mathias Spaliviero for the support during the study research.

I do thank to Mexico's government for sponsoring me by the Consejo Nacional de Ciencia y Tecnologia (CONACyT) to perform the studies in The Netherlands. I make a special attention to the Water Resources Division who gave me the opportunity to pursue this MSc program.

Special thanks to all my classmates and friends; I will never forget the support, friendship and very good times that we shared together.

My deepest gratitude to my mum, dad, sister and brother for their moral support, encouragements and love. All my sincere gratitude to Juan for his unconditional love, faith and strength. I love you very much.

Above all I thank God who took care of me in all the way.

## Abstract

The research was conducted to examine the status and effects of economic activities - mainly flower growing, diary farming and water supply on Lake Naivasha water quality and main inflowing rivers. The water quality evaluation for drinking water and irrigation purposes of the rivers and lake, was based on WHO (1993) and FAO #29 (1985) guidelines. Two different spatial sampling schemes were carried out in Lake Naivasha; a high density distributed and a line transect sampling. Geostatistical techniques were used to estimate the spatial variability of pH, temperature, conductivity, total dissolved solids and dissolved oxygen from data collected in the first survey. The use of line transect survey data for deriving water quality maps was investigated. However, this survey method did not permit a full spatial assessment of the lake water quality water variables, but only in combination with information (e.g. variograms) from the first survey. The temporal comparison of the two spatial datasets permitted to observe and quantify the effects of river inflows in the lake. The refreshening of the lake waters with rainfall-based runoff using the EC parameter was analyzed and the contaminants inflow was observed using the N, P nutrient variables.

# Contents

# List of Figures

# List of Tables

# Chapter 1

# Introduction

## 1.1 General introduction

Surface waters from rivers and lakes are the most important freshwater resource for man. With the advent of industrialization and increasing populations, the range of requirements for water have increased together with greater demands for higher quality water. Over time, water requirements have emerged for drinking and personal hygiene, fisheries, agriculture (irrigation and livestock supply), navigation for transport of goods, industrial production, hydropower generation and recreational activities such as bathing and fishing.

Each water use, including abstraction of water and discharge of wastes, leads to specific, and generally rather predictable, impacts on the quality of the aquatic environment. In addition to these intentional water uses, there are several human activities, which have indirect and undesirable, effects on the aquatic environment. Similarly, the uncontrolled and excessive use of fertilizers and pesticides has long-term effects on ground and surface water sources.

## 1.2 Problem statement

Lake Naivasha is a highly significant Kenya freshwater resource in an otherwise water deficit area. Apart from the invaluable freshwater it also supports large and vitally important economic activities – mainly flower growing and geothermal power generation. The area is thus a major contributor to Kenya's gross domestic product and employment effort and to socio-economic development of the country as a whole. Lake Naivasha is also a Ramsar site being a wetland of international importance with a rich biodiversity, including some endangered species, and supports tourism and research activities.

The Lake and its surrounds are fragile with dynamic ecosystems and a yet uncertain water balance in a basin surrounded by intensively irrigated agricultural land and a fast growing township. The rivers and groundwater sources within the watershed provide water supply to Naivasha and Nakuru townships and adjoining human activities. Due to the intense use of the land and the Lake waters and being a closed basin system, it is extremely susceptible to pollution from farmlands, settlements and industries, and rivers inflows.

## 1.3 Objectives

The main objective of the study is the spatial and temporal assessment of surface water from Malewa and Gilgil Rivers and Lake Naivasha.

The specific objectives are:

- Water quality status of Lake Naivasha and major river inflows
- Pollution source inventory and their impacts on lake and rivers water quality
- To examine the effect of the Malewa and Gilgil river inflows into the water quality of the lake.
- To assess the spatial variability of the water quality in the water bodies
- The water quality evaluation in the area of study to determine their suitability for drinking water and irrigation purposes.

## 1.4 Specific research questions

It was tried to find some answers to the following specific research questions, which arose during the research study.

- Are Lake Naivasha and Malewa and Gilgil Rivers suitable for drinking and irrigation purposes??
- Is it possible to represent from a line transect data in the lake, water quality parameters for the entire body??
- It is possible to identify zones of rivers inflows, based on the spatial distribution of EC in the lake?

## 1.5 Methodology

**Literature review**
This stage encompasses the search and review of publications related with water quality issues in the study area and on this subject in general, that could be important for the research objectives.

**Collection and analysis of the existing data**
This step consists on gathering the data available such as topographic maps, satellite images, MSc thesis from previous years. Time series of rainfall, evaporation, water levels of Lake Naivasha and rainfall and discharge of Malewa were also collected and analysed.

**Fieldwork preparation**
Based on the objectives, the preliminary water quality survey was planned to monitor the quality of the rivers in locations near to discharge measurements stations and pollution sources. In the case of Lake Naivasha, the survey was designed to sample locations close to the river inflows, pollution sources and some others, which could represent the lake as itself. The selection of variables was governed by knowledge of the pollution sources and the expected impacts on the receiving water bodies.

The preparation of the required equipment to measure the hydrological and water quality variables was also part of this stage.

**Fieldwork survey**

This phase involves an intense programme to measure hydrological and water quality parameters of Malewa and Gilgil Rivers (upstream and downstream) and Lake Naivasha during 4 weeks of fieldwork. Some quality parameters will be measured on the field and some others will be analysed in Sulmac, Ltd. Laboratory. It has been also planned to store two water samples for location to take them back for further analysis in ITC laboratory.

**Data analysis and interpretation**

This stage comprises the ITC laboratory analysis to cross check the water quality data obtained during fieldwork; the flow, discharge and dispersion coefficient calculations in the rivers and, some statistical analysis with the water quality data. The quality variables will be described and interpreted according with the water characteristics of the water bodies and external factors (i.e. pollution sources), which affect the nature properties of the water.

**Assessment**

The water quality evaluation in the area of study will be done to determine their suitability for drinking water based on guidelines for drinking water quality. It will be analyzed through profiles in the rivers and interpolation techniques the distribution of some water quality variables in space and time.

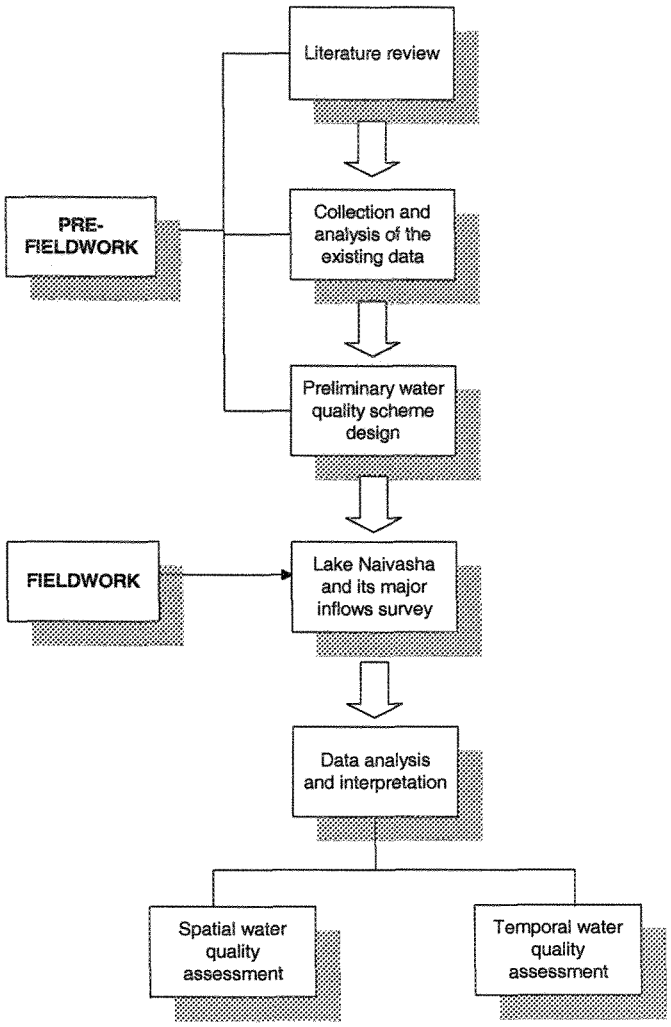


**Fig. 1.1.** Research methodology flowchart

## 1.6 Outline of the thesis

A general introduction, the main and specific objectives of the research and methodology steps is the main subjects of Chapter 1. Chapter 2 provides an introduction about the Central Rift Valley of Kenya and describes the climate, geology, hydrology, water balance, vegetation and socio-economic values of the Lake Naivasha basin. Chapter 3 summarizes the streamflow methods used during fieldwork and the theory behind geostatistical tools. This chapter concentrates as well the detail description of the chemical analysis presented next in Table 3.1. The sampling survey description, the estimation of flow, discharge and dispersion coefficient in the rivers, the choice of variables measured in the water bodies and the interpretation of these data for the purpose of assessing water quality in the Malewa and Gilgil rivers and Lake Naivasha are presented in Chapter 4. The final spatial and temporal assessment is presented in Chapter 5, describing the variability of the quality data through profiles and kriging techniques for the rivers and lake, respectively. Chapter 6 includes the conclusions and recommendations from the findings of the research.

# Chapter 2

# Study area

## 2.1 The former 'White Highlands' of Central Kenya

Development of water resource management strategies in industry and agriculture, freshwater fisheries, flood control, and hydroelectric power generation critically depends on appreciation of natural long-term climate variability. This is especially true for the vast dry land regions of East Africa, where interannual and decadal trends in rainfall have a dramatic impact on soil moisture availability, agricultural production, and the water quality of lakes and reservoirs.

Due to the lack of long (>100 years) instrumental climate records from East Africa, a truly long-term perspective of past climatic variability can only be gained by studying natural records of climate-driven environmental change. One the most important of these climate-proxy records is the sedimentary record accumulating on the bottom of suitably climate-sensitive lakes. Changes in the elevation and water chemistry of these lakes resulting from their hydrological response to seasonal and long-term trends in the regional balance of rainfall and evaporation are archived in the sediment record as characteristic lithological, geochemical, and biological signatures (Verschuren, et al. 1999).

This area was formerly part of the 'White Highlands', large tracts of land reserved by the British colonial government for farming and ranching by European settlers.

The highlands of central Kenya enjoy a famously favourable climate of yearlong warm sunny days and cool nights, and a high probability of rainfall from March through December. This long wet season results because, in addition to the two regular rain seasons associated with latitudinal passages of the Intertropical Convergence Zone, moisture is also brought in form the Atlantic Ocean by equatorial westerlies (Nicholson, 1996).

The Central Rift Valley of Kenya is an area of moderate altitude that resulted from formation of the rift. The area forms a catchment for the drainage from two extensive forest stands on both margins of the rift; the Nyandarua Mountains on the east rise to about 3960 m and Mau Escarpment on the west to above 3000 m. (Fig. 2.1). The catchment presently includes three lakes: Naivasha, Nakuru and Elmenteita.

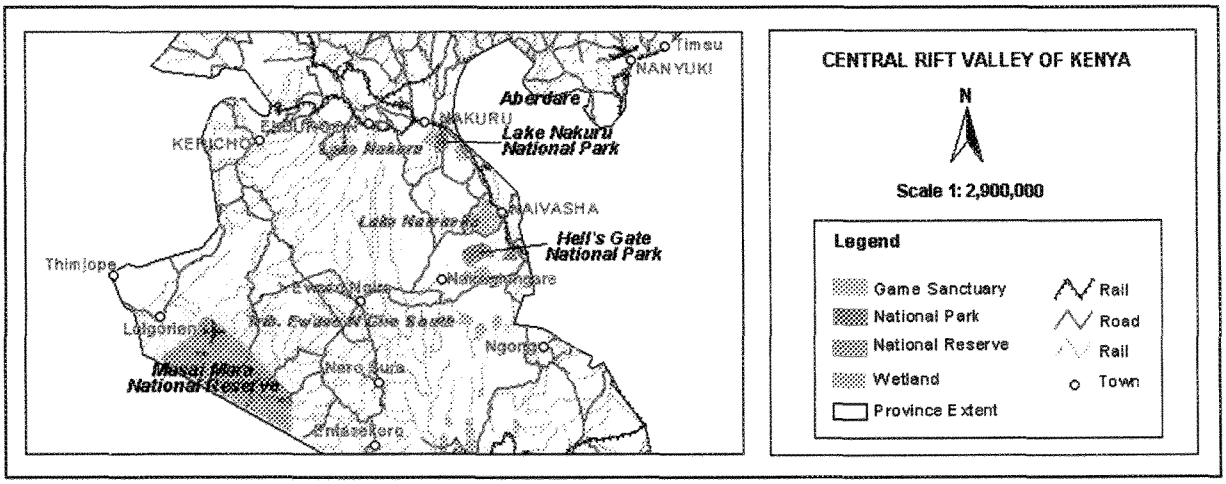


**Fig. 2.1.** Central Rift Valley of Kenya

## 2.2 Lake Naivasha basin

### 2.2.1 Physical characteristics

Lake Naivasha is a shallow freshwater lake which shares a common depression with two saline lakes, Elmenteita and Nakuru, in the eastern or Gregory Rift Valley of Kenya at a mean altitude of 1890m above sea level. It is located at 0° 45' S and 36° 20'E in Nakuru District, about 100 km northwest of Nairobi.

The lake has an average depth of about 4 m; a maximum depth of 7.6 m was recorded in 1957. An area of about 120 km$^2$ and a shoreline of approximately 50 km were recorded in 1968 (Melack, 1979). Lake Naivasha receives drainage from higher parts of the valley floor in the Kinangop Plateau and also from the mountain regions of the Nyandarua Mountains and the valley floor east of the lake.
The volcanic activity associated with the formation of the Rift Valley and tectonic faulting formed four topographically distinct water bodies (Richardson and Richardson, 1972) of varying salinity: Lake Naivasha, Crescent Island basin of Lake Naivasha, Oloidien Lake and Sonachi (or Naivasha) Crater Lake. Lake Naivasha and the Crescent Island basin are the most dilute, and Oloidien and Sonachi Crater lakes are appreciably more concentrated.

Lake Naivasha has no outlet at present but is thought to have discharged during the middle Holocene through Njorowa Gorge to the south (Richardson and Richardson, 1972).

Lake Naivasha proper contributes over 90% of the total water surface in the basin and because of the shallow depth and gently sloping sides its surface area and that of the fringing papyrus and littoral lagoons, is extremely sensitive to changes in water level.

The Lake Naivasha catchment covers an area of approximately 3300 km$^2$ and several rivers feed the lake from the north, where the Malewa River forms the main inlet.

The Malewa River (1730 km$^2$ watershed), which obtains its water from the Aberdare range and Kinangop Plateau contributes about 90% of the discharge into Lake Naivasha. Most of the remainder is

provided by the Gilgil River (420 $km^2$ watershed), which drains the Bahati highlands to the north of the Elmenteita – Nakuru basin. Consumption of water and irrigation and natural losses, often eliminate flow in the Gilgil before the lake is reached. The two rivers enter the northern side of the lake after passing under North Swamp for several kilometres. The major portion of the northern swamp consists of a floating mat of Cyperus papyrus.

### 2.2.2 Climate

The climate of the area is warm and semi-arid (East African Meteorological Dept., 1964). Air temperatures are moderate with monthly means varying from 15.9 to 18.5 °C. Seasonal variations in water temperature are also slight ranging from 19.5 to 23 °C.

Prevailing winds are from the east and northeast. The Rift Valley itself is located in the rain shadow of these highlands and therefore semiarid, with rainfall and evaporation averaging 600 mm and 1800-1900 mm $yr^{-1}$ (Ase, et al. 1986).

The combination of moderate temperature, low relative humidity and low rainfall make January and February the months with the highest evaporation. Average rainfall near the lake has a muted bimodality with a main pulse in April and May and a minor pulse in November (Melack, 1976). The highlands surrounding the drainage basin receive more rain than the lakes and valley floor and provide most of the water that maintains the lake.

### 2.2.3 Geology

The oldest rocks in the area to which a definite age has been ascribed are sediments and pyroclastics on the Kinangop. The rocks of the area fall into two main groups: 1) lavas and pyroclastics and 2) lacustrine deposits. The lavas range from under saturated basic rocks (tephrites) to acid rocks (rhyolites and obsidians) with numerous gradations in between. The pyroclastics, some consolidated and others incoherent, cover the greater part of the surface area, and compose great thickness in the flanks, particularly in the Mau escarpment, where they rise to heights of over 10,000 feet.

The lake deposits, though covering large areas are not thick. Their configuration is closely allied to the present day Rift Valley lakes, which are the remnants of the much greater lakes that existed in Pleistocene times.

### 2.2.4 Water balance

The hydrological equilibrium of a drainage basin is maintained by the dynamic balance between sources of water and water losses. Principal sources which bring water into a lake basin are affluent rivers, seepage-in and precipitation; while water may be lost through effluent rivers, seepage-out and evaporation.

Much of the rainfall designated for the Rift valley is intercepted by the surrounding highlands. The main basin of Lake Naivasha and its enclose basins, Lake Oloidien and Crescent Island are maintained primarily by the Malewa River. The remaining input comes from seasonal streams, direct pre-

cipitation and groundwater seepage. The basin losses water via evaporation, groundwater seepage and abstractions. The evaporation output is about 80% and approximately 20% of the total water lost corresponds to seepage out and utilization (Gaudet and Melack, 1981; Darling et al., 1990).

Water input by seepage occurs in the northeast and northwest sections, and seepage out in the south and southeast sections of the main lake (Thompson & Dodson, 1963).

The water balance is predominantly controlled by river discharge, rainfall and evaporation. Compared to river discharge and rainfall, seepage plays a minor role in the main lake water balance, and the lake level fluctuates much as in closed basin lakes (Gaudet and Melack 1981).

### 2.2.5 Lake level fluctuations

The interest in Lake Naivasha lies in its likely role as an indicator of a set of climatic parameters and related to upper-level air flow over East Africa. The mountainous zones of East Africa enjoy their own unique climate (Griffiths, 1972). The Aberdare Mountains rise to 3994 m and the interactions between the mountains and the air flow above the sub-tropical inversion have considerable repercussions on the lake level.

Daily records of lake level were initiated in 1909 and show repeated fluctuations [Sikes, 1936; Kenya Ministry of Works (Hydrology), 1958, 1964]. Up to 1965 the last major fluctuation was a 5.1 m increase from 1961 to 1964. Subsequently, the level has remained high but had a net decline with yearly oscillations associated with rainy and dry seasons.

Vincent, Davies & Beresford (1979) have found a highly significant correlation between levels of the main lake and rainfall at highland stations in Kenya with a periodicity of about 7 years.

### 2.2.6 Vegetation

The arid climate and the porous soils of most of the drainage basin of Lake Naivasha have a strong influence upon the vegetation. The Kedong valley, to the south of Lake Naivasha, has according to Trump (1967), natural vegetation referred to as "evergreen bush land". Large parts of the area have an appearance of dry savannah, which might partly due to fire and downcutting of the bushes. Even grasslands frequently occur in the less arid parts of the landscape. The "whistling thorn tree" (Acacia seyal) is characteristic for the "secondary vegetation". The most characteristic tree of the shores of Lake Naivasha is the yellow fever tree (Acacia xantophloea).

### 2.2.7 Socio economic values of Lake Naivasha

Much of the drainage basin is used for ranchland with some forest clearance and farming in the north on the mountain slopes. The lake basin has become an important area for vegetable production and supports a large vegetable drying factory. Cut flowers are grown on large plantations along the southern shore for export. This intensive agricultural production is made possible by the readily available irrigation water, good quality volcanic soil and tropical climate.

**Agriculture**

Horticultural farms using lake water for irrigation surround the lake. Fruits, vegetables and flowers are grown both for local and export market. Horticulture is of national importance as a source of foreign exchange and employment to some 30,000 people. The irrigated land under production is over 10 , 000 ha. Farms range in size from large companies with hundreds of hectares under intensive flower production, to small farms growing vegetables for export. Dairying around the lake is well established and irrigated Lucerne farms have supported the industry since the late 1950s. However, intensive, export-oriented horticultural production has developed only over the last 10-15 years. It is still expanding.

**Geothermal power generation**

A large volume of water is pumped from the lake by the Kenya Power Company (KPC). The plant provides roughly 15% of national electric power requirements. Being a relatively cheap source of energy for Kenya, power from geothermal resources is planned to increase for at least the next 20 years to about 28% of the country's demand.

**Domestic water supplies**

This is obtained from the lake either directly or from wells or boreholes adjacent to the lake. Three boreholes with a maximum output of 50, 100 $m^3h^{-1}$ supply the town of Naivasha.

**Commercial fishing**

The lake supports a thriving commercial fishery which started in 1959. The fish species exploited are the large mouth bass ( *Micropterus salmoides* Lacepede), tilapine species (*Oreochromis leucostictus* Trewavas and *Tilapia zilli* Gervais), and crayfish (*Procambrus clarkii* Girard). All are introduced species. Crayfish is exploited both for export and local consumption.

**Tourism and recreation**

The lake offers outstanding aesthetic scenery and recreational facilities. The latter include boating, water-skiing, sport fishing, game viewing and bird watching. There are many tourist hotels, campsites, hostels and marinas for accommodation and leisure around the lake.

**Ranching and game farming**

The lake is a source for water for game such as giraffe, buffalo, zebra, antelope and waterbuck found within a number of ranches and game sanctuaries around the lake. A number of ostrich farms are also developing around the lake.

# Chapter 3

# Methods of analysis

## 3.1 Streamflow measurements

Streamflow is the combined result of all climatologically and geographical factors that operate in a drainage basin. It is the only phase of the hydrological cycle in which the water is confined in well-defined channels, which permit accurate measurements to be made of the quantities involved.

### 3.1.1 Current meters

The current meter is still the most universally used instrument for velocity determination. The principle is based upon the relation between the speed of the water and the resulting angular velocity of the rotor. By placing a current meter at a point in a stream and counting the number of revolutions of the rotor during a measured time interval, the velocity of the water at that point can be determined. The number of revolutions of the rotor is obtained by various means depending on the design of the meter but normally an electric circuit through the contact chamber achieves this. In all types of design the electrical impulses produce either a signal, which registers a unit on a counting device or an audible signal in a headphone. Intervals of time are measured by a stopwatch or by an automatic timing device.

### 3.1.2 Velocity – area method

The velocity area method for the determination of discharge in open channels consists of measurements of stream velocity, depth of flow and distance cross the channel between observation verticals. The velocity is measured at one or more points in each vertical by current meter and an average velocity determined in each vertical. The discharge is derived from the sum of the product of mean velocity, depth and width between vertical. The discharge so obtained is normally used to establish a relation between water level and stream flow.

#### 3.1.2.1 0.2 and 0.8 depth method

Velocity is observed at two points at 0.2 and 0.8 of the depth from the surface and the average of the two readings is taken as the mean for the vertical. This assumption is based on theory and on the study of vertical velocity curves, and experience has confirmed its essential accuracy. Generally the minimum depth of flow should be about 0.75 m when the 0.2 and 0.8 depth method is used.

### 3.1.3 Dilution gauging

The basic principle of the dilution method is the addition of a suitably selected tracer to the flow. Downstream of the injection point, when dispersion throughout the flow is affected, the discharge may be calculated from the determination of the dilution of the tracer.

If the tracer was present in the flow before the injection, the increase in concentration of tracer due to the injection is know as the concentration of added tracer.

The main disadvantage of the method is the difficulty in obtaining complete mixing of the tracer.

#### 3.1.3.1 Integration ('gulp' or sudden injection method)

A volume V of a solution of concentration $C_1$ of a suitably chosen tracer is injected over a short period into a cross section located at the beginning of the measuring reach, in which the discharge Q remains constant for the duration of the gauging. A simple steady emptying of a flask of tracer solution often performs the injection. At a second cross section downstream for this reach, beyond the mixing length, the concentration of added tracer, $C_2$, is determined over a period of time sufficiently long to ensure that all the tracer has passed through the second (sampling) cross section.

If the entire tracer injected passes through the sampling cross section, the discharge is calculated from the following equation.

$$M = VC_1 = Q\int_{t_0}^{\infty} C_2(t)dt \qquad \text{Eq. (3.1)}$$

where,
$M$ is the mass of tracer injected;
$V$ is the volume of injected solution;
$C_1$ is the concentration of tracer in the injected solution;
$Q$ is the river discharge;
$C_2(t)$ is the concentration of added tracer at the fixed sampling point over the time interval d$t$;
$t$ is the elapsed time, taking as the origin the instant at which the injection started;
$t_o$ is the time interval of the first molecule of tracer at the sampling cross section.

#### 3.1.3.2 Tracers

The various substances chosen as tracers are selected for their properties, which provide ease of detection at low concentrations.

There are three main types of tracer used in dilution gauging: chemical, fluorescent and radioactive. The chemical tracer is the only that will be explained in this chapter because it was used by the dilution method during fieldwork. Information about the fluorescent and radioactive tracers will be found in the stream flow references.

**Chemical tracers**

The usual tracers are sodium chloride, in the form of common salt, sodium dichromate, lithium chloride, sodium nitrate and manganese sulphate.

The cheapest and most convenient tracer to use in many countries is common salt (NaCl), preferable fine-grained table salt that dissolves quickly. The amount of salt required per $m^3s^{-1}$ of stream discharge depends on the mixing length. The background conductivity (natural conductivity measured when no salt solution is present) of natural water also affects the minimum amount of salt that can be used. As a rule of thumb, 0.2 kg of salt per $m^3s^{-1}$ of discharge is considered sufficient for natural waters with low background conductivity. Under good conditions, however, discharges of up to 140 $m^3s^{-1}$ have been measured by the use of not more than 12 kg of salt (86g of salt per $m^3s^{-1}$ of discharge).

Colorimetric analysis permits the measurement of very low concentrations of sodium dichromate. With final concentrations between 0.2 and 2 mg/l, the accuracy of the analysis depends upon the concentration used, and the sensitivity and accuracy of the colorimetric apparatus. The solubility of sodium dichromate in water is relatively high at 600 g/l (600 $kg/m^3$).

In the UK, lithium chloride has also been used as a tracer and has a solubility of 637 g/l at 0 °C; the element lithium can be detected in concentrations down to about $10^{-4}$ mg/l in the laboratory with specialized flame photometers.

## 3.2 Geostatistical tools

Although the presence of correlation was long known, no way existed to quantify the amount of spatial correlation until the development of Geostatistical methods, most specifically the variogram. The variogram determines the relationship between the distance separating nearby samples and the amount of correlation present. Through the process the variogram analysis, one, two or three dimensional spatial correlation structures of the variable of interest can be identified and quantified.

The variogram, departing from classical statistics, demonstrates that all samples are not equal for estimation purposes. Rather, the usefulness of a sample for prediction purposes is related to its spatial location.

This relationship can be shown graphically in Fig. 3.1. The $x$ axis represents the distance between sample points; the $y$ axis shows the variance, which is related to the uncertainty or difficulty in estimating unsampled locations. The graph shows that, as the distance from known sample locations to unsampled point increases, the uncertainty or difficulty in estimating these unsampled locations also increases. At a certain distance, the difficulty reaches a maximum and remains constant.

Whereas variograms provide the assessment of the spatial correlation structure present, the technique of kriging provides the machinery that enables the geostatistics to use more fully the information derived from the variogram. The estimate of the unsampled location produced by kriging has been designed to minimize the error associated with the estimate. This puts kriging in the class of best estimators.

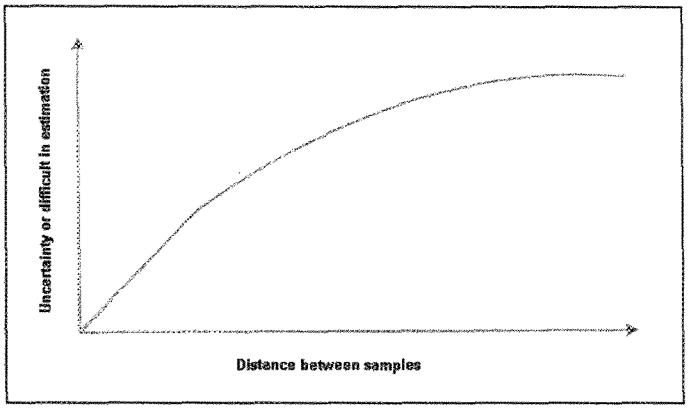


**Fig. 3.1.** Idealized variogram

### 3.2.1 Variograms

Variograms are fundamental tools in Geostatistical appraisal and the GEM process. The variogram and statistics, in general, focus on the dissimilarity. The variance provided by the variogram uses a slightly different twist on the variance and covariance approach. First, the variogram compares pairs of sample data $(Z_x - Z_{x+h})^2$ at different locations and at distance $h$, not a datum to the mean $(x_l - m)^2$. Pairing of samples is done so that a second feature may be included: the distance between the two samples. Mathematically, the difference of two values $Z(x)$ and $Z(x+h)$ is determined and then squared to produce a variance.

Having the squared difference of one pair of points is not sufficient; rather, it is necessary to obtain the average value of all such pairs of points at that distance. Thus, the variogram function may be defined:

$$\gamma(h) = \frac{1}{2N(h)} \sum_{i=1}^{N} [Z(x-h)]^2 \qquad \text{Eq. (3.2)}$$

It is important to notice that the variogram is a vector function, that is, a function of both distance and direction. The variogram quantifies how values of the variable $Z(x)$ differ (on the average) as distance $h$ increases along a given direction. The process of increasing the lag distance by $h$ ($h$, $2h$, $3h$, etc.) continues until such time as $nh$ is close to or greater than the largest distance between any two samples. Once all the values of $\gamma(h)$ have been obtained, they are plotted as a function of distance to produce the variogram graph.

The ideal variogram rises from the origin and then reduces its rate of increase until it eventually levels off. The distance at which the graph flattens is called the **range**. The height at which this plateau is reached is called the **sill**. In practice, the height of the sill is generally equal or close to the population variance $s^2$.

The variogram graph embodies three basic concepts that were qualitatively known to those working with earth science or spatial data. These are continuity, zone of influence and anisotropies.

### 3.2.1.1 Variogram models

A well-behaved experimental variogram provides a clear picture of the spatial continuity present at a site for samples of a given support. It is limited in practical usefulness, however, in that $\gamma(h)$ values are available for only those specific distances corresponding to the average separation distances between samples derived in the calculation of the experimental variogram. The number of average separation distances is almost always less than 20. The kriging process will require the knowledge of the variogram value between the locations at which estimates need to be made. It is, therefore, extremely unlikely that the 20 or less $h$ distances available will satisfy the multitude of distances required during the kriging process.

The solution comes in the form of a mathematical model for the experimental variogram. A number of functions are commonly used to model variograms and will be described in this section.

Models are loosely grouped into two categories: 1) those with sills and 2) those without. Those will sills or plateaus, sometimes called transitive models, include the spherical, exponential, Gaussian, and hole effect models. Those without sills include the nugget effect and the linear model.

**Spherical model**

The spherical model is, in all probability, the most frequently used function for modeling variograms. Its shape is presented in Figure 3.2, the beginning portion of the graph, indicating small separation distances, displays a linear component. The linear behavior is lost at larger distances; and the curve flattens, eventually reaching a plateau. A line tangent at the origin will intersect the sill at two-thirds the range.

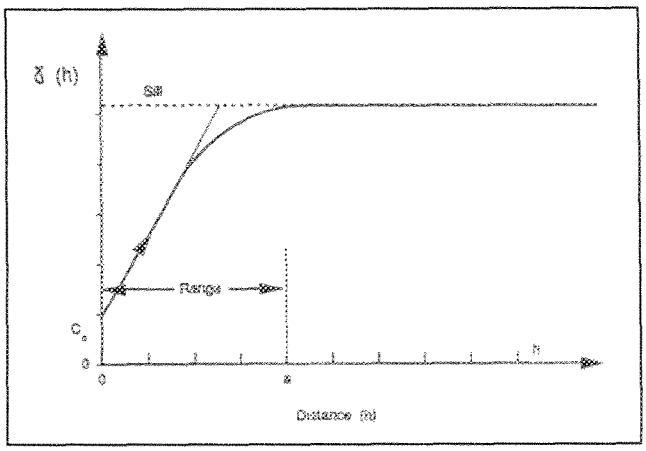


**Fig. 3.2.** Spherical variogram model

The equation for the spherical model is

$$\gamma(h) = C\left[\frac{3}{2}\frac{h}{a} - \frac{1}{2}\frac{h^3}{a^3}\right] + C_0 \qquad h \le a \qquad \text{Eq. (3.3)}$$

$$\gamma(h) = C - C_0 \qquad h > a \qquad \text{Eq. (3.4)}$$

$$\gamma(0) = 0 \qquad \text{Eq. (3.5)}$$

where,
$a$ is the range;
$C_0$ is the nugget effect,;
$C+C_0$ is the sill.

**Exponential model**

The exponential model is visually similar to the spherical (Fig. 3.3) but represents a more continuous process. It rises more steeply from the origin than the spherical model but then flattens at a more leisurely rate. In fact, it approaches a sill only asymptotically, with a practical range usually defined to be the variogram value representing 95% of the sill. As with the spherical model, it is linear at the origin. With the exponential model, the linear component exists only for very small distances. A line tangent at the origin will intersect the sill at one-fifth the range. The equation for the exponential model is

$$\gamma(h) = C_0 - C\left[1 - \exp\left(-\frac{|h|}{a}\right)\right] \qquad \text{Eq. (3.6)}$$

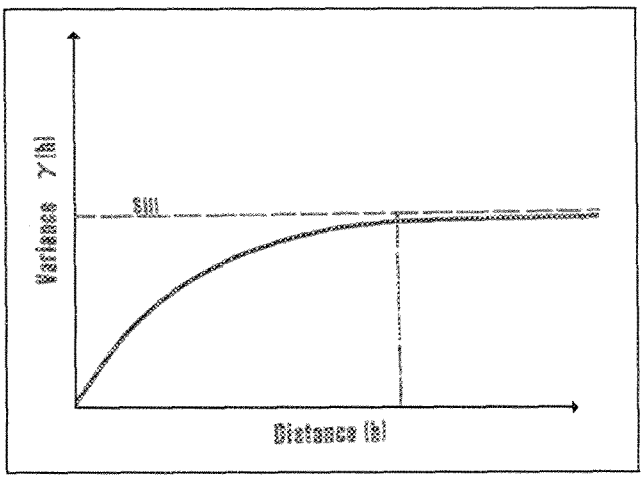


**Fig. 3.3.** Exponential variogram model

**Gaussian model**

The Gaussian model is typically used to model processes that show extremely low variation at short distances, to the extent that the model is parabolic at the origin (Fig. 3.4). As with the exponential model, the Gaussian model asymptotically approaches its sill, the practical range again defined as the distance at which the variogram value achieves 95% of the sill. The equation is:

$$\gamma(h) = C_0 + C\left[1 - \exp\left(-\frac{3h^2}{a^2}\right)\right] \qquad \text{Eq. (3.7)}$$

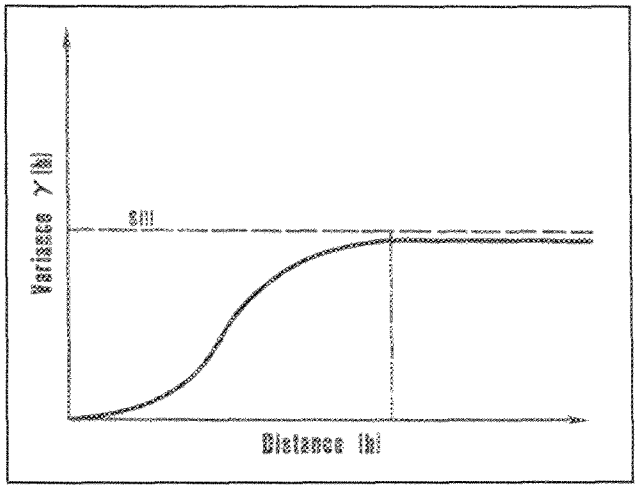


**Fig. 3.4.** Gaussian variogram model

**Hole effect model**

The hole effect model is used to model periodic behavior. This type of phenomenon is encountered where a series of high and low concentration areas exist in succession in an area of multiple spills, in lagoons, or in process areas, for example. The graph is slightly parabolic at the origin, although not so much as for the Gaussian model. After reaching a maximum, the graph oscillates up and down in a sine wave of ever decreasing amplitude (Fig. 3.5). The equation for the hole effect model is a combination of the exponential model with a sine model:

$$\gamma(h) = C\left(1 - \frac{\sin ah}{ah}\right) \qquad \text{Eq. (3.8)}$$

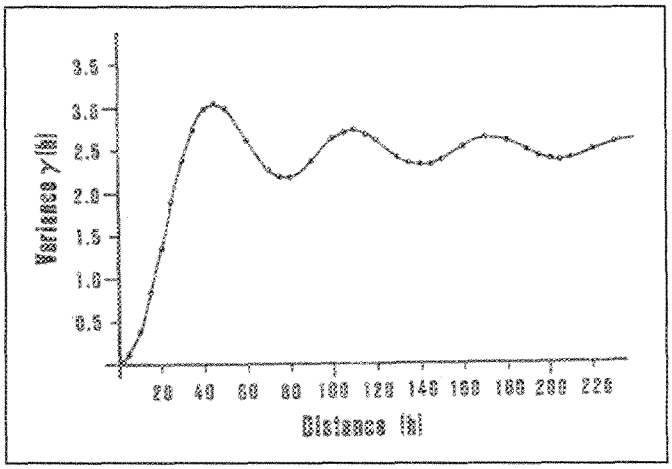


**Fig. 3.5.** Hole effect variogram model

**Nugget effect model**

Many variogram graphs do not begin at the origin. Rather, a vertical discontinuity exists at distance zero. By definition, $\gamma(0)$ is always zero, but it is known that variation may exist (fundamental error, analytical error, etc.). Also, variation may exist at very small distances. The nugget effect is defined as a constant $C_0$ and is simply added to the other variogram model or models being used. For purposes of estimation, $C_0 = 0$ when $h = 0$.

**Linear model**

Aside from the nugget effect model, the linear model is the simplest of the variogram models. The linear model does not reach a sill; instead, it grows in a linear fashion as a function of distance $h$ (Fig. 3.6). Its equation is written

$$\gamma(h) = ah + B \qquad \text{Eq. (3.9)}$$

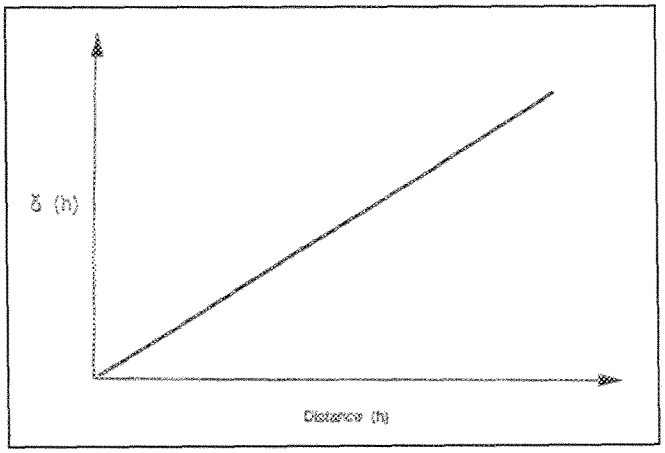


**Fig. 3.6.** Linear variogram model

### 3.2.1.2 Types of variograms

**Cross variograms**

Occasionally, it is desired or necessary to predict the value of one variable at a location using the value of a second variable at the same location.

The process by which this estimation is performed is called cokriging. In order to perform cokriging, however, it is necessary to determine the simultaneous variability between a primary variable at distance h and the variability of a secondary variable at the same distance.

Measurement of covariability is performed by means of the cross variogram. The spatial structure of the cross variogram is estimated by using the following formula:

$$\lambda_{PS}(h) = \frac{\sum_{i=1}^{n}\left(\left[Z_P(x_i) - A_p(x_i + h)\right]\left[Z_s(x_i + h)\right]\right)}{2n(h)} \qquad \text{Eq. (3.10)}$$

where,
$Z_P(x)$ is the primary variable at location $x_i$;
$Z_s$ is the secondary variable at location $x_i$;
$N(h)$ is the number of sample pairs of $Zp(x_i)$;
$Z_s(x_i)$ is a given lag interval.

The linear model of coregionalization requires that the variance of any possible linear combination of the two variables be positive. This can be assured if the cross variogram function satisfies the Cauchy – Schwartz inequality given by (Myers, 1984):

$$\left|\gamma_{Z_{PS}}(h)\right| \leq \left|\left[\gamma_{Z_S}(h)\right]\right|^{1/2} \qquad \text{Eq. (3.11)}$$

## 3.2.2 Optimizing estimation: Krigging

### 3.2.2.1 Introduction

Given a quantification of the expected error, it is possible to find a set of sample weights that will minimize the magnitude of the error variance. This is kriging, named for South African mining engineer Dannie Krige. Using the time honored method of taking the derivative with respect to the appropriate variables, the estimation variance equation produces a series of equations that, when solved, will produce the minimum variance optimal estimate.

### 3.2.2.2 The kriging equations

Starting with the definition of the estimation variance,

$$\sigma_e^2 = \sigma_{Z(X_0)}^2 - 2\sum_{i=1}^{n} a_i COV\left[Z(X_i), Z(X_0)\right] + \sum_{i=1}^{n}\sum_{j=1}^{n} a_i a_j COV\left[Z(X_i, Z(X_j))\right] \qquad \text{Eq. (3.12)}$$

To determine the set of weights $a_i$ ( $i$=1, …, $n$) that will allow the weighted average

$$Z^* = \sum_{i=1}^{n} a_i Z(X_i) \qquad \text{Eq. (3.13)}$$

to be the minimum variance estimator of $Z(V)$, where $Z(V)$ is the true unknown concentration of block $V$, and $Z(X_i)$ represents a series of samples ($i$ = 1,…, $n$) with known concentrations.

For notational simplicity, equation 1 can be rewritten as

$$\sigma_e^2 = \sigma_v^2 - \sum_{i=1}^{n} a_i \sigma_{VX_i} + \sum_{i=1}^{n}\sum_{j=1}^{n} a_i a_j \sigma_{X_i X_j} \qquad \text{Eq. (3.14)}$$

where,

$\sigma_V^2$ is the variance of the blocks being estimated (block variance);

$\sigma_{VX_i}^2$ is the covariance COV[$Z(V)$,$Z(X_i)$] of the concentration of block $V$ and the concentration of sample $X_i$;

$\sigma_{X_iX_j}$ is the covariance COV[$Z(X_i)$,$Z(X_j)$] of the concentrations of sample $X_i$ and sample $X_j$.

The $n$ sample weights $a_i$ ($i$ = 1,..., $n$) will produce $n$ equations with $n$ unknowns when the $n$ partial derivatives are taken. One problem still remains, however. The unbiasedness constraint (sum of the weights = 1) adds and additional equation yet does not contribute an additional unknown. Thus, the system has $n$+1 equations and $n$ unknowns, a very difficult solution to obtain.

The Lagrange multiplier may be used to circumvent this problem. A new unknown $\mu$ is introduced to stand for the estimated variance of the errors. The Lagrange principle states that, when a constraint $C$ (note: $C = 0$) is present, the function

$$F = Q + 2\mu C \qquad \text{Eq. (3.15)}$$

must be minimized. Combining equations 3.14 and 3.15, the short form of the equation becomes

$$F = \sigma_e^2 + 2\mu\left(\sum_{i=1}^{n} a_i - 1\right) \qquad \text{Eq. (3.16)}$$

Note that the equality of the equation is not affected by adding the Lagrange parameter. Because

$$\sum_{i=1}^{n} a_i - 1 = 0 \qquad \text{Eq. (3.17)}$$

it also follows that

$$2\mu\left(\sum_{i=1}^{n} a_i - 1\right) = 0 \qquad \text{Eq. (3.18)}$$

Thus, zero is added to $Q$ in the general equation 3.15 and to the estimation variance in equation 3.16, causing no net effect to the equality.

To obtain the error variance for the model, it is necessary to take the $n$+1 partial first derivatives corresponding to the $n$ sample weights and $\mu$. This yields $n$+1 equations with $n$+1 unknowns. In addition, the unbiasedness condition is fulfilled by setting the partial first derivative with respect to $\mu$ equal to zero. The derivatives can be written as follows:

$$\frac{\partial F}{\partial a_i} = -2\sigma_{VX_i} + \sum_i a_j \sigma_{X_iX_j} + 2\mu = 0 \qquad \text{Eq. (3.19)}$$

for each of the $i = 1,\ldots, n$ sample weights corresponding to the $n$ samples to be used in the estimate, long with the unbiasedness constraint

$$\frac{\partial F}{\partial \mu} = \sum_i a_i - 1 = 0 \qquad \text{Eq. (3.20)}$$

The more usual form of these equations can be given by

$$\sum_j a_j \sigma_{X_i X_j} + \mu = \sigma_{VX_i} \qquad \text{Eq. (3.21)}$$

and

$$\sum_i a_i = 1 \qquad \text{Eq. (3.22)}$$

Expanding equation 3.21 produces the $n$ equations needed for each of the $n$ sample weights. The system of equations can be written in matrix form

$$[\Sigma][A] = [D] \qquad \text{Eq. (3.23)}$$

and is generally known as the ordinary kriging system.

The $\Sigma$ matrix is symmetric and contains information dependent solely on the known sample concentrations and the covariances between them. The $D$ matrix depends on both the block and the sample data (point-to block covariance). The $A$ matrix contains the $n$ as yet unknown sample weights and the Lagrange multiplier.

To solve for the weights, the equation becomes,

$$[A] = [\Sigma]^{-1}[D] \qquad \text{Eq. (3.24)}$$

where,
$[\Sigma]^{-1}$ is the inverse of the $[\Sigma]$ matrix.

With the weights determined, the kriging estimate becomes simply a matter of calculating the weighted average of the sample data used. This gives a minimum variance and unbiased estimate for the block in question. The weights obtained by multiplying the $[\Sigma]^{-1}$ can be substituted into equation 3.10 since the kriging weights were obtained by minimizing the estimation variance. This tedious process can be simplified by using the following formula:

$$\sigma_K^2 = \sigma_V^2 - \sum_i a_i \sigma_{VX_i} - \mu \qquad \text{Eq. (3.25)}$$

where,

$\sigma_K^2$ is the minimized error variance, which will be called the kriging variance.

The kriging variance may also be expressed in matrix form by

$$\sigma_K^2 = \sigma_V^2 - A \cdot D \qquad \text{Eq. (3.26)}$$

Since all values on the right side of equation 3.26 are available in the kriging system, the kriging variance is easily obtained.

### 3.2.3 Influence of the variogram on kriging

The variogram has been touted as the means by which the unique spatial continuity characteristics can be quantified and input to the site model. Fitting an appropriate model to the experimental variograms is a very important step.

**Influence of the Sill**

Two spherical variogram models are shown in Fig. 3.7. Both have the same range but differ in the height of the sill. The model $\gamma_a(h)$ is described with a nugget effect of 0, a sill of 500 and a range of 100:

$$\gamma(h) = 0 + 500\left[(1.5)\frac{h}{100} - (0.5)\frac{h^3}{(100)^3}\right] \qquad \text{Eq. (3.24)}$$

Model $\gamma_b(h)$ is identical to $\gamma_a(h)$ except that the sill is twice as large:

$$\gamma(h) = 0 + 1000\left[(1.5)\frac{h}{100} - (0.5)\frac{h^3}{(100)^3}\right] \qquad \text{Eq. (3.25)}$$

Both models yield exactly the same kriging weights and estimated value for point *P*. When the height of the sill is changed, no corresponding effect has been realized on the estimate. However, the estimation variance has doubled as a result of the higher sill in model $\gamma_b(h)$. This result is a rule in rescaling: the estimate remains unaffected while the estimation variance increases by the factor used to rescale the variogram sill.

**Influence of the Nugget Effect**

Figure 3.8 presents two variogram models: the model used in the kriging example (Eq. 3.24) and the same model with a nugget effect equal to 50% of the sill. The nugget effect influences the kriging system so that the estimate produced is closer to a simple average than it would be without a nugget value. Taken to the limit, a pure nugget effect will, in fact, simply average the available data. The resulting weights are all equal and nice for the kriging system but not good for the kriging variance.

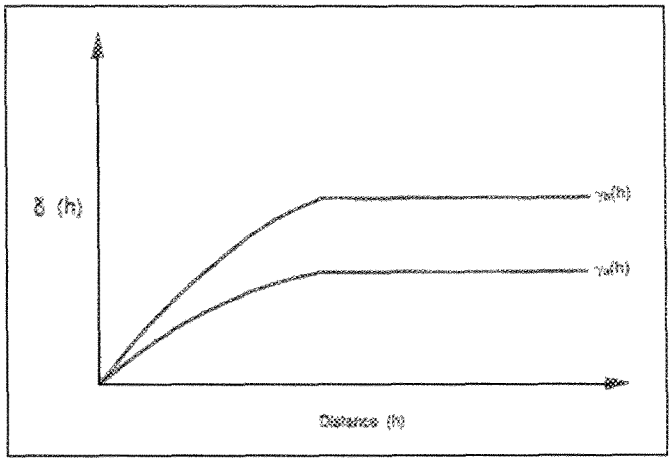


**Figure 3.7.** Two variograms that differ only in the height of the sill

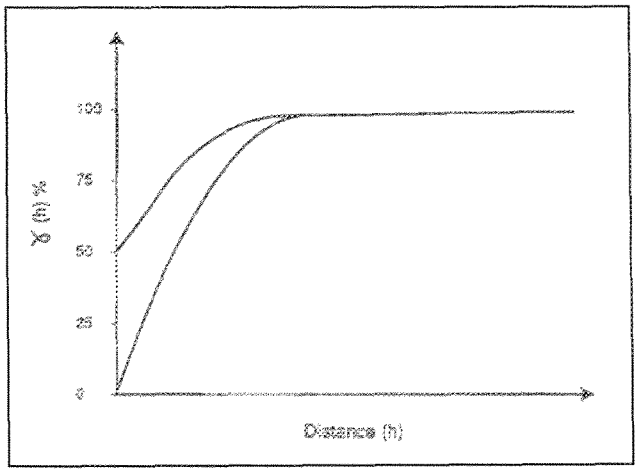


**Figure 3.8.** Two variograms that differ only in the nugget effect

### Influence of the Range

Figure 3.9 shows the original variogram model and the model, which the range has been doubled. Despite the increased spatial continuity, little change is noticed in either the weights or the value of the point estimate. The most noticeable change is to the kriging variance, which has been cut approximately in half. This is to be expected as, in terms of statistical distance, the samples now appear twice as close to before. The opposite becomes true for shorter ranges, and samples all appear equally far away.

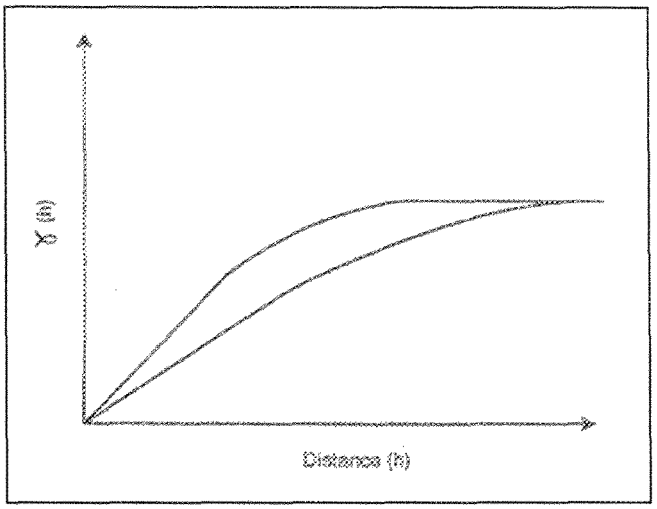


**Fig. 3.9.** Two variograms that differ only in the range

## 3.3 Water quality analysis and methods

The chemical analysis of surface water comprises the chloride, sulfate, nitrate, ammonia, phosphate, chemical oxygen demand, alkalinity and total hardness determinations which followed the methods described in each test manual. A summary of the procedures is presented next in Table 3.1. Major cations and metals were analyzed by inductivity-coupled plasma – atomic emission spectroscopy (ICP-ASE). The description of this specific method is shown below (section 3.3.1).

**Table 3.1.** Chemical methods

| Parameter | Method | Required Reagents | Required Apparatus |
|---|---|---|---|
| Sulfate | Sulfate ions react with barium in the SulfaVer 4 Sulfate Reagent and form insoluble barium sulphate turbidity. The amount of turbidity formed is proportional to the sulfate concentration. | SulfaVer 4 Sulfate Reagent Powder Pillows | Sample Cell, 25 mL, matched pair |
| Phosphate | Orthophosphate reacts with molybdate in an acid medium to produce phosphomolybdate complex. Ascorbic acid then reduces the complex, giving an intense molybdenum blue color. | PhosVer 3 Phosphate Reagent Powder | Test 'N tube vials; COD vial Adapter, DR 2010; funnel; pipet, tensette, 1.0 to 10 mL; pipet tips for 19700-10 tensette pipet; test tube rack |
| Nitrate, HR | Test 'N Tube NitraVer X Nitrate Reagent procedure. Nitrate in the sample reacts with chromotropic acid under strongly acidic conditions to yield a yellow product with a maximum absorbance at 410 nm. | NitraVer X reagent A Test 'N tubes, NitraVer X reagent B powder pillows | COD vial adapter, DR/2010; funnel; pipet, tensette, 0.1 to 1.0 mL; pipet, tips for 19700-01; tensette pipet; test tube rack |

| Parameter | Method | Required Reagents | Required Apparatus |
|---|---|---|---|
| Chemical Oxygen Demand (COD) | The mg/L COD results are defined as the mg of $O_2$ consumed per litre of sample under conditions of this procedure. In this procedure, the sample is heated for two hours with a strong oxidizing agent, potassium dichromate. Oxidizable organic compounds react, reducing the dichromate ion (Cr2O72-) to green chromic ion ($Cr^{3+}$). When the 0-150 mg/L colorimetric or tritimetric method is used, the amount of Cr6+ remaining is determined. | COD Digestion reagent vial: low range, 0 to 150 mg/l COD, demineralized water | COD reactor 120/240 Vac; COD vial adapter, DR/2010; pipet, tensette, 0.1 to 1.0 mL; pipet, volumetric, class A, 2 .0 mL; pipet filler, safety bulb; test tube rack |
| Chloride | Chloride in the sample reacts with mercuric thiocyanate to form mercuric chloride and liberate thiocyanate ion. Thiocyanate ions react with the ferric ions to form an orange ferric thiocyanate complex. The amount of this complex is proportional to the chloride concentration | Chloride reagent set, ferric ion solution, mercuric thiocyanate solution, demineralized water | Pipet, volumetric, 1.0 mL; pipet, volumetric, 2.0 mL, pipet filler, safety bulb; pipet, tensette, 0.1 to 1.0 mL; pipet tips, for 19700-01 tensette pipet; sample cell, 25 mL, matched pair |
| Nitrogen – Ammonia | Ammonia compounds combine with chlorine to form monochloramine. Monochloramine reacts with salicylate to form 5-aminosalicylate. The 5-aminosalicylate is oxidized in the presence of a sodium nitroprusside catalyst to form a blue colored compound. The blue color is masked by the yellow color from the excess reagent present to give a green solution | AmVer diluent reagent, ammonia salicylate reagent powder pillows, ammonia cyanurate reagent powder pillows | Clippers, large; COD Vial Adapter, DR/2010; funnel; pipette, 2mL, class A; test tube rack |
| Alkalinity (0 – 10 mmol/L) | The alkalinity is determined by direct titration of the water sample with hydrochloric acid. The positive p value is determined against phenolphthalein (color change pH 8.2) and the positive m value against a mixed indicator (colour change pH 4.3) | Reagent kit with graduated titration pipette (graduation: 0.1 mmol/l) for 170 determinations at 10 mmol/l | |
| Total Hardness (0.2 – 10 mmol/L) | The tritant is added dropwise to the water sample until the added indicator changes colour. The titration is based on a complexation reaction in which the calcium and/ or magnesium ions present in the water combine quantitatively with Titriplex III. The indicator also forms a complex with the calcium and magnesium ions and its complex is red. On addition of the Titriplex III, the indicator is liberated; the colour changes from red via grey-green to green. | Reagent kit with graduated titrating pipette (graduations: 0.2 mmol/l and 0.2 °d) | |

| Parameter | Method | Required Reagents | Required Apparatus |
|---|---|---|---|
| Conductivity | The conductivity electrode is plugged into the blue 5-pin connector of the sens*ion*. The electrode is placed in the water sample then the con/TDS/sal key has to be pressed for the reading, and after agitate the electrode for 5-10 sec to dislodge air bubbles, the electrode measures the conductivity electro-chemically. | | Portable sens*ion* HACH 156 multi-parameter meter; con-ductivity probe. |
| Total dissolved solids (TDS) | The conductivity electrode is plugged into the blue 5-pin connector of the sens*ion*. The electrode is placed in the water sample then the con/TDS/sal key has to be pressed for the reading, and after agitate the electrode for 5-10 sec to dislodge air bubbles, the electrode measures the TDS electrochemically. | | Portable sens*ion* HACH 156 multi-parameter meter; con-ductivity probe. |
| PH | The conductivity electrode is plugged into the black 5-pin connector of the sens*ion*. The electrode is placed in the water sample then the pH key has to be pressed for the reading, and after agitate the electrode for 5-10 sec to dislodge air bubbles, the electrode measures the pH electrochemically. | | Portable sens*ion* HACH 156 multi-parameter meter; pH probe. |
| Dissolved oxygen (DO), % oxygen saturated and temperature | Connect sensor to the meter then the sensor is immediately ready for meas-urement. Pressing the concentration and saturation key ($O_2$), the sensor starts doing the reading. | | Oxygen sensor CellOx 325 |

### 3.3.1 Inductively coupled plasma (ICP) method

**General**

ICP-AES, stands for Inductivity-Coupled Plasma – Atomic Emission Spectroscopy, is a multi-element analysis technique that will dissociate a sample into its constituent atoms and ions and cause them to emit light at a characteristic wavelength by exciting them to a higher energy level. This is accomplished by the use of an inductively coupled plasma source, usually argon. A monochromator can separate specific wavelengths of interest, and a detector is used to measures the intensity of the emitted light.

The plasma is used as a sample cell that will excite atoms. When these excited atoms return to the ground state, they will emit energy of a characteristic wavelength. The monochromator can direct these wavelengths to a detector.

A typical plasma source is shown below in Figure 3.10. The green arrow represents the argon flow, and the blue arrow indicates the sample flow. Initially, argon gas will pass through the quartz tube and exit from the tip. The tip of the quartz tube is surrounded by induction coils that create a magnetic

field. The ac current that flows through the coils is at a frequency of about 30 MHZ and a power level around 2kW. The stream of argon gas that passes the coil has been previously seeded with free electrons from a Tesla discharge coil. The magnetic field excites these electrons, and they then have sufficient energy to ionize the argon atoms by colliding with them. The cations and anions present from the initial Tesla spark accelerate due to the magnetic field in a circular pattern that is perpendicular to the stream exiting from the top of the quartz tube. By reversing the direction of the current in the induction coils, the magnetic field is also reversed. This changes the direction of the excited cations and anions, which causes more collisions with argon atoms. This results in further ionization of the argon atoms and intense thermal energy. As a result, a flame shaped plasma forms on top of the torch.

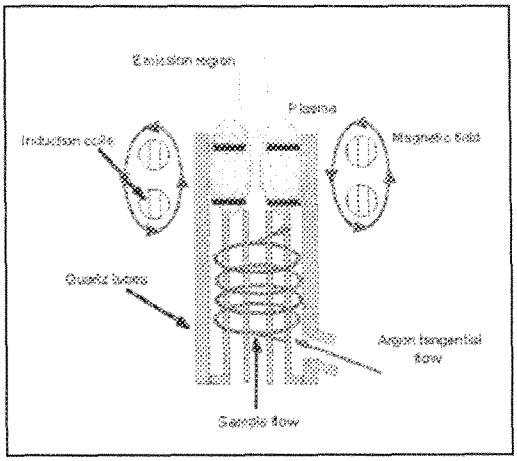


**Fig. 3.10.** Schematic diagram of a typical ICP-AES instrument

A second stream of gas is usually needed to cool down the inside of the quartz tube. This is provided by a stream of argon that provides a vortex flow. The flow also provides a way of centering and stabilizing the plasma.

When the sample flows into the plasma (in an aerosol form), the atoms present are excited by the extreme temperatures. These excited atoms will emit energy at a characteristic wavelength.

In an ICP analysis, the plasma will reach a temperature in the range of 6,000 – 10,000 °C, which will efficiently atomize most elements. The resulting detection limits are very low, and they usually range from 1-10 ppb.

There is no electrode contact in the plasma source, which results in spatially separated excitation and emission zones. This creates a simple background spectra and a high signal to noise ratio. The sample is introduced as an aerosol by use of a nebulizer or atomizer. Pneumatic nebulation is the most often used method.

A simultaneous ICP instrument can easily analyse up to 60 different elements at the same time without compromising the precision of the analysis or the detection limits.

**Interferences**

Interferences may be categorized as follows:

1. Spectral interferences: Light emission from spectral sources other than the element of interest may contribute to apparent net signal intensity. Sources of spectral interference include direct spectral line overlaps, broadened wings of intense spectral lines, ion-atom recombination continuum emission, molecular band emission, and stray (scattered) light from the emission of elements at high concentrations.

2. Non spectral interferences
    a. Physical interferences are effects associated with sample nebulization and transport processes. Changes in the physical properties of samples, such as viscosity and surface tension, can cause significant error.
    b. Molecular compound formation, ionization effects, and thermochemical effects associated with sample vaporization and atomization in the plasma cause chemical interferences.

# Chapter 4

# Materials and data collection

## 4.1 Sampling sites

Based on the research objectives, the sampling survey was planned to collect data from the lake Naivasha and its main inflows: Malewa and Gilgil rivers (see Fig. 4.1). There were not considered some other stream courses because often do no reach the lake as surface water. The Karati River, a seasonal river located on the northeast side of the lake, was not incorporated in the sampling because was dried during that period.

Before establishing definitely the sample locations in the river near to discharge measurements stations and pollution sources, the assistance of toposheets, satellite images and some previous studies were needed as well as some fieldtrips for areas recognition supervised by Kenyan hydrologists. At this point, it was quite useful to obtain the assessment from the Water Resources Ministry of Nakuru District in order to determine exactly the most convenient sampling places in terms of accessibility, security because of wildlife in the surroundings such as buffalos and hippos; and permission from owners if the location chosen belongs to a private farm.

The water quality survey in the Lake Naivasha concentrated the collection of samples from locations as much near to the rivers inflow, pollution sources and as much locations, which can represent the lake itself.

**The rivers**

The Malewa River accounts for about 90% of the river discharge into Lake Naivasha. Perennial flow is maintained in the Malewa (1730 $Km^2$ watershed) by rains on the Aberdare Mountains and Kinangop plateau.

Rains on the Bahati highlands keep perennial flow in the Gilgil River (420 $Km^2$ watershed) to at least the 2,100 m contour but consumption for irrigation and natural losses often eliminate the flow before the lake is reached.

Both of the rivers enter the papyrus swamp on the northern side of the lake and pass under the large swamp for several kilometers before reaching the lake (Gaudet, et al, 1981).

**The lake**

Lake Naivasha, ~150 $km^2$ in total area and constantly fluctuating, is a closed basin, shallow, freshwater lake surrounded by alkaline lakes.

The lake has three distinct components: the main lake, which is the most important; Oloidien Bay, which at low water – levels is a separate lake and has a considerably higher pH; and Crescent Island Bay, which forms the deepest part of the lake, presently ~15 m deep. Due to the present low water-levels, Crescent Island Bay is almost a separate lake and is chemically distinct from the main lake. Lake Sonachi, a small crater lake, 3 km form the main lake, is also part of the Lake Naivasha system.

Lake Naivasha has an average depth of 4 - 6 m and its level is 1886.5 m.a.s.l. Total water volume is estimated at 680 x 106 $m^3$, but varies with water – levels. The lake receives 90% of its inflow from the perennial Malewa and Gilgil rivers. The remaining input comes from seasonal streams, direct precipitation and ground seepage. The area is semi-arid, receiving on average 620 mm of rainfall each year, while annual evaporation is approximately 1735 mm (Abiya, 1996).

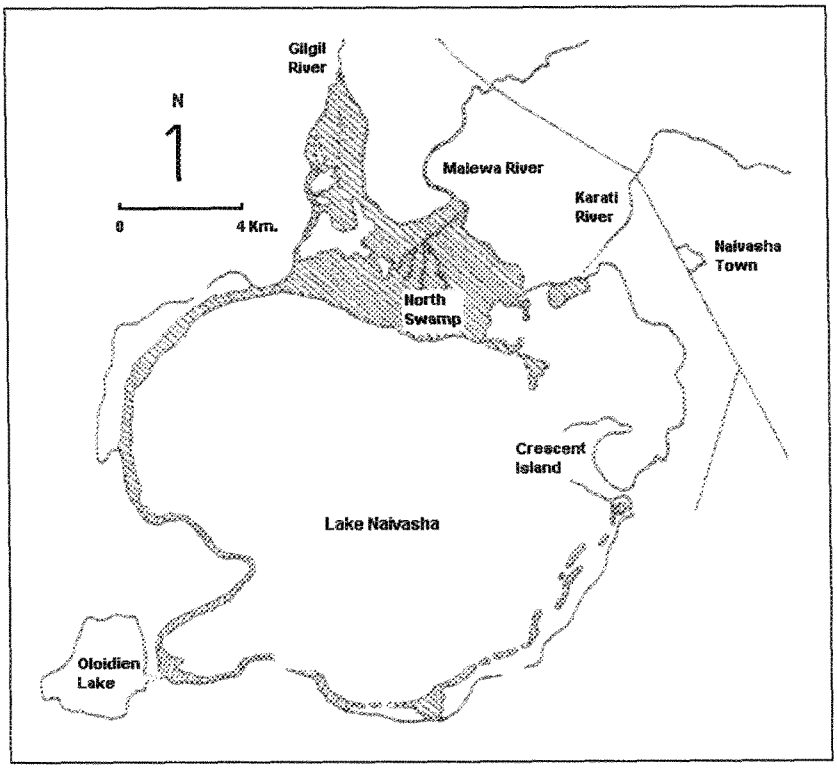


**Fig. 4.1.** Study area

## 4.2 Hydrological variables

Determining the hydrological regime of a water body is an important aspect for a water quality assessment. For example, knowledge of water velocity enables the prediction of the time of arrival downstream, of a contaminant accidentally discharged upstream. On the other hand, discharge measurements are necessary for mass flow or mass balance calculations and as inputs for water quality models (Chapman, 1996).

### 4.2.1 Malewa and Gilgil streamflow measurements

**Velocity - Area Method**
The velocity – area method was performed in 5 different locations (Fig. 4.2). Three locations (M1, M2 and M4) belong to Malewa River and the others to Gilgil River (G1 and G2).

The selection of the places to perform the tests was carefully chosen to avoid obtrusions due to rocks, tree branches, falls, among others; that could affect the velocity measurements. Once the place was selected, the rivers cross section was divided into segments by spacing verticals at a sufficient number of observations in order to describe the bed shape and the horizontal velocity distributions. The spacing verticals depended largely on the flow conditions, the geometry of the cross-section and the width of each location (see Figs. 4.3, 4.4, 4.5, 4.6 & 4.7).

The current meter used was an Ott propeller-type, which has a horizontal axis rotor. This type of current meter registers the velocity normal to the cross section and is not so susceptible to vertical currents. A stopwatch measured the intervals of time.

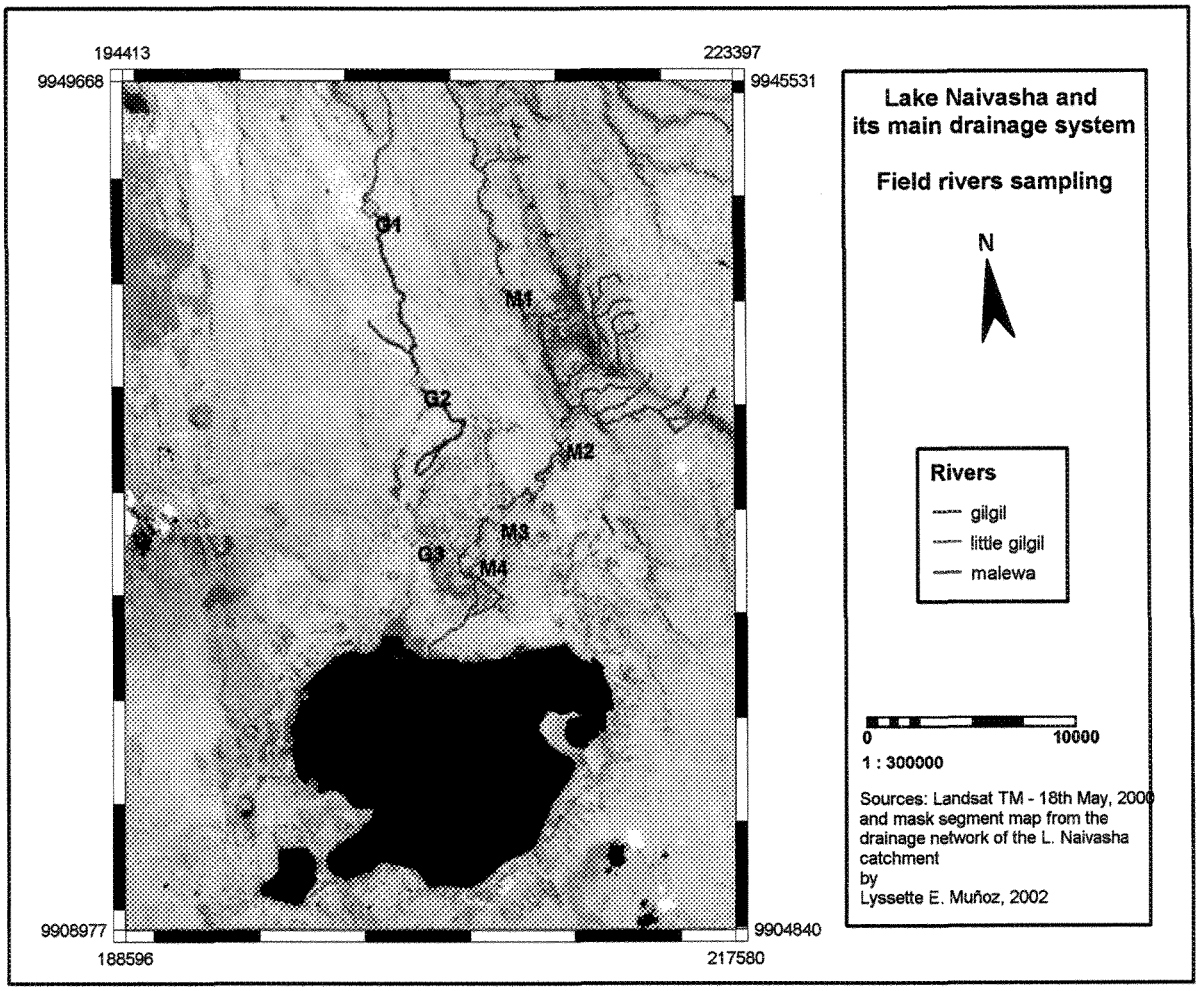


**Fig. 4.2.** Sampling points

**River:** Malewa River at 2GB1 (Location M1)
**Coordinates:** UTM Zone: 37 M; UTM Y: 9937504; UTM X: 210953
**Date:** 19/09/01

**Table 4.1.** Computation for a current meter measurement by the 0.2 and 0.8 depth method

| Vertical Number | Distance from base (cm) | Width (cm) | Depth (cm) | Veloc. 0.2 depth (cm/s) | Veloc. 0.8 depth (cm/s) | Area ($cm^2$) | Discharge ($m^3/s$) | Average velocity (cm/s) |
|---|---|---|---|---|---|---|---|---|
| 1 | 30 | 65 | 0 | 0 | 0 | 4875.0 | 00.0 E+0 | 0.00 |
| 2 | 130 | 100 | 300 | 38.76 | 46.39 | 30000.0 | 1.3E+0 | 42.58 |
| 3 | 230 | 100 | 270 | 48.08 | 48.08 | 27000.0 | 1.3 E+0 | 48.08 |
| 4 | 330 | 100 | 330 | 46.39 | 48.08 | 33000.0 | 1.6E+0 | 47.24 |
| 5 | 430 | 115 | 280 | 38.76 | 44.69 | 32200.0 | 1.3E+0 | 41.73 |
| 6 | 560 | 65 | 0 | 0 | 0 | 4550 | 00.0E+0 | 0.00 |
| | | | | | Σ | **131625.0** | **5.5E+0** | |

**Fig. 4.3.** Cross section (Location M1)

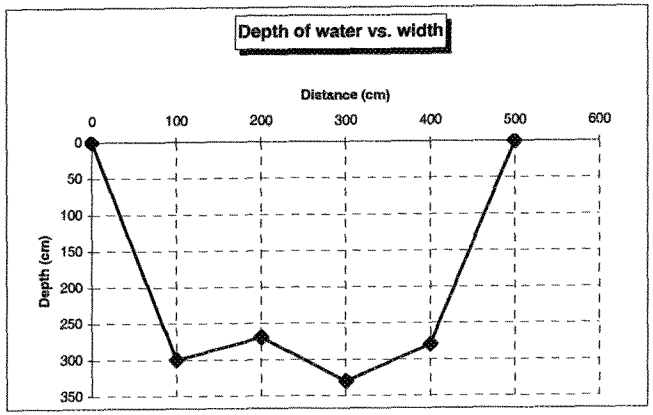


**River:** Malewa River at Diary Training School, Marula Estate (Location M2)
**Coordinates:** UTM Zone: 37 M; UTM Y: 9929754; UTM X: 212774
**Date:** 21/09/01

**Table 4.2.** Computation for a current meter measurement by the 0.2 and 0.8 depth method

| Vertical Number | Distance from base (cm) | Width (cm) | Depth (cm) | Veloc. 0.2 depth (cm/s) | Veloc. 0.8 depth (cm/s) | Area ($cm^2$) | Discharge ($m^3/s$) | Average velocity (cm/s) |
|---|---|---|---|---|---|---|---|---|
| 1 | 40 | 120 | 0 | 0 | 0 | 1200.0 | 00.0 E+0 | 0.00 |
| 2 | 240 | 200 | 40 | 23.49 | 23.49 | 8000.0 | 187.9 E-3 | 23.49 |
| 3 | 440 | 200 | 45 | 44.69 | 44.69 | 9000.0 | 402.2 E-3 | 44.69 |
| 4 | 640 | 200 | 50 | 83.70 | 83.70 | 10000.0 | 837.0 E-3 | 83.70 |
| 5 | 840 | 200 | 48 | 109.11 | 109.11 | 9600.0 | 1.0 E+0 | 109.11 |
| 6 | 1040 | 620 | 55 | 101.51 | 101.51 | 34100.0 | 3.5 E+0 | 101.51 |
| 7 | 1240 | 200 | 45 | 86.24 | 86.24 | 9000.0 | 776.2E-3 | 86.24 |
| 8 | 1440 | 820 | 26 | 59.96 | 59.96 | 21320.0 | 1.3 E+0 | 59.96 |
| 9 | 1640 | 180 | 18 | 42.15 | 42.15 | 3240.0 | 136.6E-3 | 42.15 |
| 10 | 1800 | 0 | 0 | 0 | 0 | 0 | 00.0E+0 | 0.00 |
| | | | | | Σ | **105460.0** | **8.1E+0** | |

**Fig. 4.4.** Cross section (Location M2)

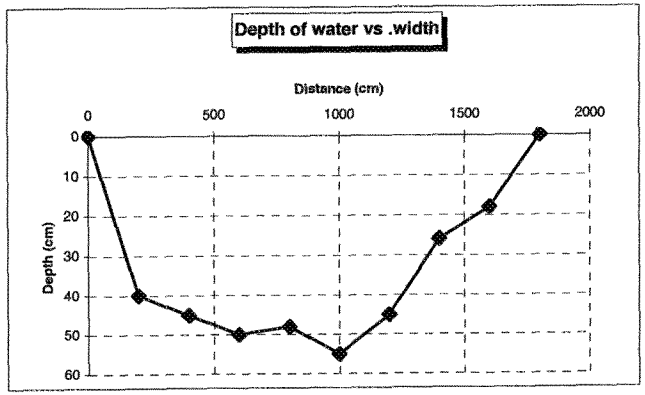

**River:** **Malewa River downstream at 2 km. before the lake (Location M4)**
**Coordinates:** UTM Zone: 37 M; UTM Y: 9924762; UTM X: 207893
**Date:** 20/09/01

**Table 4.3.** Computation for a current meter measurement by the 0.2 and 0.8 depth method

| Vertical Number | Distance from base (cm) | Width (cm) | Depth (cm) | Veloc. 0.2 depth (cm/s) | Veloc. 0.8 depth (cm/s) | Area ($cm^2$) | Discharge ($m^3/s$) | Average velocity (cm/s) |
|---|---|---|---|---|---|---|---|---|
| 1 | 0 | 150 | 0 | 0 | 0 | 1500.0 | 00.0 E+0 | 0.00 |
| 2 | 300 | 250 | 40 | 81.16 | 81.16 | 10000.0 | 811.6 E-3 | 81.16 |
| 3 | 500 | 200 | 40 | 93.00 | 93.00 | 8000.0 | 744.0 E-3 | 93.00 |
| 4 | 700 | 200 | 30 | 58.26 | 58.26 | 6000.0 | 349.6 E-3 | 58.26 |
| 5 | 900 | 550 | 25 | 38.76 | 38.76 | 13750.0 | 533.0 E-3 | 38.76 |
| 6 | 1100 | 200 | 20 | 26.88 | 26.88 | 4000.0 | 107.5 E-3 | 26.88 |
| 7 | 1300 | 200 | 48 | 43.84 | 43.84 | 9600.0 | 420.9 E-3 | 43.84 |
| 8 | 1500 | 0 | 0 | 0 | 0 | 0 | 00.0E+0 | 0.00 |
| | | | | | Σ | **52850.0** | **3.0 E+0** | |

**Fig. 4.5.** Cross section (Location M4)

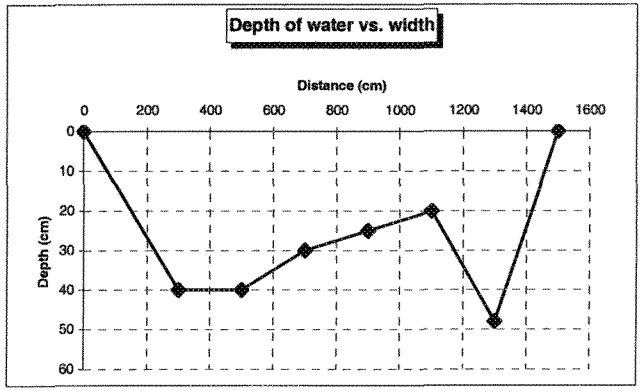

**River:** Gilgil after Little Gilgil (Location G1)
**Coordinates:** UTM Zone: 37 M; UTMY: 9941932; UTM X: 205279
**Date:** 17/09/01

**Table 4.4.** Computation for a current meter measurement by the 0.2 and 0.8 depth method

| Vertical Number | Distance from base (cm) | Width (cm) | Depth (cm) | Veloc. 0.2 depth (cm/s) | Veloc. 0.8 depth (cm/s) | Area ($cm^2$) | Discharge ($m^3/s$) | Average velocity (cm/s) |
|---|---|---|---|---|---|---|---|---|
| 1 | 0.0 | 61.25 | 0 | 0 | 0 | 612.5 | 00.0 E+0 | 0.00 |
| 2 | 122.50 | 122.5 | 40 | 53.43 | 53.43 | 4900.0 | 261.8E-3 | 53.43 |
| 3 | 245.00 | 122.5 | 70 | 42.15 | 42.15 | 8575.0 | 401.4E-3 | 46.82 |
| 4 | 367.50 | 122.5 | 40 | 12.45 | 12.45 | 4900.0 | 61.0E-3 | 12.45 |
| 5 | 490.00 | 61.25 | 0 | 0 | 0 | 612.5 | 00.0E+0 | 0.00 |
| | | | | | Σ | **19600.0** | **724.3E-3** | |

**Fig. 4.6.** Cross section (Location G1)

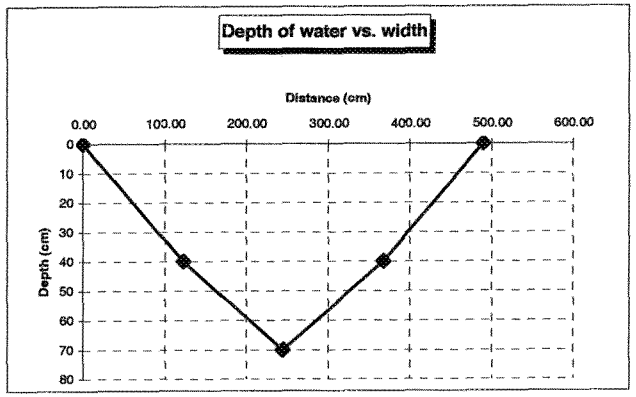


**River:** Gilgil at 2GA1 (Location G2)
**Coordinates:** UTM Zone: 37 M; UTM Y: 9933272; UTM X: 206379
**Date:** 18/09/01

**Table 4.5.** Computation for a current meter measurement by the 0.2 and 0.8 depth method

| Vertical Number | Distance from base (cm) | Width (cm) | Depth (cm) | Veloc. 0.2 depth (cm/s) | Veloc. 0.8 depth (cm/s) | Area ($cm^2$) | Discharge ($m^3/s$) | Average velocity (cm/s) |
|---|---|---|---|---|---|---|---|---|
| 1 | 0.0 | 25 | 0 | 0 | 0 | 187.5 | 00.0 E+0 | 0.00 |
| 2 | 50 | 75 | 30 | 44.69 | 44.69 | 2250.0 | 100.6 E-3 | 44.70 |
| 3 | 150 | 100 | 30 | 46.052 | 46.052 | 3000.0 | 138.2 E-3 | 46.05 |
| 4 | 250 | 100 | 30 | 41.30 | 41.30 | 3000.0 | 123.9 E-3 | 41.30 |
| 5 | 350 | 50 | 30 | 35.36 | 35.36 | 3000.0 | 106.1 E-3 | 35.37 |
| 6 | 450 | 75 | 30 | 38.76 | 38.76 | 2250.0 | 87.2 E-3 | 38.76 |
| 7 | 500 | 25 | 0 | 0 | 0 | 187.5 | 00.0E+0 | 0.00 |
| | | | | | Σ | **13875.0** | **555.9 E-3** | |

**Fig. 4.7.** Cross section (Location G2)

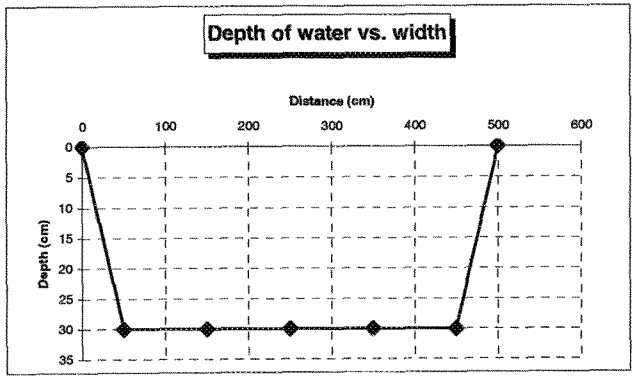

The velocity measurements were carried out three times at each vertical cross the channel to calculate an average number of revolutions. At location M1 (Malewa River at 2GB1), the velocity was observed at two points at 0.2 and 0.8 of the depth from the surface and the average of the two readings was taken as the mean for the vertical. For the other locations, the velocity was observed at 0.5 of the depth from the surface because the streams were shallow (mean depth of 40 cm) therefore it was not necessary to measured at two points in order to find differences, because the velocities in the verticals at any depth were similar.

The calibration was done satisfying the following conditions:

- The counting of pulses and the measurements of time and distance were taken as much accurate as possible.
- The axis of the meter stayed perpendicular to the water surface.

The cross-section area, the velocity and discharge estimations at each location are presented in Tables 4.1, 4.2, 4.3, 4.4 & 4.5. The velocity through the segments was calculated using the rating equations at which this type of current meter was calibrated (Eq. 4.1 & 4.2).

$$v = 0.2222 * n + 0.026 \qquad (n \leq 0.62) \qquad \text{Eq. (4.1)}$$

$$v = 0.2544 * n + 0.006 \qquad (0.62 \leq n \leq 9.85) \qquad \text{Eq. (4.2)}$$

where,
$v$ is the velocity through the segments [cm/s];
$n$ is the number of turns/30 s [rev/30s].

The discharge calculation was computed as

$$Q = V * A \qquad \text{Eq. (4.3)}$$

where,
$Q$ is the discharge [$m^3/s$];
$V$ is the velocity [cm/s];
$A$ is the cross section area [$cm^2$].

#### 4.2.1.1 Field observations

The Malewa and Gilgil are meander rivers. The Malewa is a turbulent and well-mixed stream, characterized by sand bars, deltas, irregular bed shapes, high velocities and heterogeneous flows and discharges influenced by gradients and anthropogenic factors.

On the other hand, the Gilgil River is defined by regular shapes, small velocities and discharges compared to Malewa. Its stream color is brownish because carries more sediments than Malewa do. Gilgil River is highly influenced by human activities, its flow has been changed by requirements of water uses, such as irrigation and other water supply needs.

Because of the river's depth and strong flow at location M1 (Malewa river at 2GB1), an air pump boat assisted the sampling. The river flow was characterized by high velocities because of the terrain's steep gradient. The boat helped to conduct the experiment moving through the verticals in the stream cross section. During the test, it was hardly tried to keep the boat stable for two reasons: 1) to maintain the axis propel perpendicular and to the water flow and 2) to avoid completely interferences from the boat to the water movement. However, some measurements were small disturbed and influenced the final calculations (5.5 $m^3/s$) therefore the discharge estimation was considered underestimated at location M1 (Malewa river at 2GB1).

As it is observed, there is an increase of flow at location M2 (Diary Training School at Marula Estate), which can be attributed to the Biazi, Mahindu streams which join the Malewa River at 5 and 1.5 Km. upstream, respectively. At this location, Malewa River becomes more wide and less deep than the previous location.

The last measurement point in the Malewa River was done at 8 km before reaching the lake (location M4). At this place, the Malewa continues being wide and shallow and it was noticed that became more calm and its flow has been reduced due to the gentle gradient and perhaps for some water abstraction works from Marula Estate. It was observed looking from the top that the river had heterogeneous flows; in some parts the water remained stagnant while others the water flowed fast due to deltas placed in the stream center.

Regarding to the Gilgil graphs and tables, the eminent decrease of flow and discharge from location G1 to G2 can be caused by consumption of water, irrigation and natural losses. Gilgil reaches the lake like a small channel because its flow is diverted and utilized by human activities.

### 4.2.2 Dilution Gauging

The dilution test was carried out in the Malewa and Gilgil rivers for discharge and dispersion coefficient estimations. The integration ('gulp' or sudden injection) method explained in section 3.1.3.1 and some relations from the time-concentration curves (section 4.3.2.1) were involved in the calculations.

The sampling sites were selected according with the accessibility of the rivers and its suitability to represent that section of the river. In general, the cross sections were chosen downstream of physical

structures resulting in mixing of the water, e.g. waterfalls or river bends producing a helical mixing pattern.

The test was done in the same locations as the velocity – area test, except in the location M4 (Malewa River downstream), because in this location the stream conditions were difficult to set the measuring points walking or navigating into the river due to high velocities and holes in the river's bottom.

The conditions satisfied for calibration purposes were:

- The duration of the injection was as short as possible, so as to reduce the duration of sampling and the mass of tracer required for a given precision.
- It was necessary to calibrate the bottle of salt to have the real amount of salt dissolved in the bucket, so the next consideration was taken:

| Weight of polythene bottle | Weight of polythene bottle filled with salt | Total weight of polythene bottle filled with salt | Water volume in the bucket |
|---|---|---|---|
| 24 gr. | 369 gr. | 345 gr. | 20.5 l |

The conditions in the Gilgil allowed performing the test at 3 distances: 50, 100 and 150 m. However, in the Malewa the distances were set at 45, 75 and 100 m because the accessibility was normally not easy.

The sampling was done using a Portable sens*ion* HACH 156 multiparameter meter as sensing element immersed directly in the flow at the center of the rivers, except in the location M1 which was done from the right bank. It was observed that maximum velocities occurred in the center of the rivers but were reduced to almost zero at the bank by frictional forces exerted by the shallow bank zone and the bank itself.

Gilgil River maintained regularly small velocities and laminar flow contributing to stagnate the salt but bends in the river induce mixing by overturn. The combination of high velocities, river bends and rapids or waterfalls in the Malewa River, allowed obtaining a well mix of the salt in the water by turbulence. Both rivers are considered dilute (Gaudet, 1978), so the chemical properties of waters helped on the dilution of the salt. Thus, the mixing length was determined mainly by the flow characteristics of the rivers and water quality properties of the water.

It was possible to sample every 3 seconds during the experiment. When the EC readings started to reach the background conductivity at the end of the experiment, the readings were taken with time periods of 6, 12 and 18 seconds depending how the readings came in.

It was used a common salt as a tracer. The amount of salt in each experiment depended on the discharge and natural conductivity of the river (see Table 4.6). For example, the Malewa River required at least 3 kg of salt dissolved in a bucket of 20.5 l to obtain a good concentration – time curve (see Fig. 4.10 & 4.11) while Gilgil river needed with 1.3 kg of salt dissolved in the same volume of water to produce a good response and peak (see Fig. 4.8 & 4.9) because of its small dimension compared to Malewa.

At the time that the first attempt in the location M1 was run, the amount of salt injected was not enough to obtain a good concentration peak so it was inserted more salt up to 3 kg. Once the gauging was done for the 100 and 75 m., the last gauging at 45 m. had to be delayed because of rainfall. The missing test was carried out the day after successfully. Owning to the changes of the natural conductivity in the Malewa influenced by rainfalls, pollution, among others; the background conductivity registered during the gauging at 45 m of distance was 86 and not 82 as the day before. This difference generated the offset observed in the 45 m curve from the Fig. 4.10.

The conductivity data recorded have been converted in NaCl concentration, applying the equivalence of 1μS/cm = 0.65 mg/l of NaCl.

**Table 4.6.** Background conductivity and salt concentration applied for each location

| Location | Conductivity (μS/cm) | Temperature (°C) | Concentration of tracer in the injected solution (gr/L) |
|---|---|---|---|
| G1 | 70 | 19 | 67 |
| G2 | 70 | 19.1 | 67 |
| M1 | 82 | 17 | 146 |
| M2 | 89 | 16.5 | 146 |

#### 4.2.2.1 Discharge calculation

The discharge calculation was performed using the next formula

$$Q = M/Area\ under\ the\ time\text{-}concentration\ curve \qquad \text{Eq. (4.4)}$$

where,
$Q$ is the discharge [lit/s];
$M$ is the mass of salt injected [gr].

The integral is evaluated to determine the area under the time – concentration curve

$$\int_{t}^{T} C_2(t)dt \qquad \text{Eq. (4.5)}$$

where,
$C_2(t)$ is the concentration of added tracer at the fixed sampling point over the time interval d$t$;
$t$ is the elapsed time, taking as the origin the instant at which the injection started.

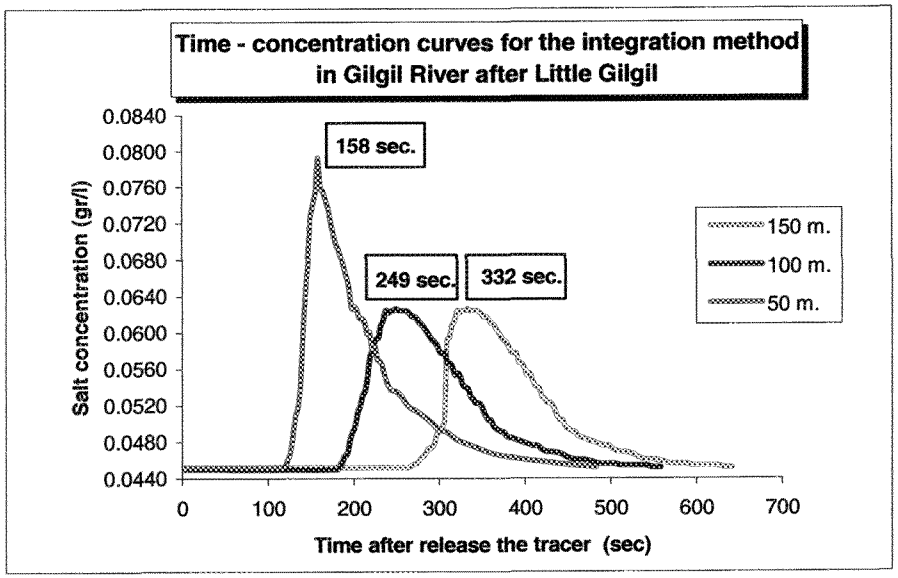


**Fig. 4.8.** Time – concentration curves (Location G1)

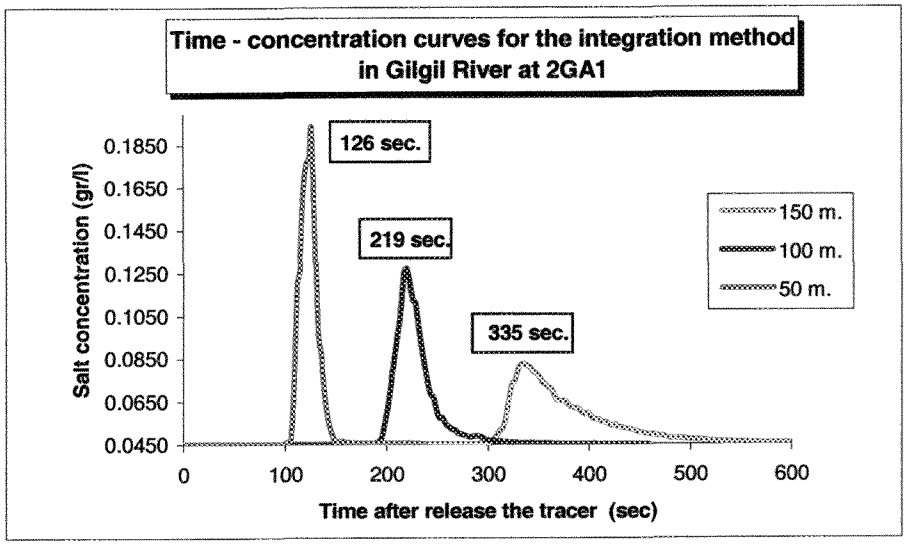


**Fig. 4.9.** Time – concentration curves (Location G2)

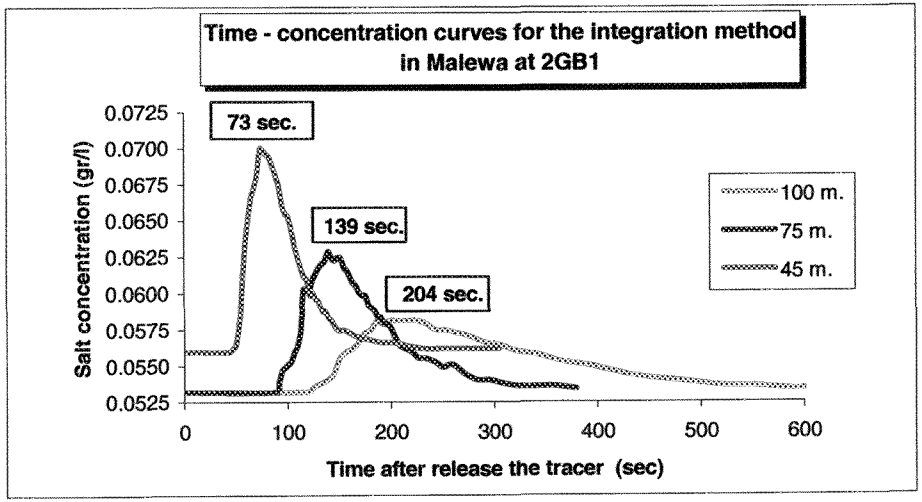


**Fig. 4.10.** Time – concentration curves (Location M1)

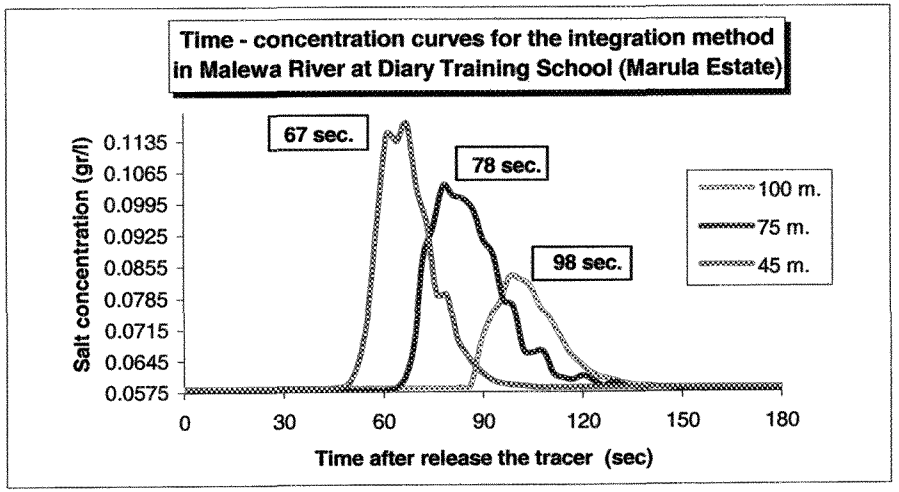


**Fig. 4.11.** Time – concentration curves (Location M2)

The discharge obtained is presented in Tables 4.7 and 4.8. As it was expected, the discharge determinations are closed each other in the different tests carried out at same location. The small variations can be attached to inaccurate conductivity readings when the readings were requested according with the time and to salt mixing problems, which are specially observed in the gauging at location M2 (Malewa River at Dairy Training School).

**Table 4.7**. Estimated discharge for Gilgil river locations

| | Locations | | | | | |
|---|---|---|---|---|---|---|
| | G1 | | | G2 | | |
| Length | 50m | 100 m | 150 m | 50 m | 100 m | 150 m |
| Discharge ($m^3/s$) | 0.513 | 0.572 | 0.685 | 0.484 | 0.489 | 0.501 |

**Table 4.8**. Estimated discharge for Malewa River locations

| | Locations | | | | | |
|---|---|---|---|---|---|---|
| | M1 | | | M2 | | |
| Length | 45 m | 75 m | 100 m | 45 m | 75 m | 100 m |
| Discharge ($m^3/s$) | 3.60 | 3.36 | 3.03 | 2.61 | 2.45 | 5.33 |

### 4.2.2.2 Dispersion coefficient

**Theoretical frame**

A river contamination transport is not caused by plug flow, but also by dispersion forces and other processes (like decay).

The mass balance equation, assuming a constant cross-sectional area and a constant river flow, and considering only one outfall input and the effects of advection, dispersion and decay, is

$$\frac{\partial C}{\partial t} = -v\frac{\partial C}{\partial x} + D\frac{\partial^2 C}{\partial x^2} - KC \qquad \text{Eq. (4.6)}$$

where,

$C(t,x)$ is the concentration of outfall [$Kg/m^3$];

$v$ is the flow velocity [m/s];

$D$ is the dispersion coefficient [$m^2/s$];

$K$ is the decay coefficient [1/t].

A mixing process along the length of the river occurs principally because of the horizontal and vertical gradients of velocity, influenced by the channel characteristics. Changes of concentration with

depth are neglected, since it is a shallow river where there is a complete mixing from side to side and from top to bottom, therefore the studied phenomenon is called longitudinal dispersion.

For this experiment it is assumed that a certain amount of salt has been instantaneously pored into the river at different locations, so the related equation to apply is:

$$C(x,t) = \frac{M}{2A\sqrt{\pi Dt}} \exp\left[\frac{-(x-vt)^2}{4Dt} - Kt\right] \qquad \text{Eq. (4.7)}$$

where,
$C(t,x)$ is the concentration of outfall [Kg/m$^3$];
$v$ is the flow velocity [m/s];
$D$ is the dispersion coefficient [m$^2$/s];
$K$ is the decay coefficient [1/t];
$A$ is the cross-section area of flow [m$^2$];
$M$ is the mass of pollutant [kg];
$t$ is the time [s].

Since NaCl, which is a very stable substance, is used as input, the decay process of the substance can be neglected ($Kt$=0).

Perhaps the Eq. 4.7 is recognized as the mathematical form of the normal probability density function with a mean = $vt$ and a variance $\sigma^2 = 4Dt$. Therefore, if $x$ is considered the independent variable and $t$ is fixed, the plot of the concentration $C$ as a function of $x$ is a symmetrical and bell-shaped around the peak concentration.

The spread of the curve is a measure of the dispersion phenomenon related with the **coefficient *D***. Note that the spread increases with time and the overall peak decays (see Fig. 4.12). Since in a normal distribution the "spread" is equivalent to the standard deviation $\sigma^2 = 4Dt$, low values of $D$ (little mixing) approach plug flow, while larger values of $D$ result in an increasing spreading due to increasing mixing.

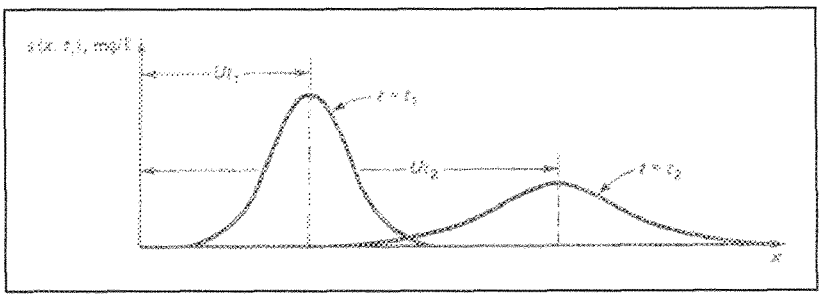

**Fig. 4.12.** Dispersive stream quality response to pulse input

When time $t$ is used as a variable while $x$ is fixed, it is observed (see Fig. 4.13) that the impulsive response is right skewed. The processes of mixing for large time periods are more significant than for short time periods, due to the kinetic of the process.

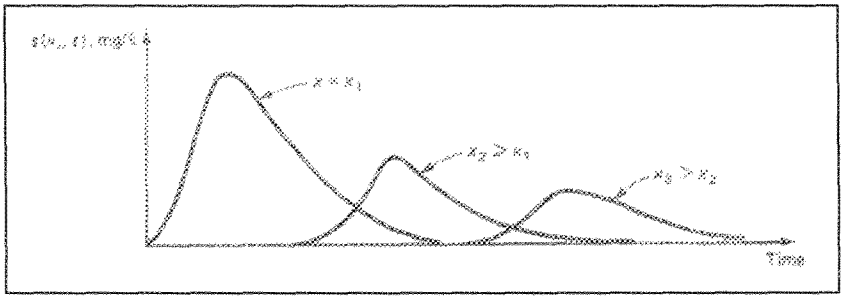

**Fig. 4.13.** Response over time at distance $x_1$ and $x_2$

To estimate a dispersion coefficient several theoretical and empirical relationships can be used. In this work the **coefficient *D*** was calculated using a simple procedure, which evaluates the peak concentration $C_{peak}$ and the related time $t_{peak}$, knowing $t=x/v$.

$$C_{peak} = \frac{M}{2A\sqrt{\pi D t_{peak}}} \qquad \text{Eq. (4.8)}$$

$C_{peak}$ is plotted versus $\frac{1}{\sqrt{t_{peak}}}$ and **coefficient *D*** is then derived from the slope.

### Dispersion coefficient calculation

As it is mention before, the conditions in the Gilgil allowed performing the test at 3 distances: 50, 100 and 150 m. However, in the Malewa the distances were set at 45, 75 and 100 m because the accessibility was normally not easy. Despite, the data obtained in each experiment show, in general, a very good correlation ($0.89<r^2>0.999$), thus the plot was used for the slope calculation (Fig. 4.14, 4.15, 4.16 & 4.17).

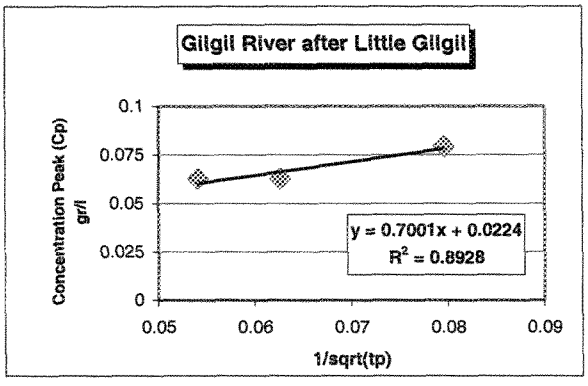


**Fig. 4.14.** Slope calculation (Location G1)

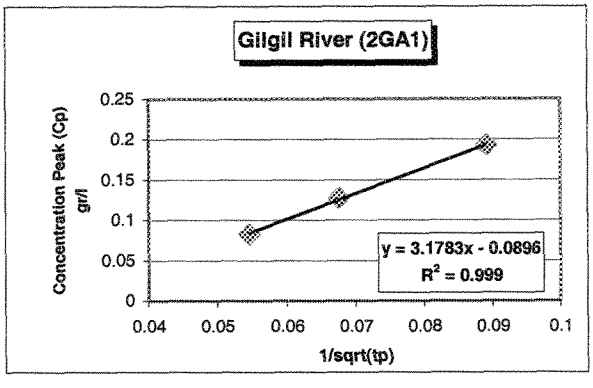


**Fig. 4.15.** Slope calculation (Location G2)

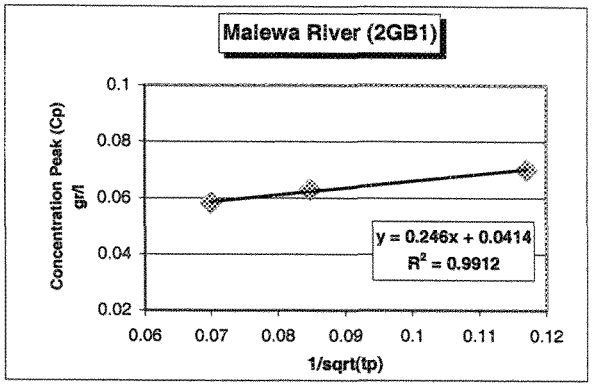


**Fig. 4.16.** Slope calculation (Location M1)

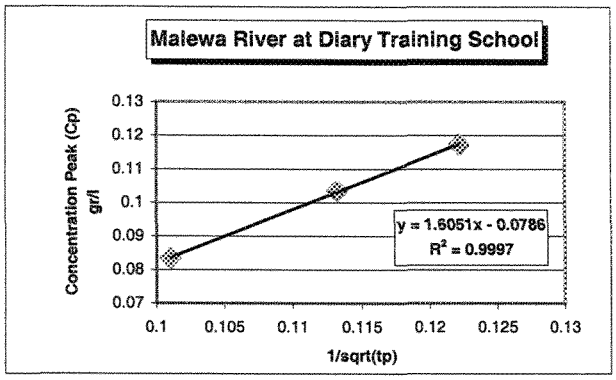


**Fig. 4.17.** Slope calculation (Location M2)

The slope is derived from the next relation

$$Slope = \frac{C_{peak}}{1\sqrt{t_{peak}}} \qquad \text{Eq. (4.9)}$$

and also is equal to

$$Slope = \frac{M}{2A\sqrt{\pi D}} \qquad \text{Eq. (4.10)}$$

then

$$D = \frac{M^2}{4A^2 \cdot \pi \cdot Slope^2} \qquad \text{Eq. (4.11)}$$

The dispersion coefficient results are presented in Tables 4.9 & 4.10. For its calculation, the area was taken from the spreadsheet computed using the 0.2 and 0.8 depth method reported in Section 3.2.1.

**Table 4.9.** Dispersion coefficient for each location in Gilgil River

| | Locations | | | | | |
|---|---|---|---|---|---|---|
| | G1 | | | G2 | | |
| Length | 50m | 100 m | 150 m | 50 m | 100 m | 150 m |
| $C_{peak}$ (gr/L) | 0.0793 | 0.062 | 0.062 | 0.192 | 0.127 | 0.082 |
| $t_{peak}$ (s) | 158 | 249 | 332 | 126 | 219 | 335 |
| Dispersion Coefficient ($m^2/s$) | 0.0804 | | | 0.0078 | | |

**Table 4.10.** Dispersion coefficient for each location in Malewa River

| | Locations | | | | | |
|---|---|---|---|---|---|---|
| | M1 | | | M2 | | |
| Length | 45 m | 75 m | 100 m | 45 m | 75 m | 100 m |
| $C_{peak}$ (gr/L) | 0.070 | 0.062 | 0.058 | 0.117 | 0.103 | 0.083 |
| $t_{peak}$ (s) | 73 | 139 | 204 | 67 | 78 | 98 |
| Dispersion Coefficient ($m^2/s$) | 0.0683 | | | 0.0025 | | |

### 4.2.3 Comparison between velocity- area and dilution gauging

In general, the estimated discharges using the velocity –area method have given reasonable values based on the field observations and have been verified by the rating curves performed by Rupashinga.

The discharge estimation, which is not so much reliable, is the one in the location M1 (Malewa River at 2GB1) because sometimes the boat interrupted the river flow during the test and this problem affected indubitably the final result.

Regarding to the dilution method, the discharges calculated are particularly small compared to the other ones. The reason is that factors such as turbulences, sand bars, among others; influence easily the salt course taking it away of the measuring point.

## 4.3 Lake Naivasha ecosystem: water quality issues

Concern has been expressed about the possible effects of the intensive horticultural activity around the lake on water quality, and the possible effects of pollution of the lake by fertilizers and chemicals. Of chemicals applied to crops 30-90% terminate in the soil, some of which drain to the lake during heavy rainfall. The lake is under threat from nutrient enrichment from urban and agricultural growth in the catchment and surrounding areas.

Untreated sewage from the Naivasha Township also finds its way into the lake, enhancing the levels of nitrates and phosphates and giving rise to eutrophication with resultant loss in transparency and to reduce oxygen levels.

Anthropogenic pressure presents a considerable threat to the lake environment. The Naivasha Township, situated on the northeastern shore of the lake, is a rapidly growing agricultural, tourist and commercial center, with a population of 50,000. Elsewhere around the lake, there has been a high influx of people due to increased job opportunities; this has resulted in an additional population of some 200,000, often living in inadequate housing and unsanitary conditions.

The tendency by some Riparian farmers to reclaim more land for cultivation as the lake recedes results in the destruction of fringing marshland and papyrus zones; this subsequently increases siltation and reduces the buffering effects of agrochemical and nutrients on surface run-off.

Reclamation of swamps for irrigated agriculture enhances utilization of lake waters. Additionally, the trend by illegal fishermen to burn fringing papyrus from fear of hiding hippos and buffaloes results in the re-release of bioaccumulated toxins into the lake in the form of ash.

Finally, the rapid expansion of the tourist industry around Naivasha mayo outstrip the provisions of infrastructural facilities such as sewage disposal and also cause disturbance to natural breeding places and the fragile lake ecosystem itself (Abiya, 1996).

## 4.4 Selection of water quality variables in relation to pollutant sources

The selection of variables was performed in relation to major sources of pollutants affecting the Lake Naivasha ecosystem and its impacts.

**Sewage and municipal wastewater**

Municipal wastewater consists of sewage effluents, urban drainage and other collected wastewater. They usually contain high levels of faecal material and organic matter. Therefore, to assess the impact of such wastewaters it is advisable to measure variables, which are indicative of organic waste such as **BOD, COD, chloride, ammonia and nitrogen compounds.**

**Urban run-off**

Rivers running through, or lakes adjacent to, large urban developments are inevitably subjected to urban run-off during periods of heavy rain. In some cities, rainwater is collected in drains and directed through the sewage collection and treatment facilities before discharge to the rivers or lakes. In the case of Naivasha town, rainwater is channeled directly into the lake. Variables associated with urban run-off are largely the same as those selected for municipal wastewater. However, water quality problems particularly associated with urban run-off are high levels of oil products and **lead** as well as a **variety of other metals and contaminants associated with local industry activities.**

**Agricultural activities**

Impacts relating to agricultural activities principally concern organic an inorganic matter and those chemicals incorporated in fertilizers and pesticides. Irrigation, especially in semi-arid and arid areas, can lead to salinisation of surface and groundwater and, therefore, inclusion of **conductivity, chloride, alkalinity, sulphate and sodium, among others**.

**Atmospheric sources**

Studies of atmospheric pollutants are also important to be included in the water quality assessment to analyze acidic depositions lead to a loss of the acid neutralizing capacity or alkalinity, which in turns decreases the pH and affects the normal chemical balance of water bodies. The variables, which can indicate atmospheric interferences, are **alkalinity, pH, sulphate and nitrate**. However, widespread atmospheric transport has been proven for lead, cadmium, arsenic, certain pesticides and other organic compounds.

## 4.5 Water quality survey

The water quality survey has been done from September 17th to October 3rd to analyze the water quality status of Lake Naivasha, Malewa and Gilgil rivers. Water quality data for the study was taken from the lake itself and from the visited locations in the rivers when the streamflow tests were conducted. There were added two locations more, one in the safest downstream part of the Gilgil that it was possible to reach and the other in the Malewa River at washing clothes bridge.

Lake Naivasha recognition and sampling were performed using an engine boat (maximum capacity = 7 persons), a Fish finder Sonar and 2 GPS's. The Fish Finder sonar was required for the bathymetric survey performed by R.A.P Rupashinga. The Fish Finder sensor was placed in the same side of the engine looking at the bottom of the lake. Once the harbour had been left, the sonar started to display continuously the depth, temperature and the lake's bottom profile. Unfortunately, the sonar did not have an option to store the readings automatically therefore the readings were noted down with the position given by GPS.

The bathymetric and water quality survey were carried out at the same time. It was an intensive work for the two parts and the task consisted on taking readings of position and depth for bathymetric purposes as well as temperature, pH, total dissolved solids (TDS), conductivity, dissolved oxygen (DO), percentage of oxygen saturated ($\%O_{sat}$) and turbidity for water quality objectives. The water samples collection was also included.

As it is mentioned above, it was required two GPS's. One GPS was loaded with the UTM coordinates from the computer using a german software called GARTRIP. And the other GPS was used for two purposes: to set the coordinates when the bathymetric and water quality readings were done and to confirm the boat position.

The boat operator used the GPS loaded with the coordinates in order to guide the boat accurately to the measuring points. The measuring points and the sail direction were planned previously writing down the sequence of coordinates for visiting and finding the best rout that the boat had to follow. The boat operator was helped by the GPS compass to navigate within the lake.

Field equipment was calibrated before the sampling survey started. The calibration followed the procedures specified in the manuals of each equipment.

The lake Naivasha survey started and finished early every day (7:00 a.m. – 14:00 p.m.) so as to complete the journeys before the storms started that make the situation risky for sailing.

Specifically, the sampling of the lake was done from September 24th to 30th. The monitoring survey of the lake was designed to measure as much possible water quality parameters on spot to observe trends and variability of the quality data over the entire lake. The water quality parameters measured on the field were: temperature, pH, total dissolved solids, conductivity, dissolved oxygen and percentage of oxygen saturated at 20 cm of depth approximately. During the first six days, 158 locations were sampled as it is shown in Fig. 4.18.

Then the last day of survey, the lake was sampled in a line transect with the purpose of collecting data of conductivity and temperature, putting a special attention in those regions where the rivers enter into the lake (North portion of the lake). 349 locations were measured in Sept. 30th (Fig. 4.19).

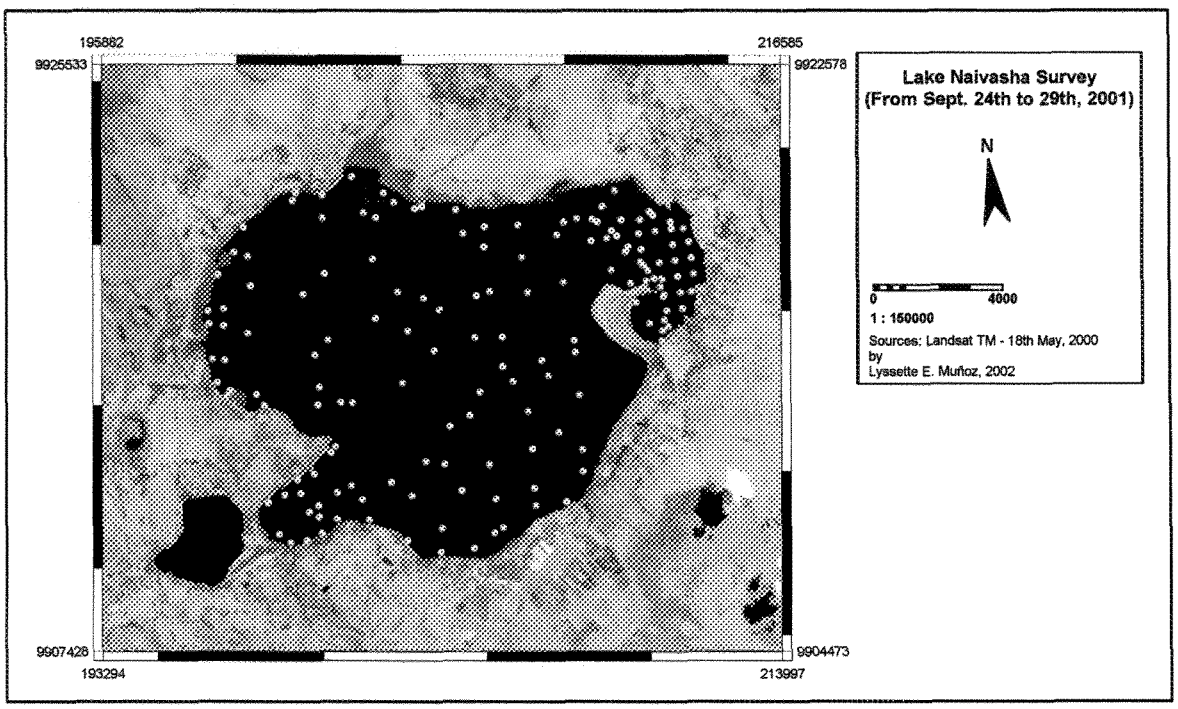


**Fig. 4.18.** First survey

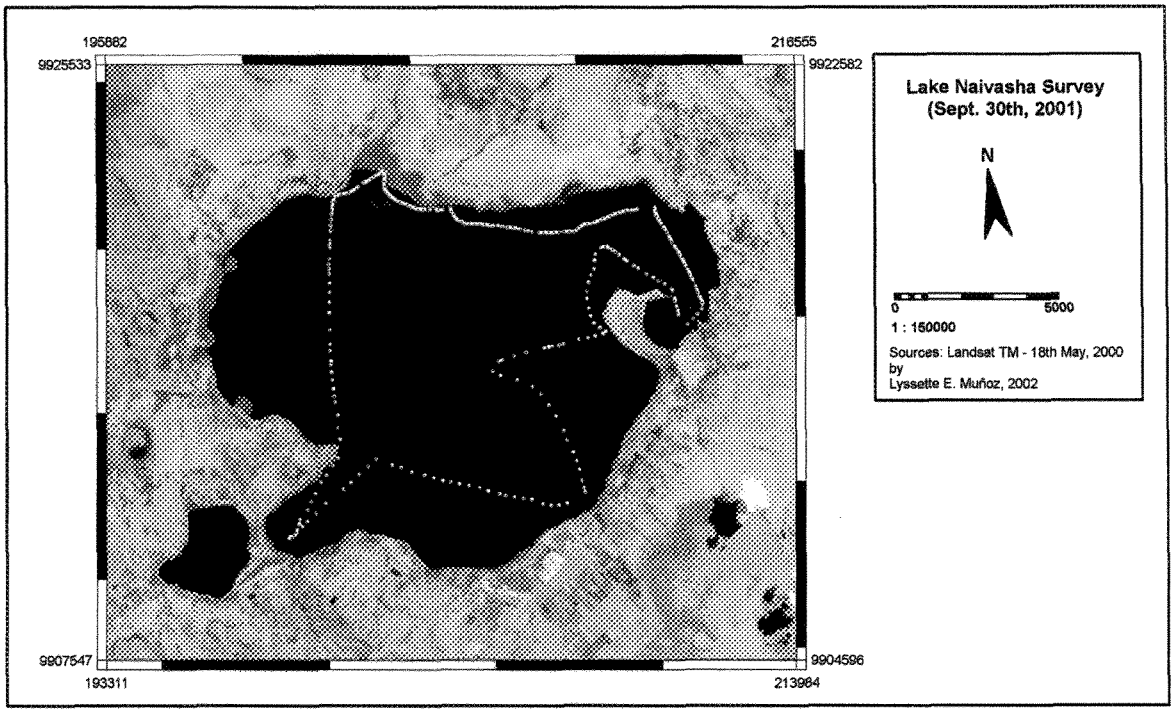


**Fig. 4.19.** Second survey

### 4.5.1 Sample collection and treatment

The samples were taken after their registration using a Global Positioning System (GPS). Every sample was assigned with a unique identification code.

All equipment in contact with water quality samples was carefully cleaned before by rinsing distilled water inside them. The water samples for analysis were filtered with filter papers of 0.45micras.

The data for this study was based on samples collected from 21 locations. Seven locations were sampled in the rivers and 14 samples were taken from the Lake Naivasha, shown in Fig. 4.20. Different sampling points are given designations as presented below, data for location M1 through M4 represent surface water samples of Malewa River, G1 through G3 represent surface water samples of Gilgil River and L1 through L14 represent surface water sample of Lake Naivasha.

The temperature, pH, total dissolved solids (TDS) and conductivity were determined *in situ* using a Portable sens*ion* HACH 156 multiparameter meter. The dissolved oxygen (DO) and the percentage of oxygen saturated ($\%O_{sat}$) were also measured *in situ* using an oximeter/WTW Oxi340. The turbidity was measured *in situ* using a turbidimeter/HACH.

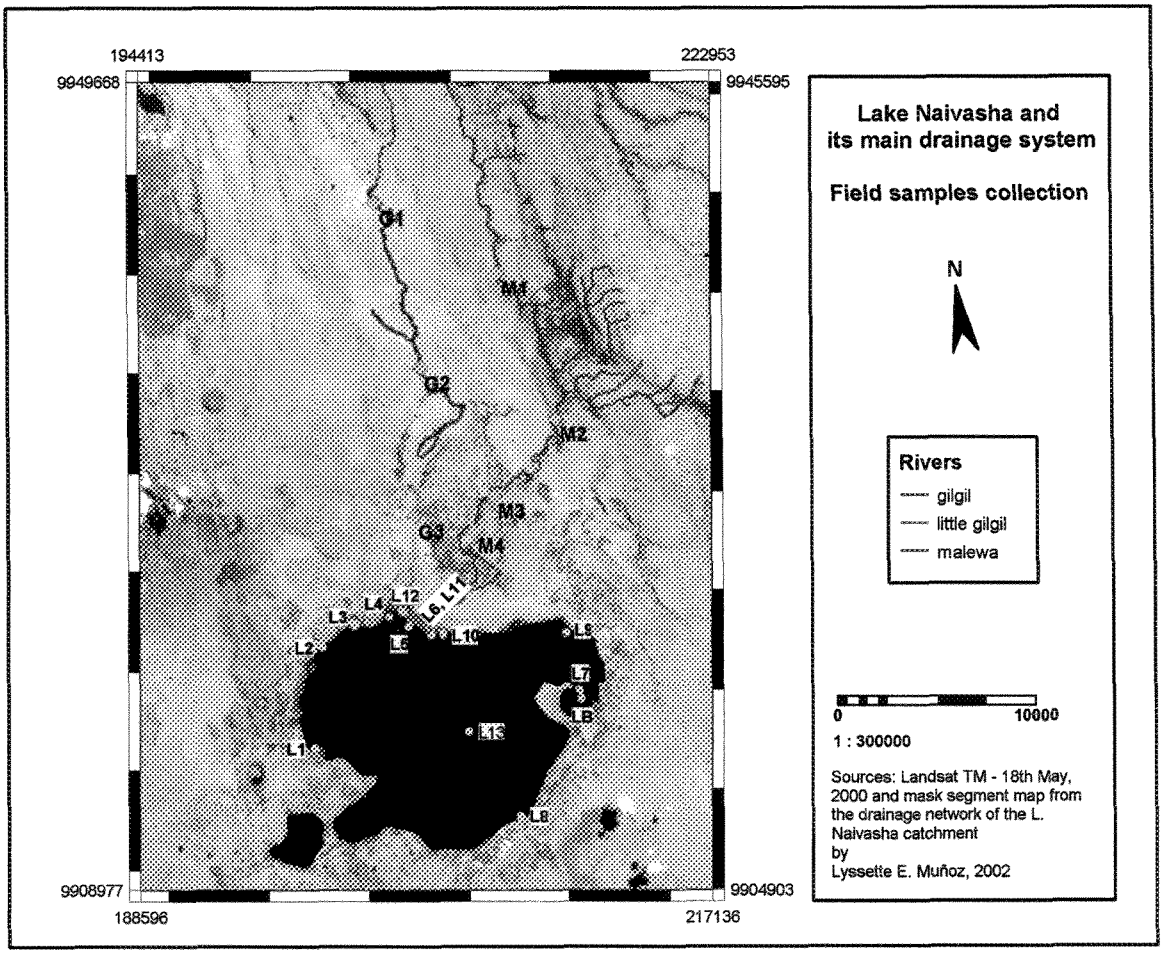


**Fig. 4.20.** Sample location map

* Same location, different days.

| S/N | Coordinates | Stream/Lake location | Code |
|---|---|---|---|
| Malewa, Gilgil Rivers | | | |
| 1 | 37M 0210953, 9937504 | Malewa at 2GB1 | M1 |
| 2 | 37M 0212775, 9929758 | Malewa at Diary Training School (Marula Estate) | M2 |
| 3 | 37M 0209114, 9926320 | Malewa at washing clothes bridge | M3 |
| 4 | 37M 0207863, 9924752 | Malewa at Britzia properties | M4 |
| 5 | 37M 0205314, 9941904 | Gilgil after Little Gilgil | G1 |
| 6 | 37M 0206379, 9933272 | Gilgil at 2GA1 (Marula Estate) | G2 |
| 7 | 37M 0204987, 9925862 | Gilgil at 5 km before the lake (Marula Estate) | G3 |
| Lake Naivasha | | | |
| 8 | 37M 0203697, 9921152 | Close to Gilgil inflow | LA |
| 9 | 37M 0198336, 9914935 | West shore | L1 |
| 10 | 37M 0199462,9919914 | North-west shore | L2 |
| 11 | 37M 0201213, 9920745 | North shore | L3 |
| 12 | 37M 0202993, 9920999 | North shore close to Gilgil inflow | L4 |
| 13 | 37M 0203877, 9920359 | North shore (between Malewa and Gilgil inflows) | L5 |
| 14 | 37M 0204981, 9919777 | Malewa inflow (II) | L6* |
| 15 | 37M 0211960, 9915940 | Crescent Island | L7 |
| 16 | 37M 0208075, 9910030 | Channel farm discharges | L8 |
| 17 | 37M 0211727, 9918911 | Sewage inlet | L9 |
| 18 | 37M 0205578, 9919694 | Malewa inflow (I) | L10 |
| 19 | 37M 0204957, 9919782 | Malewa inflow (II) | L11* |
| 20 | 37M 0203734, 9921135 | Gilgil inflow | L12 |
| 21 | 37M 0209680, 9917527 | Center of lake | L13 |

The Malewa and Gilgil rivers and Lake Naivasha samples were then collected and stored in 250 ml polythene bottles. All the samples were collected filling a bucket at once (grab method), rinsing the container with the sample stream water and finally filling the bottle with the sample avoiding turbulence and air bubbles. Four sets of samples were obtained at each location. One of the samples was acidified later with nitric acid for chloride ($Cl^-$), sulfate ($SO_4^{2-}$), TDS and major cations ($Na^+$, $Ca^{2+}$, $Mg^{2+}$, $K^+$) determinations. Another sample was acidified with sulphuric acid to analyse nitrate ($NO_3^-$), ammonia ($NH_4^+$), phosphate ($PO_4^{3-}$) and chemical oxygen demand (COD). Another sample stayed without any treatment for suspended solids determinations. This three-set of samples were storage in the refrigerator during fieldwork to preserve them for the further analysis in the ITC laboratory. The fourth sample was used to carry out all the analyses at Sulmac laboratory in Naivasha, Kenya, except for the phosphate, sulfate and major cations.

The reminder analysis (phosphate, sulfate and major cations determinations) was done in the ITC laboratory one month after the arrival from Kenya due to a delay in Naivasha for sending the missing samples and field equipment. For this reason, it was not possible anymore to do a cross check with results obtained in Sulmac laboratory therefore the analysis was concentrated only in the water quality parameters that could not be obtained during fieldwork.

The field measurements and laboratory analysis are presented in Tables 4.11 & 4.12.

**Table 4.11.** Lake Naivasha: field and laboratory results

| Parameters/Sample locations | Units | LA | LB | L1 | L2 | L3 | L4 | L5 | L6 |
|---|---|---|---|---|---|---|---|---|---|
| Coordinates (x,y) | m | 203697, 9921152 | 211996, 9915496 | 198336, 9914935 | 199462, 9919914 | 201213, 9920745 | 202993, 9920999 | 203877, 9920359 | 204981, 9919777 |
| (1) Temperature | °C | 25.0 | 20.6 | 23.9 | 26.6 | 24.1 | 25.2 | 21.4 | 21.0 |
| (1) pH | | 8.1 | 9.0 | 8.7 | 8.8 | 8.1 | 8.6 | 9.0 | 9.0 |
| (1) Conductivity | µS | 247.05 | 402.21 | 326.84 | 324.19 | 321.86 | 285.01 | 310.24 | 287.67 |
| (1)TDS | mg/L | 131.4 | 192.8 | 156.7 | 155.4 | 154.3 | 136.6 | 148.7 | 137.9 |
| (1) Turbidity | NTU | - | - | - | - | 27.7 | 36.2 | 42.8 | 50.8 |
| (1) Dissolved oxygen | mg/L | - | - | 6.70 | 6.49 | 4.35 | 6.27 | 5.82 | 6.40 |
| (1) Oxygen saturated | % | - | - | 95.0 | 100.0 | 68.0 | 95.0 | 80.0 | 88.0 |
| (2) COD | mg/L | 70 | 66 | 54 | 59 | 64 | 48 | 61 | 60 |
| (3) $K^+$ | mg/L | 15.83 | - | 16.90 | 17.37 | 16.96 | 15.56 | 16.09 | 15.40 |
| (3) $Na^+$ | mg/L | 27.06 | - | 27.43 | 27.80 | 27.35 | 25.49 | 26.44 | 25.84 |
| (3) $Ca^{2+}$ | mg/L | 13.79 | - | 14.29 | 20.10 | 14.94 | 13.76 | 14.07 | 14.54 |
| (3) $Mg^{2+}$ | mg/L | 6.08 | - | 6.57 | 6.80 | 6.71 | 6.08 | 6.56 | 6.12 |
| (3) $Al^{3+}$ | mg/L | 1.27 | - | 0.78 | 0.96 | 0.89 | 1.10 | 1.13 | 1.10 |
| (3) $Fe^{3+}$ | mg/L | 1.44 | - | 1.30 | 1.00 | 0.81 | 1.06 | 0.95 | 0.93 |
| (3) $Mn^{2+}$ | mg/L | 0.29 | - | 0.34 | 0.31 | 0.37 | 0.46 | 0.37 | 0.33 |
| (3) $Li^+$ | mg/L | < 0.05 | - | < 0.05 | < 0.05 | < 0.05 | < 0.05 | < 0.05 | < 0.05 |
| (2) $Cl^-$ | mg/L | 13.3 | 15.6 | 15.8 | 14.0 | 14.6 | 16.0 | 13.0 | 13.0 |
| (2) $NH_4^+$ | mg/L | 4.0 | 1.2 | < LOD | 5.3 | 2.1 | < LOD | 1.4 | 0.5 |
| (2) $NO_3^-$ | mg/L | 0.6 | 0.5 | 0.8 | 0.4 | 0.6 | 0.6 | 0.8 | 0.7 |
| (3) $SO_4^{2-}$ | mg/L | 1 | - | 1 | 1 | 1 | 1 | 1 | 1 |
| (3) $PO_4^{3-}$ | mg/L | 0.28 | - | 0.18 | 0.19 | 0.26 | 0.34 | 0.22 | 0.73 |
| (2) Total alkalinity | mg/L | 152.55 | 219.67 | 176.96 | 183.06 | 167.81 | 176.96 | 176.96 | 170.86 |
| (2) Total hardness as $CaCO_3$ | mg/L | 60.5 | 90.08 | 70.06 | 75.07 | 75.07 | 70.06 | 78.07 | 70.06 |

**Table 4.11.** Continued

| Parameters/Sample locations | Units | L7 | L8 | L9 | L10 | L11 | L12 | L13 |
|---|---|---|---|---|---|---|---|---|
| Coordinates (x,y) | m | 211960, 9915940 | 208075, 9910030 | 211727, 9918911 | 205578, 9919694 | 204957, 9919782 | 203734, 9921135 | 206146, 9914633 |
| [1] Temperature | °C | 21.2 | 21.6 | 18.1 | 17.2 | 17.0 | 19.1 | 21.1 |
| [1] pH | | 9.1 | 8.7 | 9.1 | 9.1 | - | 9.0 | 8.3 |
| [1] Conductivity | µS | 401.87 | 337.47 | 399.00 | 92.00 | 92.00 | 213.00 | 332.00 |
| [1]TDS | mg/L | 192.7 | 161.8 | 191.3 | 44.1 | 44.1 | 102.1 | 159.1 |
| [1] Turbidity | NTU | 3.81 | 18.7 | - | - | - | - | - |
| [1] Dissolved oxygen | mg/L | 7.07 | 4.13 | 7.40 | 7.05 | - | 6.0 | 6.03 |
| [1] Oxygen saturated | % | 98.4 | 60.0 | 108.6 | 101.3 | - | 83.0 | 81.9- |
| [2] COD | mg/L | 55 | 66 | 66 | 19 | 12 | 59 | 65 |
| [3] $K^+$ | mg/L | 21.65 | 20.49 | 22.13 | 3.95 | 4.06 | 11.31 | 17.41 |
| [3] $Na^+$ | mg/L | 32.02 | 32.83 | 32.02 | 8.22 | 8.51 | 21.76 | 27.82 |
| [3] $Ca^{2+}$ | mg/L | 15.08 | 16.97 | 15.81 | 11.27 | 6.53 | 10.55 | 14.29 |
| [3] $Mg^{2+}$ | mg/L | 8.51 | 8.17 | 8.86 | 2.31 | 2.31 | 4.40 | 6.70 |
| [3] $Al^{3+}$ | mg/L | 0.25 | 0.53 | 1.57 | 1.33 | 1.35 | 1.53 | 0.58 |
| [3] $Fe^{3+}$ | mg/L | 0.19 | 0.74 | 1.13 | 1.93 | 1.80 | 1.85 | 0.83 |
| [3] $Mn^{2+}$ | mg/L | 0.07 | 0.45 | 0.43 | 0.35 | 0.32 | 1.23 | 0.35 |
| [3] $Li^+$ | mg/L | < 0.05 | < 0.05 | < 0.05 | < 0.05 | < 0.05 | < 0.05 | < 0.05 |
| [2] $Cl^-$ | mg/L | 15.3 | 15.2 | 19.6 | 8.3 | 7.2 | 12.8 | 20.7 |
| [2] $NH_4^+$ | mg/L | <LOD | 1.1 | 1.3 | 0.9 | 0.4 | 0.9 | 3.2 |
| [2] $NO_3^-$ | mg/L | 0.9 | 0.5 | 0.4 | 1.1 | 1 | 0.7 | 0.8 |
| [3] $SO_4^{2-}$ | mg/L | 1 | 2 | < LOD | 1 | 1 | < LOD | < LOD |
| [3] $PO_4^{3-}$ | mg/L | 0.09 | 0.16 | 0.26 | 0.59 | 0.58 | 0.44 | 0.50 |
| [2] Total alkalinity | mg/L | 234.93 | 200.15 | 231.88 | 67.12 | 48.82 | 103.73 | 259.34 |
| [2] Total hardness as $CaCO_3$ | mg/L | 79.07 | 75.07 | 85.08 | 28.03 | 29.03 | 42.04 | 80.07 |

[1] Field measurements
[2] Sulmac laboratory analysis
[3] ITC laboratory analysis

LOD Limit of detection
NTU Nephelometric turbidity units
COD Chemical oxygen demand

**Table 4.12.** Malewa and Gilgil rivers: field and laboratory results

| Parameters/Sample locations | Units | M1 | M2 | M3 | M4 | G1 | G2 | G3 |
|---|---|---|---|---|---|---|---|---|
| Coordinates (x,y) | m | 210953, 9937504 | 212775, 9929758 | 209114, 9926320 | 207863, 9924752 | 205314, 9941904 | 206379, 9933272 | 204987, 9925862 |
| (1) Temperature | °C | 16.1 | 17.4 | 17.8 | 17.0 | 18.9 | 17.5 | 17.7 |
| (1) pH | | 7.5 | 7.6 | 8.0 | 7.6 | 7.7 | 7.4 | - |
| (1) Conductivity | µS | 71.0 | 80.7 | 81.0 | 80.0 | 88.0 | 92.1 | 91.0 |
| (1)TDS | mg/L | 34.0 | 38.7 | 38.8 | 38.4 | 42.2 | 44.2 | - |
| (1) Turbidity | NTU | 197.0 | 131.0 | 191.0 | 215.0 | 60.0 | 78.2 | 107.0 |
| (1) Dissolved oxygen | mg/L | 7.90 | 7.34 | 6.57 | 7.23 | - | 7.35 | - |
| (1) Oxygen saturated | % | 99 | 88 | 85 | 94 | - | 93 | - |
| (2) COD | mg/L | 36 | 53 | 53 | 49 | 24 | 31 | 35 |
| (3) $K^+$ | mg/L | 3.69 | 3.94 | 3.34 | 3.36 | 4.65 | 4.70 | 5.25 |
| (3) $Na^+$ | mg/L | 6.29 | 7.75 | 6.68 | 6.66 | 11.47 | 11.13 | 12.07 |
| (3) $Ca^{2+}$ | mg/L | 5.22 | 5.80 | 6.03 | 6.05 | 4.04 | 5.39 | 4.44 |
| (3) $Mg^{2+}$ | mg/L | 1.92 | 2.04 | 2.18 | 2.20 | 1.18 | 1.17 | 1.23 |
| (3) $Al^{3+}$ | mg/L | 1.39 | 1.75 | 1.54 | 1.56 | 0.84 | 0.97 | 1.15 |
| (3) $Fe^{3+}$ | mg/L | 1.92 | 2.32 | 1.97 | 1.93 | 1.71 | 2.16 | 1.68 |
| (3) $Mn^{2+}$ | mg/L | 0.5 | 0.43 | 0.38 | 0.38 | 0.31 | 0.24 | 0.21 |
| (3) $Li^+$ | mg/L | < 0.05 | < 0.05 | < 0.05 | < 0.05 | < 0.05 | < 0.05 | < 0.05 |
| (2) $Cl^-$ | mg/L | 21.2 | 12.9 | 14.6 | 17.5 | 7.5 | 2.2 | 6.3 |
| (2) $NH_4^+$ | mg/L | 1 | 6.1 | 1.1 | 1 | 0.9 | 0.4 | 0.7 |
| (2) $NO_3^-$ | mg/L | 1.0 | 0.7 | 1.0 | 1.1 | 0.7 | 0.9 | 0.8 |
| (3) $SO_4^{2-}$ | mg/L | 1 | < LOD | 2 | 2 | < LOD | 2 | 2 |
| (3) $PO_4^{3-}$ | mg/L | 0.27 | 0.40 | 0.41 | 0.28 | 0.49 | 0.60 | 0.76 |
| (2) Total alkalinity | mg/L | 54.92 | 54.92 | 61.02 | 42.71 | 61.02 | 54.92 | 91.53 |
| (2) Total hardness as $CaCO_3$ | mg/L | 30.03 | 25.02 | 28.03 | 28.03 | 22.02 | 250.23 | 220.20 |

(1) Field measurements
(2) Sulmac laboratory analysis
(3) ITC laboratory analysis

LOD Limit of detection
NTU Nephelometric turbidity units
COD Chemical oxygen demand

During the laboratory works, the different chemical tests were checked through standards and through some consecutive measurements with the same samples in order to check precision, accuracy and relative error. The errors obtained for the different analysis were all in the range of ±5-10% so the concentrations measured are quite reliable. The testing measurements, the calibration curves and the information about the range of detection of each chemical test are presented in the appendix A.

A Portable case Datalogging Spectrophotometer HACH DR/2010 measured the content of sulfate ($SO_4^{2-}$) by the sulfaVer 4 method, the phosphate ($PO_4^{3-}$) by phosVer method with the test 'N tube procedure, the nitrate ($NO_3$), high range (HR) with the chromotropic acid method, the chemical oxygen demand (COD) by reactor digestion method and colorimetric determination, the chloride ($Cl^-$) by mercuric thiocyanate method and the nitrogen-ammonia ($NH_4^+$), high range (HR) with the Test 'N Tube procedure.

Alkalinity ($HCO_3^-$) was analysed using the Aquamerck 11109 based on acidimetric titration against phenolphthalein or mixed indicator method and total hardness ($CaCO_3$) was obtained from Aquamerck 8039 based on complexometric titration against Tritriplex III method with mixed incidator.

Major cations ($Na^+$, $Ca^{2+}$, $Mg^{2+}$, $K^+$) and metals ($Al^{2+}$, $Fe^{3+}$, $Mn^{2+}$, $Li^+$) were analysed by inductivity coupled plasma – atomic spectroscopy emission (ICP-ASE).

The detailed description of the chemical analysis is explained in the section 3.4.

### 4.5.2 Data analysis and interpretation

Univariate statistics were carried out for the lake Naivasha and Malewa and Gilgil parameters presented in Tables 4.13 & 4.14 to summarize the most important features of the experimental distribution of the data.

In this case, the Malewa and Gilgil values were analysed together for two reasons: the two databases separately are described for a very small number of observations and because the water quality information in both rivers are alike.

**Organoleptic parameter**

The mean temperature in the lake and its main inflows is 20.8° C and 18.9° C respectively, which is a normal temperature for surface water.

In general, the temperature is influenced by latitude, altitude, season, time of day, air circulation, cloud cover and the flow and depth of the body (Chapman, 1996).

The temperature in these water bodies was highly variable with the daytime, but unfortunately was not registered during the sampling regime.

**Table 4.13.** Lake Naivasha: summary of univariate statistics

| Parameters/Univariate statistics | Units | No. of observations | Maximum | Minimum | Mean | Median | Standard deviation | 1st quartile | 3rd quartile | 1st percentile | Ninetieth percentile | Skew coefficient |
|---|---|---|---|---|---|---|---|---|---|---|---|---|
| Temperature | °C | 507 | 26.80 | 17.00 | 20.80 | 20.80 | 1.80 | 19.50 | 21.60 | 18.70 | 22.84 | 0.76 |
| pH | | 158 | 9.30 | 8.20 | 8.85 | 8.80 | 0.24 | 8.70 | 9.10 | 8.60 | 9.10 | -0.22 |
| Conductivity | µS | 507 | 402.87 | 92.00 | 330.33 | 334.00 | 58.32 | 324.76 | 380.65 | 247.00 | 391.00 | -1.75 |
| TDS | mg/L | 158 | 193.14 | 116.90 | 166.45 | 161.22 | 14.86 | 157.80 | 183.83 | 155.10 | 187.61 | 0.07 |
| Turbidity | NTU | 100 | 72.70 | 3.28 | 19.96 | 14.55 | 14.22 | 11.98 | 23.05 | 10.97 | 39.15 | 1.80 |
| Dissolved oxygen | mg/L | 153 | 7.93 | 4.01 | 6.34 | 6.33 | 0.70 | 5.87 | 6.77 | 5.60 | 7.27 | -0.42 |
| Oxygen saturated | % | 153 | 115.00 | 58.40 | 91.21 | 90.30 | 10.76 | 83.10 | 99.70 | 80.12 | 106.64 | -0.20 |
| COD | mg/L | 15 | 70.00 | 12.00 | 54.93 | 60.00 | 16.45 | 54.50 | 65.50 | 30.60 | 66.00 | -1.94 |
| $K^+$ | mg/L | 14 | 22.13 | 3.95 | 15.37 | 16.50 | 5.35 | 15.44 | 17.40 | 6.24 | 21.30 | -1.20 |
| $Na^+$ | mg/L | 14 | 32.83 | 8.22 | 25.04 | 27.02 | 7.36 | 25.58 | 27.82 | 12.49 | 32.02 | -1.63 |
| $Ca^{2+}$ | mg/L | 14 | 20.10 | 6.53 | 14.00 | 14.29 | 3.01 | 13.77 | 15.04 | 10.77 | 16.62 | -0.63 |
| $Mg^{2+}$ | mg/L | 14 | 8.86 | 2.31 | 6.16 | 6.57 | 1.91 | 6.08 | 6.78 | 2.94 | 8.41 | -0.90 |
| $Al^{3+}$ | mg/L | 14 | 1.57 | 0.25 | 1.03 | 1.10 | 0.38 | 0.80 | 1.32 | 0.54 | 1.48 | -0.50 |
| $Fe^{3+}$ | mg/L | 14 | 1.93 | 0.19 | 1.14 | 1.03 | 0.47 | 0.86 | 1.40 | 0.76 | 1.84 | 0.14 |
| $Mn^{2+}$ | mg/L | 14 | 0.46 | 0.07 | 0.33 | 0.34 | 0.09 | 0.31 | 0.37 | 0.25 | 0.44 | -1.38 |
| $Li^+$ | mg/L | 14 | < 0.05 | < 0.05 | < 0.05 | < 0.05 | < 0.05 | < 0.05 | < 0.05 | < 0.05 | < 0.05 | - |
| $Cl^-$ | mg/L | 15 | 20.70 | 7.20 | 14.29 | 14.60 | 3.38 | 13.00 | 15.70 | 10.10 | 18.16 | -0.30 |
| $NH_4^+$ | mg/L | 15 | 5.30 | 0.00 | 1.49 | 1.10 | 1.50 | 0.45 | 1.75 | 0.00 | 3.68 | 1.40 |
| $NO_3^-$ | mg/L | 15 | 1.10 | 0.50 | 0.79 | 0.80 | 0.17 | 0.65 | 0.90 | 0.62 | 1.01 | 0.19 |
| $SO_4^{2-}$ | mg/L | 14 | 2.00 | 0.00 | 0.86 | 1.00 | 0.52 | 1.00 | 1.00 | 0.00 | 1.00 | -0.22 |
| $PO_4^{3-}$ | mg/L | 14 | 0.73 | 0.09 | 0.34 | 0.27 | 0.19 | 0.02 | 0.49 | 0.17 | 0.59 | 0.70 |
| Total alkalinity | mg/L | 15 | 259.34 | 48.82 | 171.38 | 176.96 | 57.54 | 160.18 | 209.91 | 81.77 | 233.71 | -0.78 |
| Total hardness as $CaCO_3$ | mg/L | 15 | 90.08 | 28.03 | 67.13 | 75.07 | 18.54 | 65.06 | 78.57 | 34.23 | 83.07 | -1.24 |

**Table 4.14.** Malewa and Gilgil rivers: summary of univariate statistics

| Parameters/Univariate statistics | | No. of observations | Maximum | Minimum | Mean | Median | Standard deviation | 1st quartile | 3rd quartile | 1st percentile | Ninetieth percentile | Skew coefficient |
|---|---|---|---|---|---|---|---|---|---|---|---|---|
| Temperature | °C | 7 | 18.90 | 16.10 | 17.49 | 17.50 | 0.78 | 17.20 | 17.75 | 16.64 | 18.24 | 0.04 |
| pH | | 6 | 8.00 | 7.40 | 7.63 | 7.60 | 0.19 | 7.53 | 7.68 | 7.45 | 7.85 | 1.17 |
| Conductivity | µS | 7 | 92.10 | 71.00 | 83.40 | 81.00 | 6.90 | 80.35 | 89.50 | 76.40 | 91.44 | -0.44 |
| TDS | mg/L | 7 | 44.15 | 34.04 | 39.98 | 38.83 | 3.31 | 38.52 | 42.91 | 36.63 | 43.84 | -0.44 |
| Turbidity | NTU | 7 | 215.00 | 60.00 | 139.89 | 131.00 | 57.15 | 92.60 | 194.00 | 70.92 | 204.20 | -0.04 |
| Dissolved oxygen | mg/L | 5 | 7.90 | 6.57 | 7.28 | 7.34 | 0.42 | 7.23 | 7.35 | 6.83 | 7.68 | -0.44 |
| Oxygen saturated | % | 5 | 99.00 | 85.00 | 91.80 | 93.00 | 4.87 | 88.00 | 94.00 | 86.20 | 97.00 | 0.04 |
| COD | mg/L | 7 | 53.00 | 24.00 | 40.14 | 36.00 | 10.67 | 33.00 | 51.00 | 28.20 | 53.00 | -0.04 |
| $K^+$ | mg/L | 7 | 5.25 | 3.34 | 4.13 | 3.94 | 0.69 | 3.52 | 4.67 | 3.35 | 4.92 | 0.39 |
| $Na^+$ | mg/L | 7 | 12.07 | 6.29 | 8.86 | 7.75 | 2.38 | 6.67 | 11.30 | 6.51 | 11.71 | 0.31 |
| $Ca^{2+}$ | mg/L | 7 | 6.05 | 4.04 | 5.28 | 5.39 | 0.73 | 4.83 | 5.92 | 4.28 | 6.04 | -0.72 |
| $Mg^{2+}$ | mg/L | 7 | 2.20 | 1.17 | 1.71 | 1.92 | 0.45 | 1.21 | 2.11 | 1.18 | 2.19 | -0.25 |
| $Al^{3+}$ | mg/L | 7 | 1.75 | 0.84 | 1.31 | 1.39 | 0.31 | 1.06 | 1.55 | 0.92 | 1.63 | -0.24 |
| $Fe^{3+}$ | mg/L | 7 | 2.32 | 1.68 | 1.96 | 1.93 | 0.21 | 1.81 | 2.07 | 1.70 | 2.23 | 0.43 |
| $Mn^{2+}$ | mg/L | 7 | 0.43 | 0.21 | 0.33 | 0.33 | 0.07 | 0.28 | 0.38 | 0.23 | 0.40 | -0.38 |
| $Li^+$ | mg/L | 7 | < 0.05 | < 0.05 | < 0.05 | < 0.05 | < 0.05 | < 0.05 | < 0.05 | < 0.05 | < 0.05 | - |
| $Cl^-$ | mg/L | 7 | 21.20 | 2.20 | 11.74 | 12.90 | 6.22 | 6.90 | 16.05 | 4.66 | 18.98 | -0.03 |
| $NH_4^+$ | mg/L | 7 | 5.30 | 0.00 | 2.00 | 1.40 | 1.85 | 0.60 | 3.05 | 0.00 | 4.52 | 0.80 |
| $NO_3^-$ | mg/L | 7 | 1.10 | 0.80 | 0.94 | 0.90 | 0.12 | 0.83 | 1.05 | 0.80 | 1.07 | 0.19 |
| $SO_4^{2-}$ | mg/L | 7 | 2.00 | 0.00 | 1.29 | 2.00 | 0.88 | 0.50 | 2.00 | 0.00 | 2.00 | -0.76 |
| $PO_4^{3-}$ | mg/L | 7 | 0.76 | 0.27 | 0.46 | 0.41 | 0.16 | 0.34 | 0.55 | 0.28 | 0.66 | 0.76 |
| Total alkalinity | mg/L | 7 | 91.53 | 42.71 | 60.15 | 54.92 | 14.00 | 54.92 | 61.02 | 50.04 | 73.22 | 1.70 |
| Total hardness as $CaCO_3$ | mg/L | 7 | 250.23 | 22.02 | 86.26 | 28.03 | 94.58 | 26.53 | 125.25 | 23.82 | 232.21 | 1.26 |

It was observed that the temperature affects physical, chemical and biological processes. At water temperature increased in the lake, the pH increased and the dissolved oxygen (DO) decreases because the respiration rates increases leading to increase oxygen consumption and increased decomposition of organic matter.

**Physio-chemical parameter**

The pH of the lake and rivers indicate that waters are alkaline (ph>7). The pH of most natural waters is between 6.0 and 8.5 because pH is principally controlled by the balance between the carbon dioxide, carbonate and bicarbonate ions (Chapman, 1996).

The higher pH values in the lake were reported in the Crescent Island. This water body lies in a volcanic crater in part bounded by an exposed rim (Gaudet et al. 1981), and it is chemically distinct to the main lake, as it will be explained further in Chapter 5.

**Biological parameter**

Based on the measurements, it was observed that the maximal dissolved oxygen concentrations occurred near the surface and were mostly saturated. Lake Naivasha reported concentrations of 4.0 – 7.93 mg/l (58.4 – 115%) while Malewa and Gilgil rivers registered 6.5 – 7.9 mg/l (85 – 99%).

The mean DO value in the rivers (7.28 mg/l) are higher than the lake (6.34 mg/l) because the nature ecosystem of the rivers maintain the water moving; turbulence and waterfalls are examples of reaeration processes which take place supplying oxygen in the water. Some other factors such as photosynthesis or sediment oxygen demand, among others, determines de DO level in the water.

**Conductivity and solutes**

The conductivity is sensitive to variations in dissolved solids, mostly mineral salts. The electrical conductivity in the lake varied from the north part, near by Malewa's inflow (92 µS/cm) to the centre (330 µS/cm). The highest values were registered on Crescent Island (402 µS/cm). Regarding to the rivers, the mean conductivity value determined in the Malewa is 78.1 µS/cm. while Gilgil is 90.3 µS/cm.

In general, the lake Naivasha and its main inflows are freshwater (<1,000µS/cm). Gaudet, 1978 explained that several factors combined keep lake Naivasha's water fresh; one of them is that a large fraction of the water supplied to the lake comes from dilute rivers, which drain predominantly trachytes and tuffs, and rain.

When compared to Meybeck's (1977) typology of transport by the major rivers of the world, the total dissolved load carried by the Malewa River is similar to the loads carried by rivers with low runoff, medium relief and warm temperatures.

**Major ions**

Major ions ($Ca^{2+}$, $Mg^{2+}$, $Na^{+}$, $K^{+}$, $Cl^{-}$, $SO_4^{2-}$, $HCO_3^{-}$) are naturally very variable in surface due to local geological, climatic and geographical conditions.

The Malewa and Gilgil rivers are dilute and contain a predominance of bicarbonate. In general, the bicarbonate concentrations presented high variability; from 42.7 to 91.53 mg/l. In particular Gilgil River reported higher concentrations than Malewa. The sources of bicarbonate are attributed to atmospheric inputs in combination with weathering reactions (Gaudet et al, 1981).

In the Lake Naivasha, sodium and bicarbonate were predominant as is typical in many fresh waters in Africa (Kilham, 1971; Talling and Talling, 1965). The bicarbonate and sodium concentrations in the lake present much more variability than the rivers; from 48.8 to 259.3 mg/l and from 8.2mg/l to 32.8 mg/l respectively.

In the Malewa sodium and calcium are the major cations, while in the Gilgil sodium is the major cation, as it is observed from the chemical reports (Tables 4.13 and 4.14). The sodium and most calcium are probably derived from materials in the basin because the Malewa is a river which drains predominantly trachytes, tuffs and welded tuffs and its headwaters begin in the strongly alkaline lavas and olivine basalts that form the Aberdare and Kipipiri ranges (Gaudet et al, 1981).

The salts of calcium, together with those of magnesium, are responsible for the hardness of water. As can be observed from the univariate tables, the hardness is highly variable and the mean concentration is 65 mg/l in the streams and lake. The highest amounts were found in Gilgil River and Lake Naivasha (259 mg$CaCO_3$/l).

Potassium concentrations in the lake and rivers (3.9 >$K^+$> 22.1) are not low since the concentrations in natural waters are usually less than 10 mg/l (Chapman, 1996). Potassium salts are widely used in industry and in fertilisers for agriculture and enter freshwaters with industrial discharges and run-off from agricultural land. Gaudet and Melack (1981) carried out some chemical analyses of two surface runoff samples and of water collected in seepage meters, finding that the surface runoff contained considerably higher proportions of potassium, calcium and magnesium than the seepage, river or lake water; so it is quite possible that the surface runoff is the main source of potassium in the water bodies.

Chloride and sulphur concentrations in the lake are ranged from 7.20 mg/l to 20.7 mg/l and from <LOD[1] mg/l to 2 mg/l. It was found that chloride concentrations in the Malewa River are a little bit higher than lake Naivasha (maximum = 21.2 mg/l). The absence of chloride and sulphur in the most common rock types in the basin is evidence that nearly all the chloride and sulphur in the drainage from the basin is derived from precipitation (Gaudet et al, 1981).

**Nutrients**

Of nutrients, phosphorus, nitrate and sulphur are the most important in limiting production of freshwater ecosystems especially at the high production rates typical of the tropics.

Of the three nutrients in the water, nitrate has the highest mean concentration in the lake (0.74 mg/l) and in the rivers (0.94 mg/l), followed by phosphorus. It was found that the inflowing rivers (Malewa

[1] Limit of detection

and Gilgil) are richer in total nutrients than lake Naivasha water. Gaudet (1979) indicated that total nutrients in the rivers are carried predominantly on silts and colloids which usually sediment or are filtered out by the papyrus swamp.

The nitrate in the lake and rivers exceed for just a little amount, the natural concentrations for fresh-water ($NO_3$-N < 0.1 mg/l). When the nitrate is influenced by human activities, the concentrations can go up to 5 mg/l, but often less than 1 mg/l $NO_3$-N. The excess of nitrate usually indicates pollution by human or animal waste, or fertiliser run-off.

Phosphorus is generally the limiting nutrient for algal growth and, therefore, controls the primary productivity of a water body (Chapman, 1996). However, some recent experiments carried out in the lake Naivasha, suggest that nitrogen is one of the limiting factors and in fact it may be as often as limiting as phosphorus (Anon, 1978). The last mention was confirmed by Mclean (2001) finding that nitrogen is a more limiting nutrient than phosphorus in controlling the biomass levels of the lake.

In general, the phosphorus is rarely found in high concentrations as plants actively take it up and also because the solubility of natural phosphate minerals is very low (e.g., supatite). Nevertheless, the amounts reported in the lake and rivers indicate the presence of pollution such as domestic wastewaters and fertiliser run-off, which elevate the levels and can contribute largely for eutrophic conditions.

The ammonium occurs naturally from the breakdown of nitrogenous organic and inorganic matter in soil and water. In Gilgil river the ammonium is present but in very low amounts ($NH_4^+$ <1). However, in Lake Naivasha and Malewa River, the concentrations arise as probably indication of organic pollution such as from domestic sewage or fertiliser run-off. Ammonia is, therefore, a useful indicator of organic pollution.

**Heavy metals**

Generally, trace amounts of metals are always present in freshwaters from the weathering rocks and soils.

Among the metals analyzed from the surface waters, iron and aluminum concentrations reported the highest values. The findings can be explained through information written about the soils and geology of the lake Naivasha area. The analyses performed in 1998 detected the presence of allophane, which is characteristic in soils as a product of weathering volcanic ash and may be derived from pyroclastics rocks. It was expressed that soils that contain allophane have often high amount of aluminum and potassium. The allophane may weather further into hallosyte and into gibbsite, which is a hydrated aluminum oxide (Siderius, 1998).

**Organic matter**

For comparative purposes an indication of the amount of organic matter present can be obtained by measuring related properties, principally the biochemical oxygen demand (BOD) or the chemical oxygen demand (COD). The COD usually includes all, or most, of the BOD as well as some other chemical demands.

**Chemical oxygen demand (COD)**

The concentrations of COD observed in the different surface waters range from 12 mg/l $O_2$ to 70 mg/l $O_2$. The amounts exceed the range to consider the surface water of the lake and rivers as unpolluted. The pollution source is mainly effluents from sewage plants (i.e. Naivasha untreated sewage plant) and some domestic wastewater discharges.

### 4.5.3 Checking reliability of analyses

**Anion-cation balance**

The anion and cation sums, when expressed as milliequivalents per liter, must balance because all potable waters are electrically neutral. The test is based on the percentage difference defined as follows:

$$\%difference = 100\frac{\sum cations - \sum anions}{\sum cations + \sum anions} \qquad \text{Eq. (4.12)}$$

The electroneutrality results for the lake Naivasha and Malewa and Gilgil rivers water samples are given in the Tables 4.15 & 4.16.

The acceptance interval usually is taken around ±10% and depends on water types. High bicarbonate waters tempt to be unstable ($CO_2$ exchanges) due to interactions with colloidal and suspended mater (alkalinity changes). The differences over the acceptance criteria are related to several factors: 1) Using different kind of equipments (i.e. ICP-AES and Datalogging Spectrophotometer HACH), which also mean different precisions, 2) in some cases the samples were not analysed for all the compartments the same day so the water properties change from one day to other, bringing some result's imprecision and 3) there were not included other compartments which could neutralize electrically the waters.

**Table 4.15.** Lake Naivasha: cation-anion balance

| Samples | Anions (-) | Cations (+) | Cation-anion balance (%) |
|---|---|---|---|
| LA | 2.92 | 3.20 | 4.55 |
| L1 | 3.39 | 3.02 | -5.65 |
| L2 | 3.43 | 3.66 | 3.29 |
| L3 | 3.20 | 3.18 | -0.38 |
| L4 | 3.39 | 2.87 | -8.35 |
| L5 | 3.31 | 3.05 | -3.99 |
| L6 | 3.23 | 2.94 | -4.62 |
| L7 | 4.32 | 3.44 | -11.41* |
| L8 | 3.77 | 3.63 | -1.78 |
| L9 | 4.37 | 3.78 | -7.25 |
| L10 | 1.39 | 1.49 | 3.45 |
| L11 | 1.06 | 1.24 | 7.80 |
| L12 | 2.09 | 2.42 | 7.33 |
| L13 | 4.86 | 3.21 | -20.55* |

**Table 4.16.** Malewa and Gilgil Rivers: cation-anion balance

| Samples | Anions (-) | Cations (+) | Cation-anion balance (%) |
|---|---|---|---|
| M1 | 1.54 | 1.24 | -10.79* |
| M2 | 1.29 | 1.26 | -1.35 |
| M3 | 1.48 | 1.11 | -14.32* |
| M4 | 1.26 | 1.41 | 5.49 |
| G1 | 1.24 | 1.20 | -1.65 |
| G2 | 1.04 | 1.16 | 5.73 |
| G3 | 1.76 | 1.26 | -16.62* |

Note: From the 21 water samples, 5 samples show distinctly or discrepancy in cation-anion balance due to post reactions in the sample bottles (*).

# Chapter 5

# Spatial water quality assessment

## 5.1 Concentration profiles along Malewa and Gilgil Rivers

The chemical transport has been analyzed for different water quality parameters in the Malewa River. Because of the scarcity of Gilgil River data, the profiles along the distance could not be carried out. Nevertheless, after observing its water quality properties, it was noticed that the conductivity increases in the downstream direction and correlates with the total dissolved solids concentration. The concentrations of calcium and nitrate rise in Marula Estate at 2GA1 (location G2) having a tendency to be diluted downstream. The concentrations that increase with the distance were COD, potassium, phosphate, aluminum and bicarbonate.

### 5.1.1 Lower Malewa River concentration profiles

From the Figure 5.1 is observed that the COD concentrations started increasing nearby Marula Estate at Dairy training school (location M2) and then the river maintains approximately the same concentration downstream. The probable release into river of untreated domestic wastes results in a marked decline in oxygen concentration that is observed clearly in the graph.

In aqueous solution, un-ionized ammonia exists in equilibrium with the ammonium ion. The ammonia concentration is dependent on the temperature, pH and total ammonia concentration. The change of ammonia in relation to pH going downstream is indicated in Figure 5.2. As it is shown, substantial losses of ammonia occur in the location M3 (Malewa River at washing clothes bridge) probably due to ammonium ion exchanges due to interactions with colloidal and suspended mater. An important increase of concentration is reported when the river approaches the lake.

As the conductivity is related to the concentrations of total dissolved solids (see Figure 5.3) and major ions, the EC measurements taken along the river are very good correlated with the TDS results. In the Malewa, the conductivity at 2GB1 is the lowest registered but around 12 km. further, the conductivity increased reaching its highest value at Dairy Training School. The change in conductivity can be caused by many factors such as the join of Biazi and Mahindu streams, which can have different water quality properties, and also some non-point pollution sources coming from Marula Estate activities. Malewa River approaches the lake with a conductivity value of 80 μS/cm.

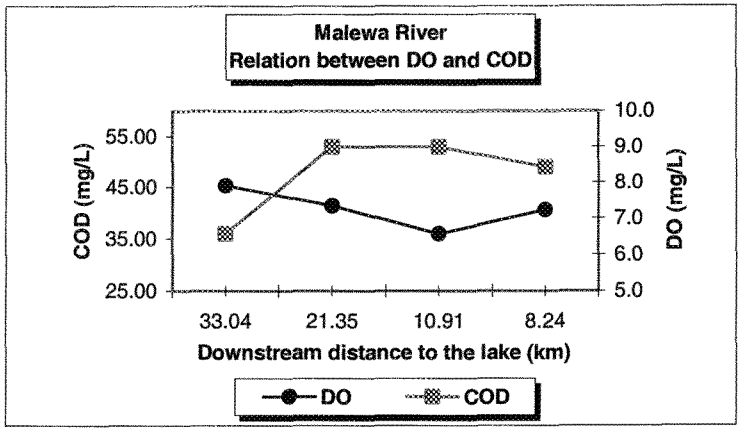


**Fig. 5.1.** Profile of DO and COD downstream

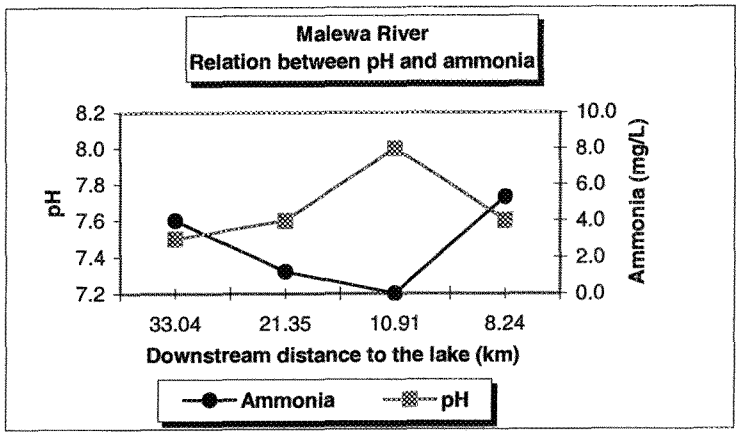


**Fig. 5.2.** Profile of ammonia and pH downstream

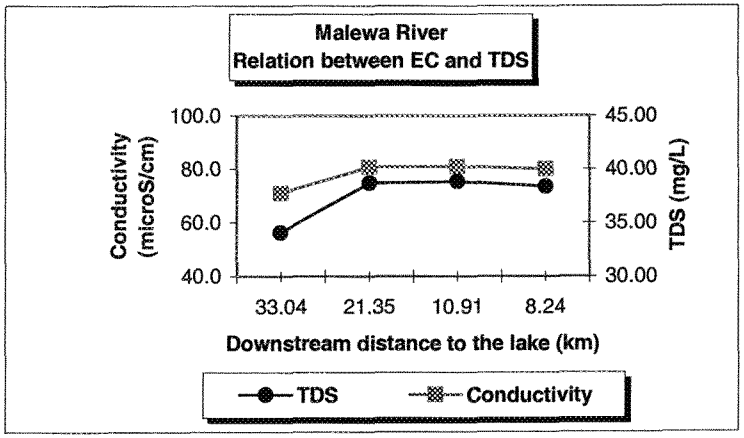


**Fig. 5.3.** Profile of TDS and conductivity downstream

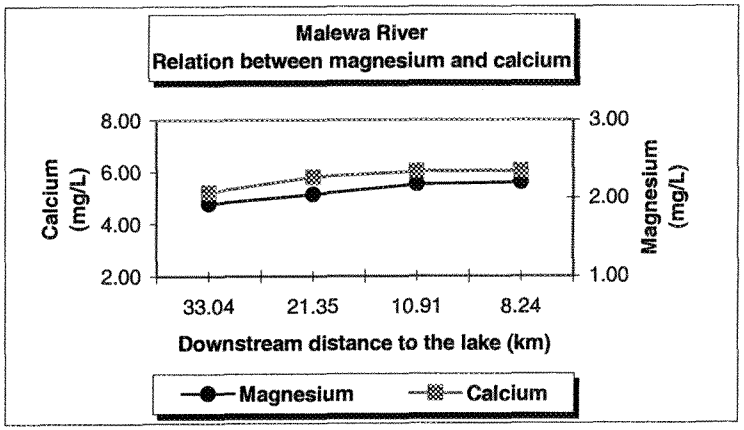


**Fig. 5.4.** Profile of magnesium and calcium downstream

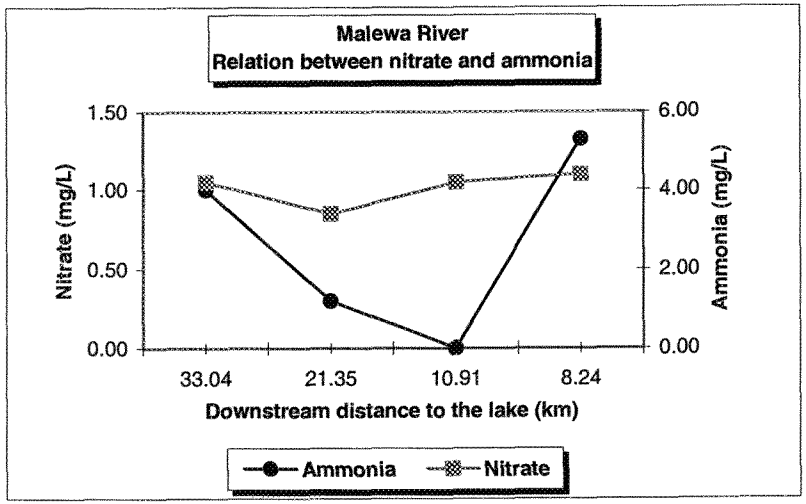


**Fig. 5.5.** Profile of nitrate and ammonia downstream

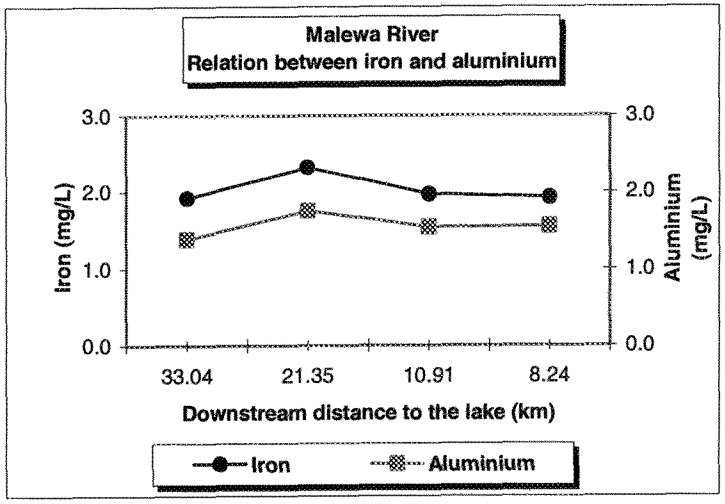


**Fig. 5.6.** Profile of iron and aluminum downstream

The Malewa's hardness can be defined as mainly carbonate hardness determined by concentrations of calcium and magnesium bicarbonates. It was found calcium concentrations higher than magnesium in the overall locations (see Fig. 5.4). In general, the calcium and magnesium amounts do not fluctuate very much and establish a good correlation each other. The tendency of these parameters is to increase slowly until reach the lake. The calcium and magnesium concentrations on the last measurement point are 6.06 mg/l and 2.20 mg/l, respectively.

The leaching of organic soils generates nitrogen ($NH_4^+$, $NO_3^-$) and dissolved organic matter in surface waters. Looking at Figure 5.5 it is found that the highest concentrations of nitrate and ammonia were registered where the Malewa is nearby the farms as a result of high nitrogen fertiliser application as well as human and animal waste.

The Figure 5.6 described the relation between the iron and aluminium along the river sampling. These trace elements are ones of the less soluble and remain in residual soil minerals and/or colloidal matter. The concentration of the metals arises at Marula Estate probably due to different environmental conditions in that region, especially oxidation and reduction in riverbed sediment, or to anthropogenic factors. The levels of iron and aluminium at 8.24 km before the lake are relatively high considering that the water is flowing and fully aerated.

## 5.2 Geostatistical analysis

Variograms often have complicated structures. The combination of nugget effects, sills, trends in so-called nested structures and various possible underlying spatial correlation models make it difficult to analyze experimental variograms. However, it is possible to adjust a mathematical model if it is fit in short distances in the experimental variograms.

On the other hand, the selection of an appropriate model to the experimental variograms is a very important step because will provide the input information (such as model type, sill, range, and nugget) for the kriging method which will estimate values for the Lake Naivasha based on the inputs or values measured.

### 5.2.1 First survey

As it is observed from the Figure 4.18, the first survey monitored the lake in a distributed sampling scheme and was performed at the same time with the bathymetric survey. The water quality survey consisted on taking measurements on spot of temperature, pH, total dissolved solids, conductivity, dissolved oxygen and percentage of oxygen saturated. The number of locations sampled was 158.

#### 5.2.1.1 Variograms

Scattered data create the need for a type of distance tolerance in experimental variogram analysis. Because all data are at different distances, all data within a specified distance interval or "lag distance" are treated together. Lag distances that are too large mask the spatial structure, whereas inappropriately small lags do not capture sufficient samples. In this case, for selecting an appropriate lag distance was chosen the average or median distance between sample data points as good starting point.

Then, the sensitivity of the lag distance was tested making it larger and smaller. The most adequate lag distance chosen was 750 m.

The number of separation pairs used in computing semivariance for pH, temperature, conductivity, total dissolved solids, dissolved oxygen and %oxygen saturated always exceeded 20. Table 5.1 and 5.2 show the estimated semivariogram models and parameters.

The values of semivariance, $\gamma^*(h)$, measurements were fit using nonlinear least squares methods (Marquardt, 1963) to the spherical model. The values of semivariance for conductivity and total dissolves solids were adjusted to the linear model.

Theoretically, the value of range (a) of the semivariogram can be considered as the scale distance beyond which pairs of observations cease to be spatially correlated. Results in Table 5.1 show that, based on the value of the range, the scale of spatial correlation varies in distance from about 2800 m for temperature to about 6500 m for pH.

**Table 5.1.** Values of nugget, range and $C_1$ for spherical semivariogram models of pH, temperature, dissolved oxygen and % oxygen saturated from the Lake Naivasha (First survey).

| Parameter | Spherical semivariogram parameters | | |
|---|---|---|---|
| | Nugget ($C_0$) | Range (a) | $C_1$ |
| pH | 0 | 6500 | 0.055 |
| Temperature | 0 | 2800 | 2.05 |
| Dissolved oxygen | 0.17 | 4000 | .410 |
| % oxygen saturated | 39 | 6000 | 108 |

**Table 5.2.** Values of nugget, and slope for linear semivariogram models of conductivity and total dissolved solids from the Lake Naivasha (First survey).

| Parameter | Linear semivariogram parameters | | |
|---|---|---|---|
| | Nugget ($C_0$) | Slope | Power |
| Conductivity | 10 | 0.13 | 1 |
| Total dissolved solids | 0 | 0.03 | 1 |

A good agreement was obtained between calculated semivariance values and the corresponding spherical and lineal models from Eq. (3.3 & 3.9) respectively; as exemplified by the results in Fig. 5.7 to 5.11.

Theoretically, for $h = 0$, $\gamma(h) = 0$ regardless of the variogram. However, very often variograms exhibit a jump at the origin as it is shown in almost all the experimental variograms. The nugget effect can be attributed to the fact that the data have not been collected with sufficient small interval to show the underlying continuous behavior of the phenomenon or also variation may exist at very small distances.

Besides the nugget effect, the temperature variogram does not reach a stable sill value but present a fluctuation around the sill value (hole effect).

A non-stationary distribution due to trend is quite clear in the dissolved oxygen experimental variograms (see Fig. 5.9). The dissolved oxygen experimental variogram exhibits the next characteristics: a nugget effect of about 0.18 $(mg/l)^2$; a spherical model with a sill value of 0.410 and a range of 4000 m., beyond 6000 m. there is a sharp increase in variogram values indicating the presence of a trend. Thus over a neighborhood of less than 6000 m. in the vertical direction the dissolved oxygen can be considered as stationary and characterized by a semivariogram with a finite range and a constant sill value.

The pH experimental variogram illustrates this situation as well, but the trend is not so remarkable as in the dissolved oxygen variogram. Nevertheless, shows a non-stationary distribution beyond 7500 m.

The conductivity and total dissolves solids experimental variograms did not reach a sill (non stationary); instead, it grows in a linear fashion as a function of distance (see Fig. 5.10 and 5.11).

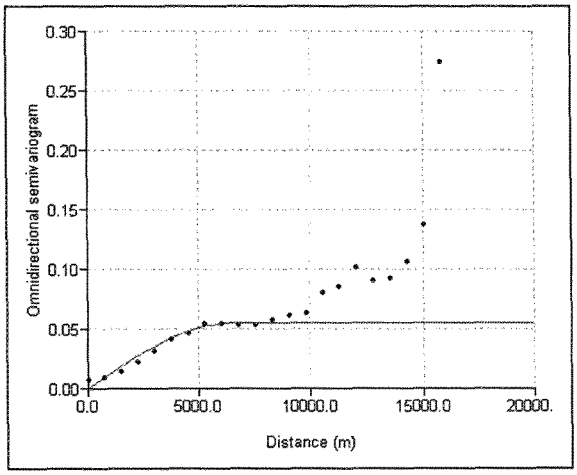


**Fig. 5.7.** Values of semivariance and the best fitting spherical semivariogram model for measurements of pH.

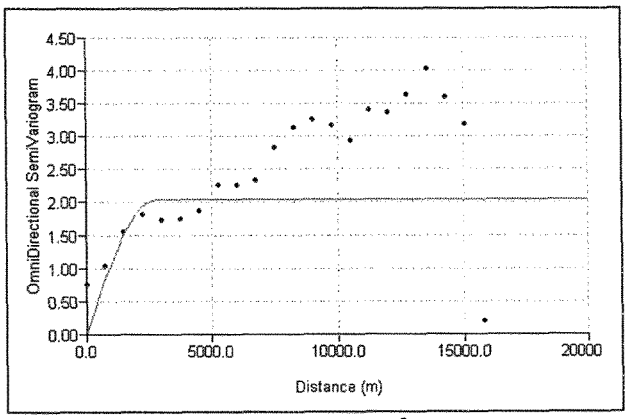


**Fig. 5.8.** Values of semivariance $(°C^2)$ and the best fitting spherical semivariogram model for measurements of surface temperature (°C).

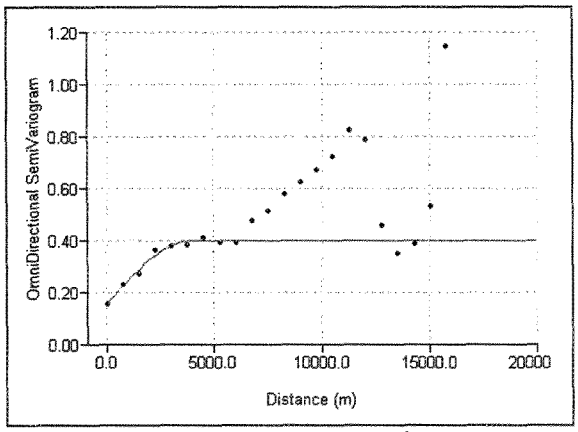


**Fig. 5.9.** Values of semivariance $(mg/l^2)$ and the best fitting spherical semivariogram model for measurements of dissolved oxygen (mg/l).

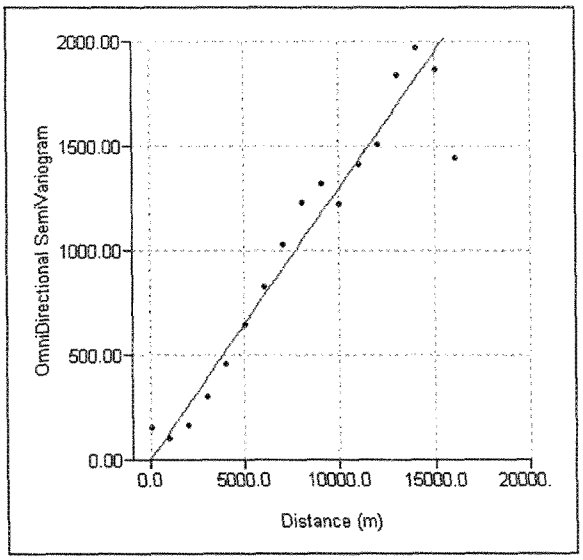


**Fig. 5.10.** Values of semivariance (μS/cm$^2$) and the best fitting linear semivariogram model for measurements of conductivity (μS/cm).

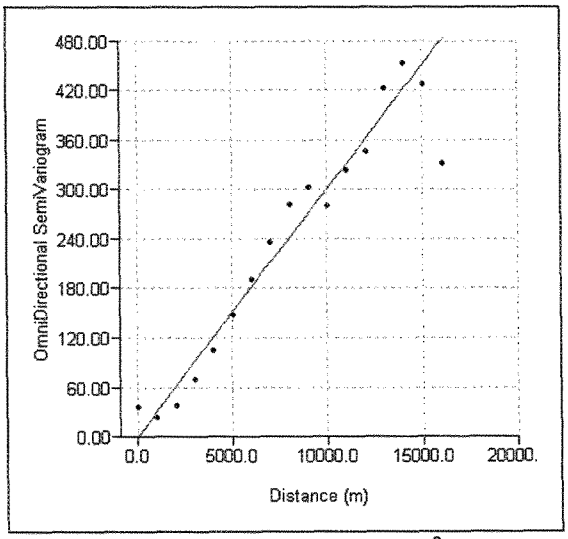


**Fig. 5.11.** Values of semivariance (mg/l$^2$) and the best fitting linear semivariogram model for measurements of total dissolved solids (mg/l).

### 5.2.1.2 Kriging

The kriging process produced two results for each location: an estimated value and a kriging standard deviation.

The parameters estimated over the Lake Naivasha were: pH, temperature, conductivity, total dissolved solids, dissolved oxygen and %dissolved oxygen, using a search neighborhood of 2300 m.

Some of the chemical properties that make the Crescent Island different from the main lake were reflected in most of the kriging maps. This particular region is described mainly by high values of pH, conductivity and dissolved oxygen compared to the main lake.

Derived from the kriging, the dissolved oxygen and %oxygen saturated maps showed high estimated values in the north caused by the inflows of the rivers; in the Crescent Island due to biological activities (i.e. photosynthesis) and the west side which is interesting because can be related to groundwater intrusions. Mostly, the low concentrations presented in the south belong to farm wastewater discharges.

Observing the conductivity map, it is remarkable how the conductivity increases from the north to the center of the lake as well as from the west to the east (anisotropic model). The hotspot in the north portion indicates the location of Malewa's inflows.

The northeast portion presented high estimated values due to the untreated sewage from the Naivasha Township which discharges directly into the lake.

Regarding to the pH map, this water quality parameter varies in a small range and the high estimated values are found in the north part of the lake and Crescent Island.

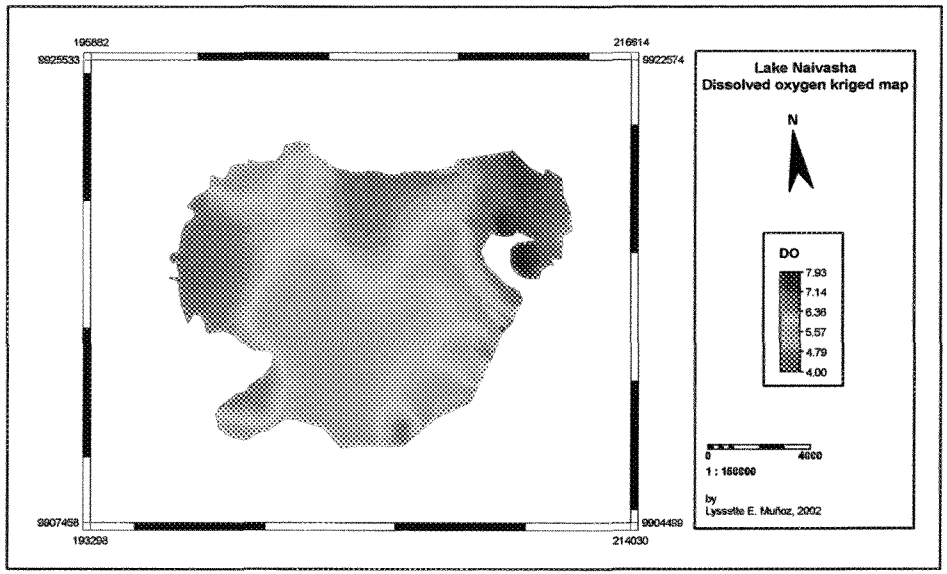


Fig. 5.12. Kriging map of dissolved oxygen in the Lake Naivasha

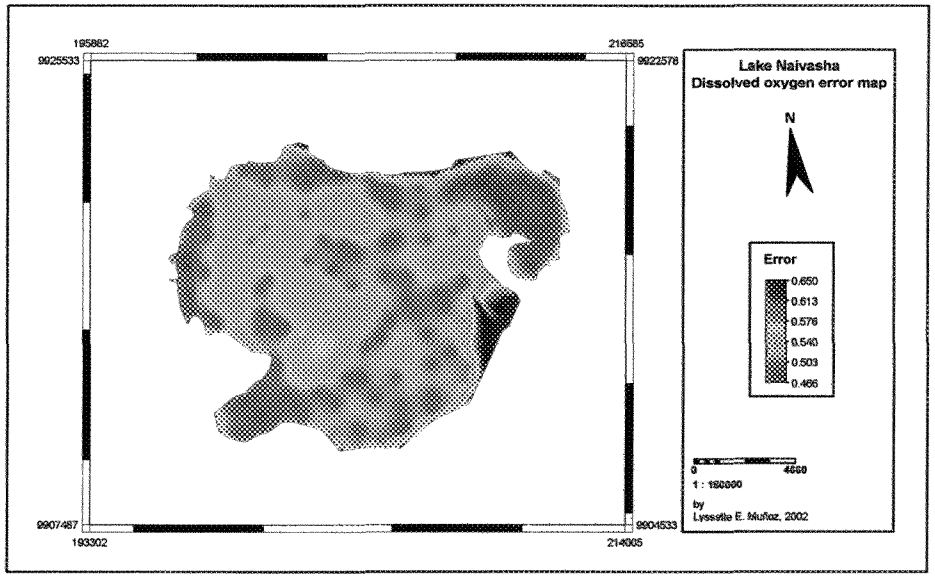


Fig. 5.12A. Kriging error map of dissolved oxygen in the Lake Naivasha

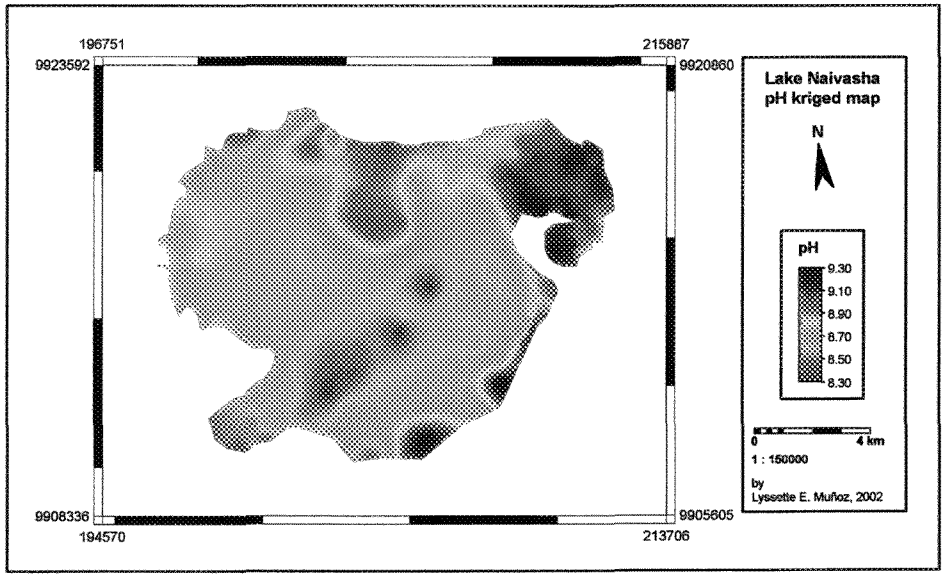


Fig. 5.13. Kriging map of pH in the Lake Naivasha

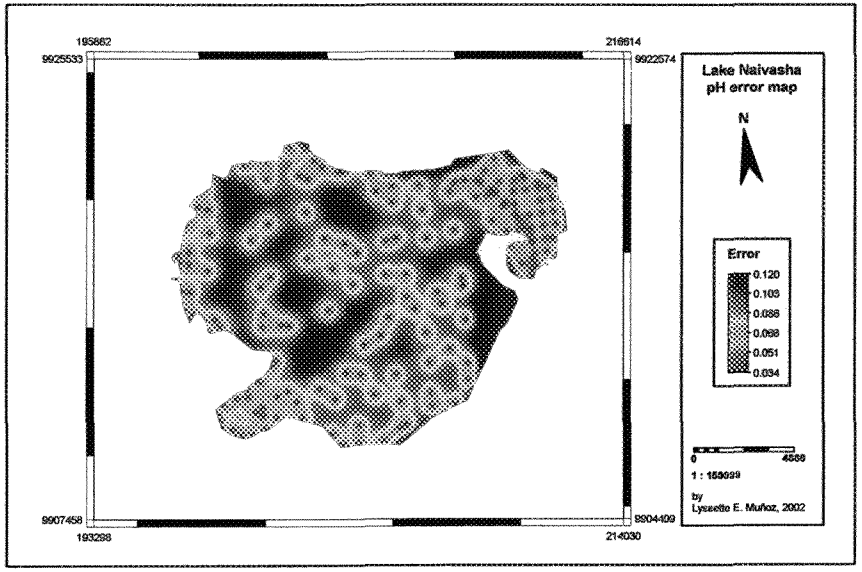


Fig. 5.13A. Kriging error map of pH in the Lake Naivasha

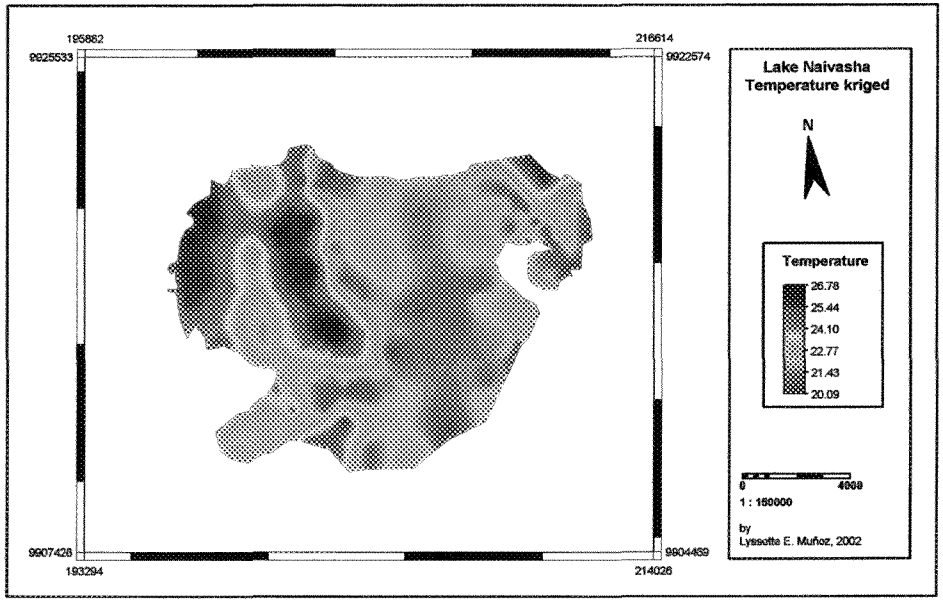


Fig. 5.14. Kriging map of temperature in the Lake Naivasha

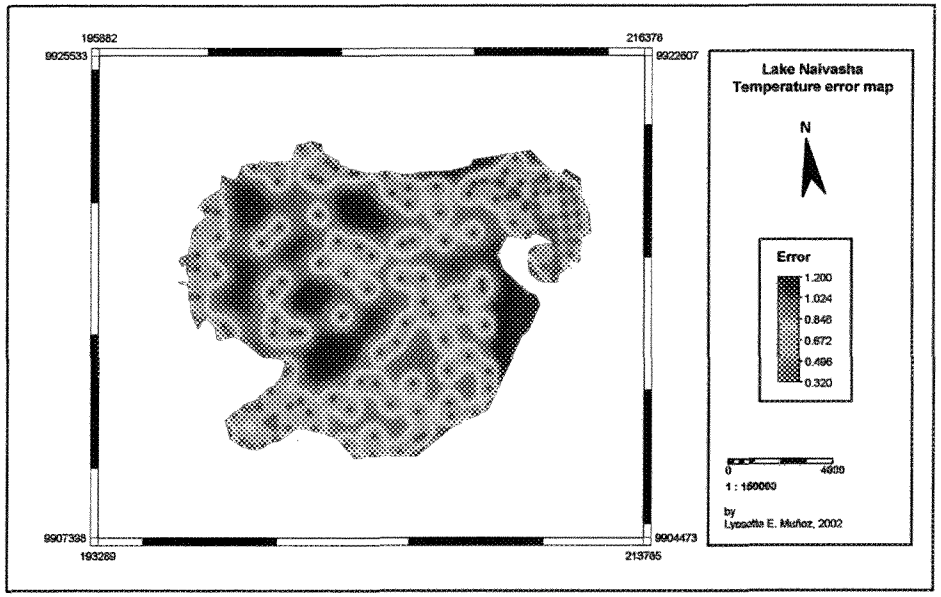


Fig. 5.14A. Kriging error map of temperature in the Lake Naivasha

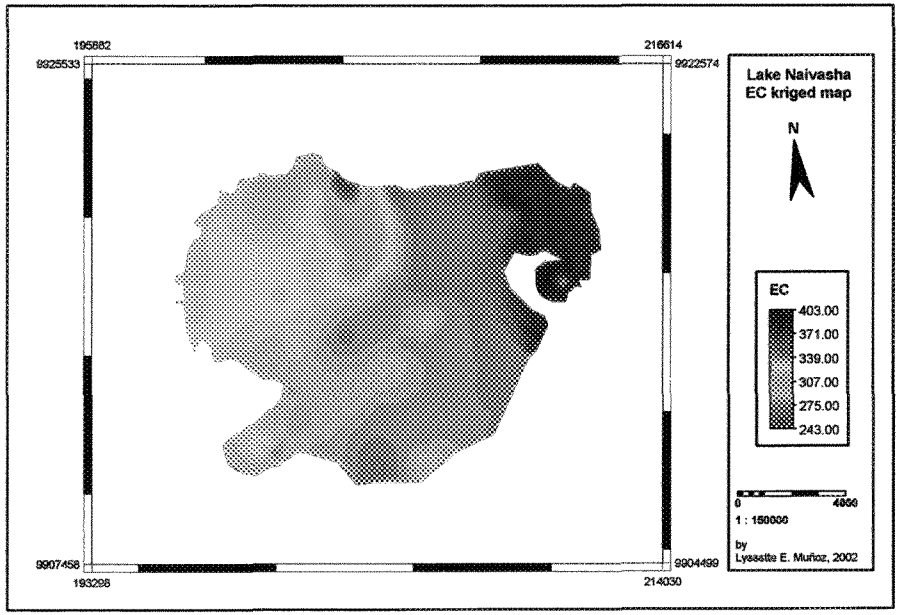


Fig. 5.15. Kriging map of conductivity in the Lake Naivasha

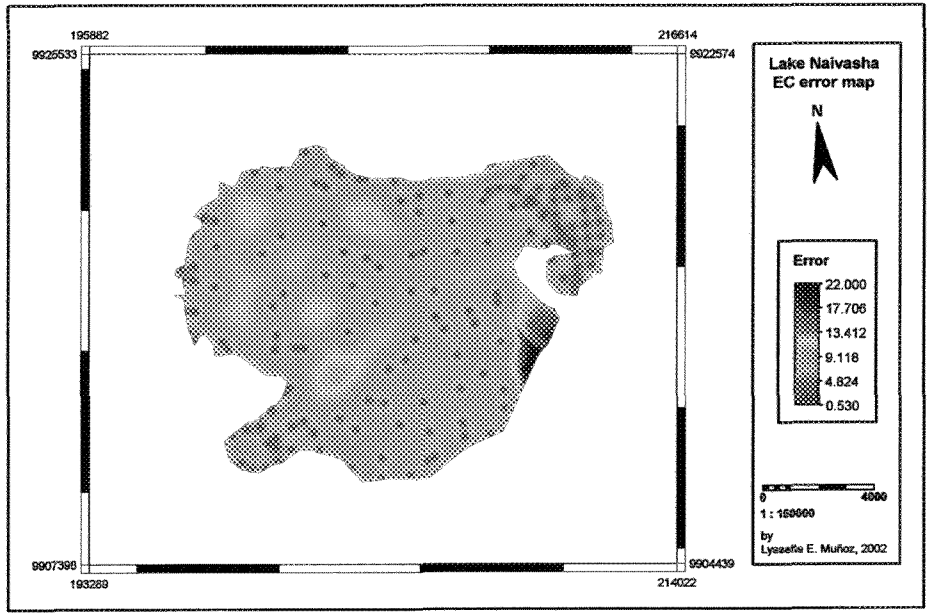


Fig. 5.15A. Kriging error map of conductivity in the Lake Naivasha

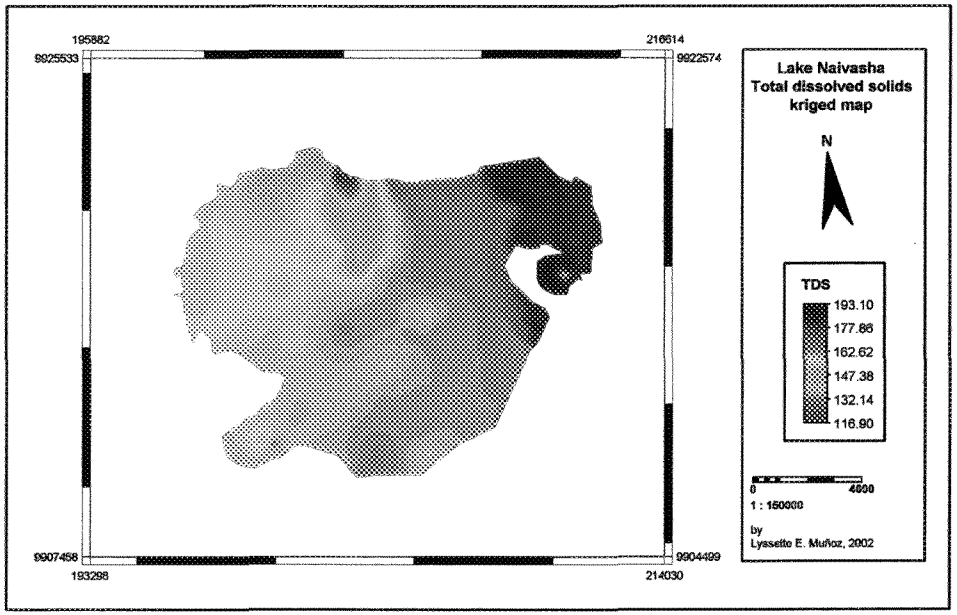


Fig. 5.16. Kriging map of total dissolved solids in the Lake Naivasha

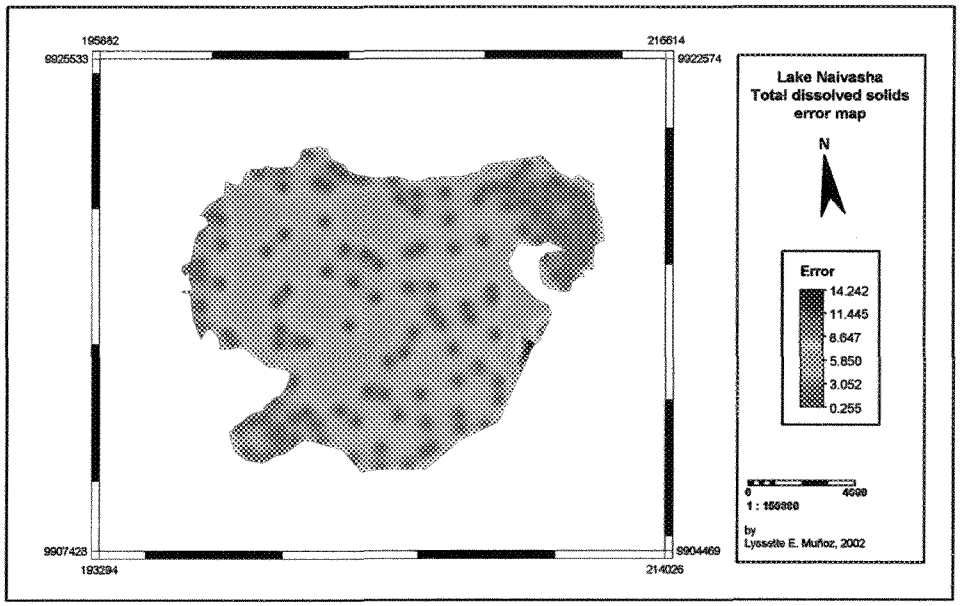


Fig. 5.16A. Kriging error map of total dissolved solids in the Lake Naivasha

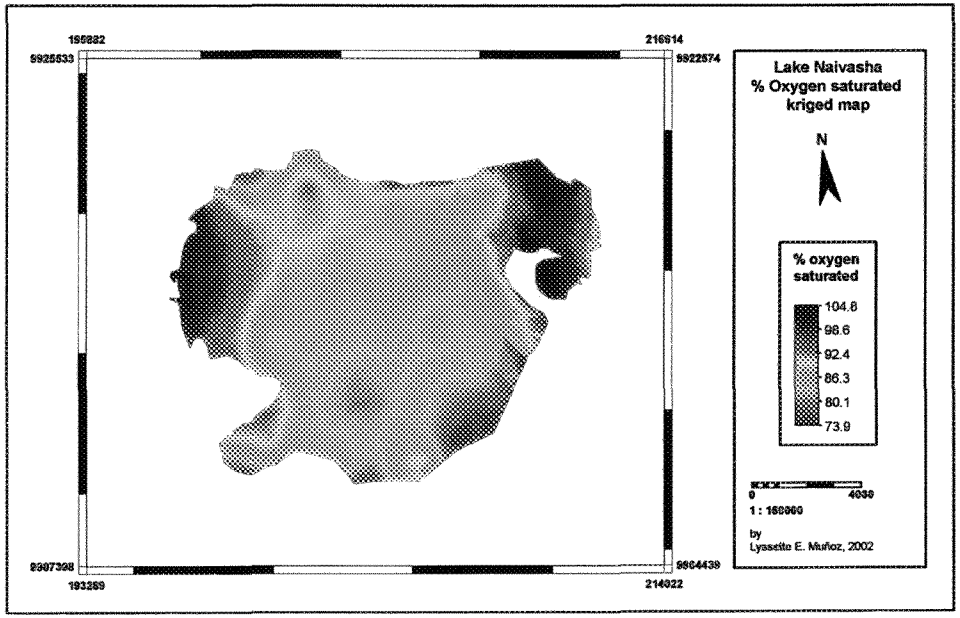


Fig. 5.17. Kriging map of %oxygen saturated in the Lake Naivasha

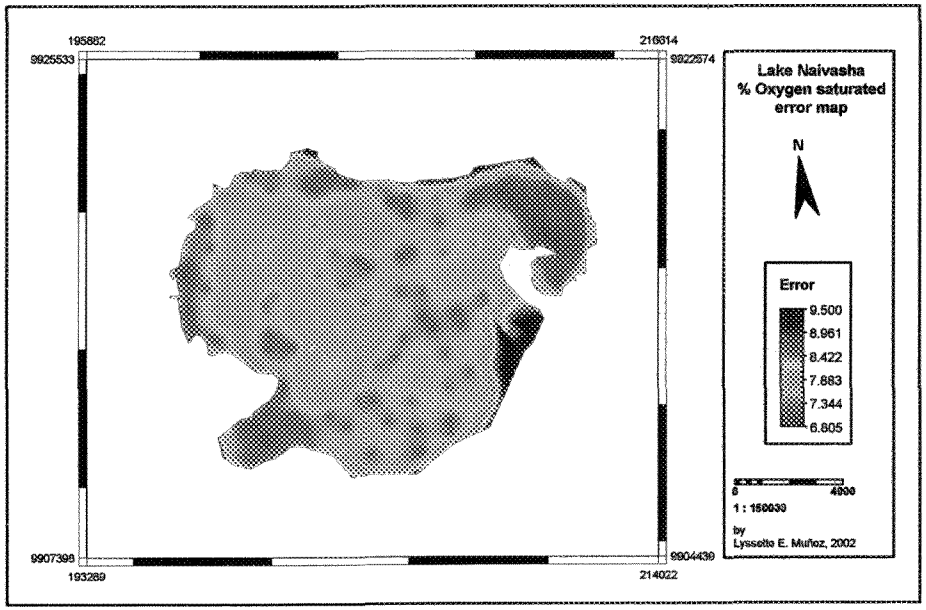


Fig. 5.17A. Kriging error map of % oxygen saturated in the Lake Naivasha

The temperature in the lake is influenced by season, time of day, air circulation, cloud cover and depth, mainly. The temperatures measurements were taken during the morning (from 7:30 – 1:30 p.m.) and as the temperature map reflects, the low temperature values were registered normally in the deepest parts of the lake (i.e. the Crescent Island and the center of the lake). The temperature varies by only a few degrees from one portion to another.

Figures from 5.12A to 5.17A illustrate a commonly observed phenomenon in error mapping. A "Swiss cheese" effected in noted, with error drawdown around each sample point on a semi regular grid. As it is observed from the maps, the error increases rapidly outside the area of sampling. Interestingly, two areas of relatively high error exist in the northeast and southeast portions of the Lake Naivasha. This reflects a large unsampled area corresponding to regions shallow, full of algae and hippos where the boat could not pass through for sampling.

Error maps can be used to evaluate the error occurring at specific locations at the site and at the site in general. Areas with high error values represent potential targets for additional sampling.

### 5.2.2 Second survey

During the second survey, the lake was sampled in a line transect (Fig. 4.19). The survey was done in only one day (30th Sept., 2001) and there were collected from 349 locations data of conductivity and temperature. Due to a storm event occurred during the afternoon and night of the day before sampling, the conductivity readings reported important differences compared to the first survey.

Figure 5.18 and 5.19 show a series of box plot graphs presenting the variation in the conductivity and temperature during the first and second survey, thus allowing a quantitative comparison of data over time.

In the conductivity graph, the outliers of the second survey are the most interesting measurements in the data set because represent the conductivity values of that area, which demonstrated to be the most sensitive. These individual points correspond to the North part of the lake quite close to Malewa's inflows.

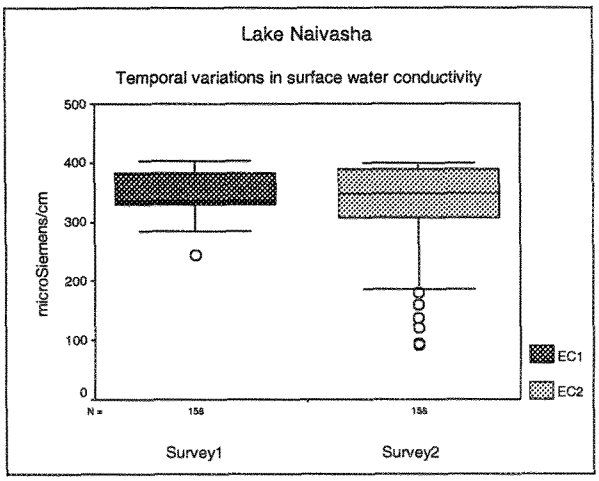


**Fig. 5.18.** Box plot of conductivity for the two surveys.

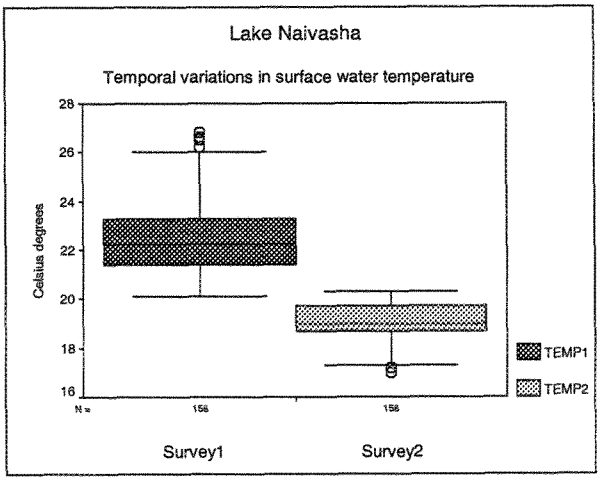


**Fig. 5.19.** Box plot of temperature for the two surveys.

### 5.2.2.1 Variograms

If the Figure 4.19 is observed, the lake was sampled in a line transect with a mean separating distance of 200 m. The north part of the lake was intensively sampled at 20 m. spacings approximately, with the objective of obtaining as much data of the lake's conductivity near the inflows in order to be precise of what exactly was coming into the lake after the storm. During the survey, it was notable the high turbidity near the shore in the northeast part due to the run-off coming from the Naivasha Township principally.

In attempting to represent the spatial structure of variability in conductivity using the data collected along the transect, some methods were tested in order to find out if it was possible to estimate values for those regions which the survey 2 did not consider, using the conductivity data collected in the survey 1.

The first step consisted on investigating the correlation between the conductivity of the survey 1 and survey 2 (Mulla, 1988). As it is observed in the Figure 5.18, the data of survey 2 contain a few outliers which do not represent the bulk of data and affected significantly the correlation (i.e. the conductivity reported in the survey 1 at Malewa's inflow was 243 μS/cm and during the survey 2 was 92 μS/cm) therefore these outside values were removed and the $r^2$ obtained was 0.917, which indicates that the correlation is good and consistent (see Fig. 5.20), so the formula acquired was applied to estimate the new values of conductivity from the survey 1.

Once the estimation was performed, it was examined carefully those locations where the data from the surveys overlapped or were closed by to verify if the estimation gave the values expected. The result was positive because the estimated values were quite closed to the observed ones (mean difference equal to 20 μS/cm) except in the North part, where the rivers enter into the lake. In this place, the estimated values were not able to describe the real situation due to the high variability of conductivity therefore those estimated values from the survey 1 were removed for that specific portion and only the values of conductivity from the survey 2 were required for the entire estimation of the lake.

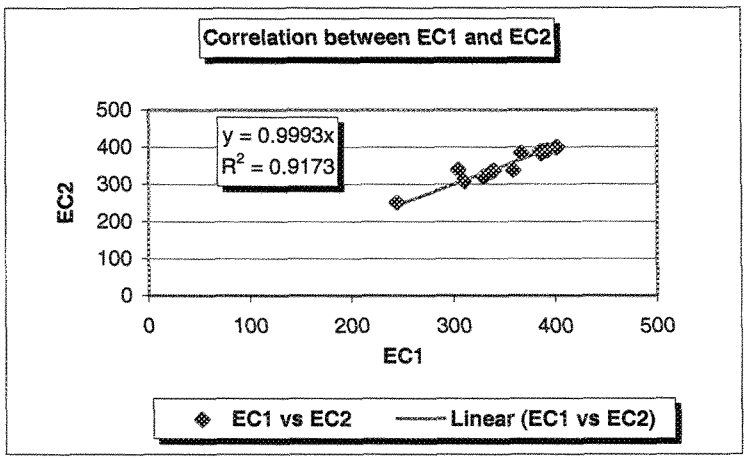


**Fig. 5.20.** Correlation between the conductivity of Survey 1 and the conductivity of Survey 2.

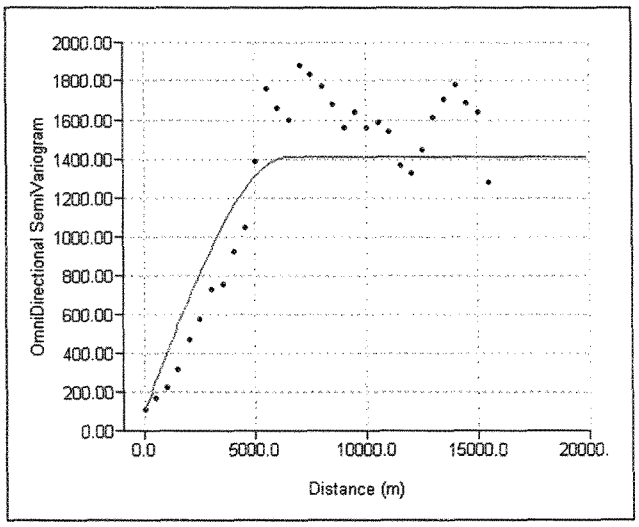


**Fig. 5.21.** Values of semivariance ($\mu S/cm^2$) and the best fitting spherical semivariogram model for measurements of conductivity ($\mu S/cm$)

The experimental variogram presented below (see Fig 5.21) represents the spatial variability in conductivity described by a spherical model. The model parameters set were: nugget: 90, sill: 1410 and range: 6500 m. The experimental variogram shows a discontinuity at the origin (nugget effect) probably caused by variations at small distances. A hole effect is also suggested.

#### 5.2.2.2 Kriging

The universal kriging was used to estimate spatial patterns in conductivity using a search neighborhood of 2400 m.

As it is observed from the Figure 5.22, the big changes are localized in the north part of the lake meaning that this region was the most dynamic at the climatic events because of the influence of rivers inflows, mainly Malewa and Gilgil, and urban run-off expressed in the water quality properties of the lake. The hotspot in the northeast portion of the lake, which is not present in the EC kriged map of the first survey (see Fig. 5.15), corresponded to the Karati River inflow. Karati River was dried when the fieldtrips of areas recognition were done, but after the storm event, the river responded and its inflow was possible to observed it through the low conductivity values registered in that specific area.

Also is interesting to observe that the conductivity property conserved almost the same spatial pattern as the conductivity of the first survey and probably, if the lake would be sampled some days after, the complete response of the lake would be detected. Anyway, the results obtained lead that the conductivity parameter is a very good water quality indicator letting know how the lake behaves after certain event.

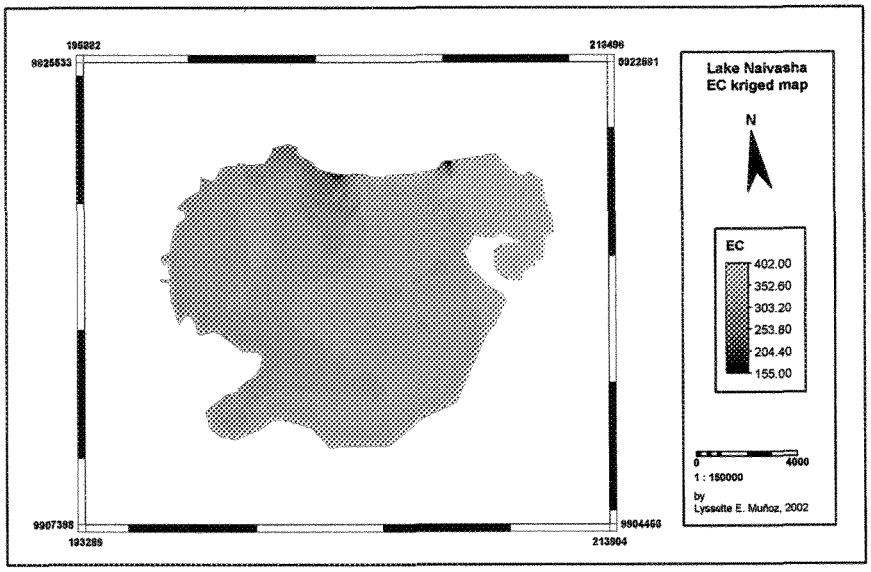


**Fig. 5.22.** Kriging map of conductivity in the Lake Naivasha

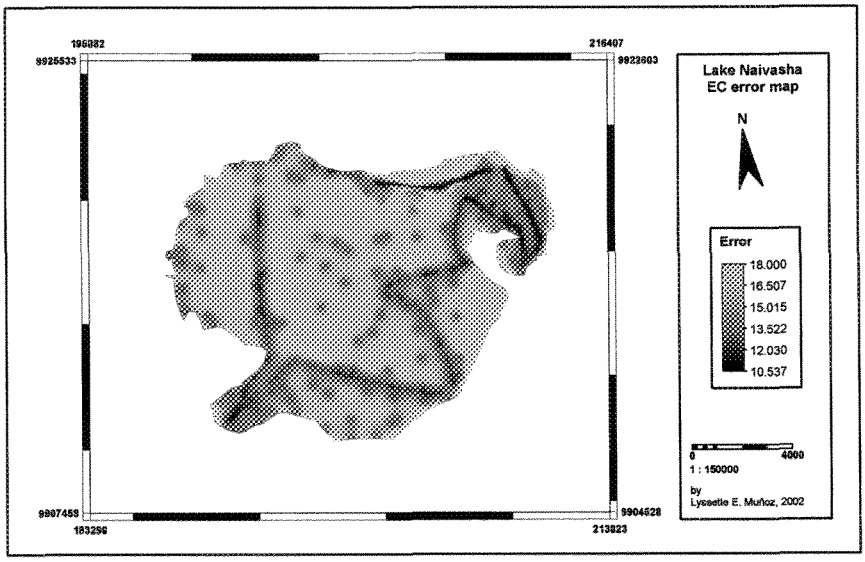


**Fig. 5.22A.** Kriging error map of conductivity in the Lake Naivasha

### 5.2.3 Anisotropy in the variogram

By calculating variograms in different directions and evaluating the associated ranges, the anisotropy was determined. Figure 5.23 shows two directional variograms for conductivity plotted in the same graph, which ranges differ according to direction. For example, the east-west range is clearly longer than the north-south range, in this case by a factor of 2. This gives an anisotropy ratio of 2:1. This also means that if is tried to predict the value of a location 1 km to the east or west of a know location, the expected error will be the same as that for an unsampled location only 500 km north or south of the know location. Thus, there is more information available along the axis of greater continuity.

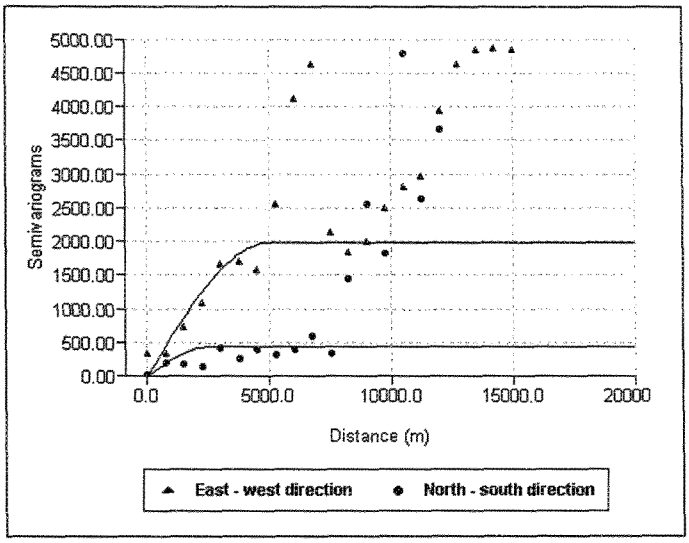


**Fig. 5.23.** Directional variogram for conductivity (survey 2), showing the good structure in both directions.

## 5.3 Lake Naivasha

### 5.3.1 Conductivity and major ions

Regression equations were developed between water conductivity and the major cations and anions from 14 samples collected during the first and second surveys on Sept. 2001. The results are presented in Table 5.3. Correlation coefficients were high for cations and the poor correlation observed in the nitrate and sulphate can be caused by low concentrations, which vary over a low narrow range or sometimes temporal variations may be responsible for differences in chemical composition of water causing correlation coefficients to be affected.

**Table 5.3.** Regression analyses relating concentrations of ions and conductivity in the Lake Naivasha (Water quality surveys of Sept. 2001)

| Parameters | Regression equation | Correlation coefficient ($r^2$) |
|---|---|---|
| Sodium | $Na^+ = 0.0785$ (Cond.) + 2.70 | 0.942 |
| Potassium | $K^+ = 0.0579$ (Cond.) – 1.17 | 0.979 |
| Calcium | $Ca^{2+} = 0.0258$ (Cond.) + 6.63 | 0.615 |
| Magnesium | $Mg^{2+} = 0.0206$ (Cond.) + 0.28 | 0.968 |
| Chloride | $Cl^- = 0.0321$ (Cond.) + 5.04 | 0.710 |
| Nitrate | $NO_3^- = 1.12 - 0.0011$ (Cond.) | 0.390 |
| Sulphate | $SO_4^{2-} = 0.944 - 0.0003$ (Cond.) | 0.002 |
| Bicarbonate | $HCO_3 = 0.5959$ (Cond.) – 2.20 | 0.878 |

### 5.3.2 Zones of Influence in the Lake Naivasha

The selection of variables that describe in general the physic-chemical characteristics of the water and, those variables which can give an indication of local changes in quality of the lake water caused by different factors such as climatic, anthropogenic, among others; in parallel with the visualization of

the mixing of rivers inflow with the lake water (plumes), obtained by kriging the EC values of the lake from the different datasets showed in Figures 5.24 and 5.25, provided information to recognize 5 zones of influence in the lake described below. The designation of low, medium and high concentrations in the description of the water quality parameters was done within the range of values found in the lake.

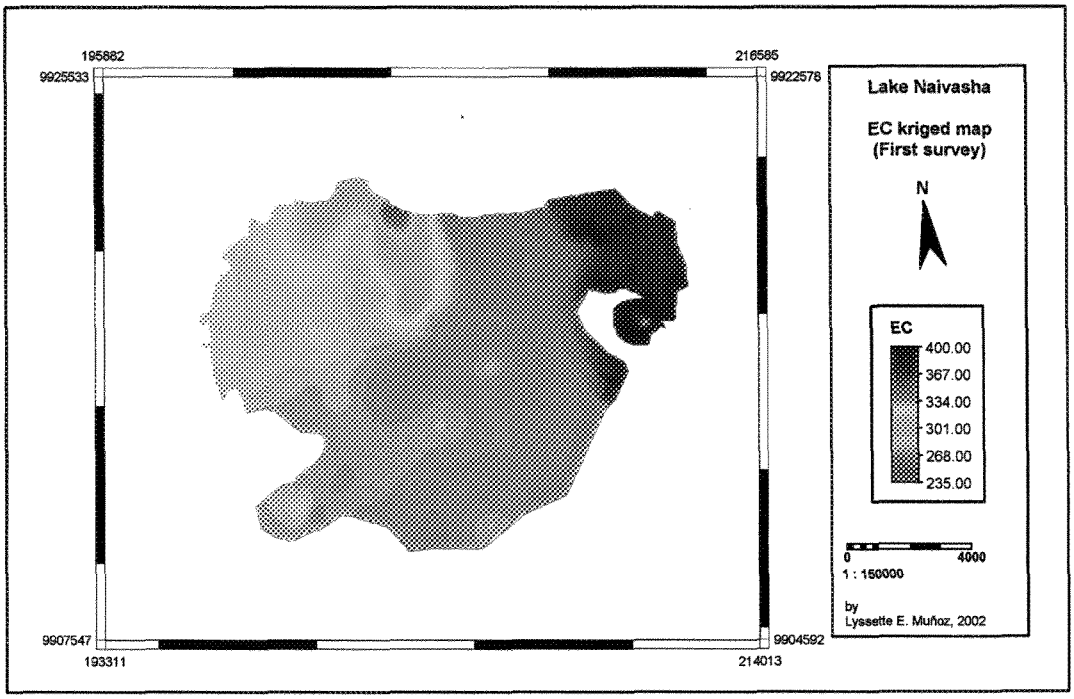


**Fig. 5.24.** Visualization of the refreshing process by rivers inflow and rainfall-based runoff through the EC kriged map (First survey).

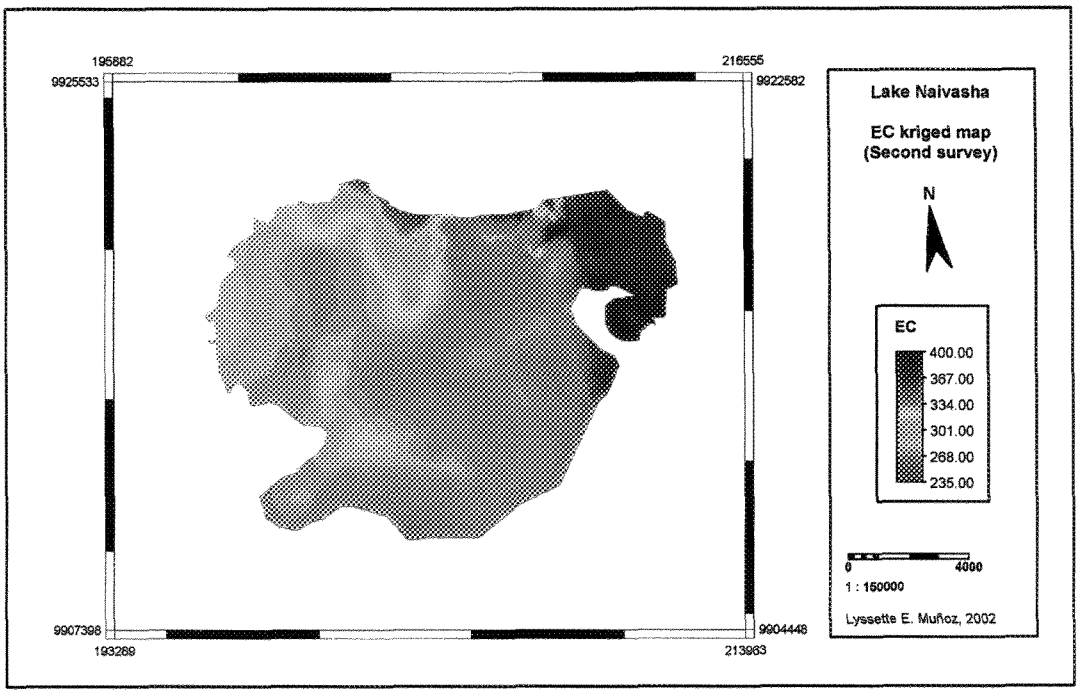


**Fig. 5.25.** Visualization of the refreshing process by rivers inflow and rainfall-based runoff through the EC kriged map (Second survey).

**Zone 1: Zone of immediate influence to rivers inflow**

The Malewa and Gilgil Rivers enter the papyrus swamp on the northern side of the lake and pass under the large swamp for several kilometers before reaching the lake. This region is shallow (<1.2m), and turbulent; keeps growing huge amounts of algae colonies and, hippos families like to stay close the rivers inflows. This zone is characterized by low values of conductivity (<320μS/cm) and within the major cations; the sodium and potassium are the predominant with mean concentration values. The chemical oxygen demand concentrations varied highly and are determined by the rivers concentration. After the storm event, it was observed that the Malewa contributed largely to decrease the chemical oxygen demand concentration. However, the dilution effect of Gilgil River was small because does not carry the same quantity of water as Malewa does. The aluminum concentration is the biggest between the metals followed by the iron, although these metals are suitable to exchange positions. High values of pH, dissolved oxygen and ammonia are common in this portion of the lake. This region can be considered the most dynamic and interesting because is sensitive to rivers inflows and to water coming as urban run-off.

**Zone 2: Western part of the lake**

Clear and well-oxygenated water are characteristics of this zone. Low to medium values of pH (8.4-8.8) and medium conductivity values (320-333 μS/cm) within the lake ranges describes this portion, where sodium and bicarbonate are the dominant ions. From the conductivity patterns in Figures 5.16 and 5.22 suggest that solutes are transported to the west from the north, via water mass movements resulting from hydraulic flow and lake circulation as induced by wind direction and velocity. The chloride and chemical oxygen demand concentrations reveal the presence of waste outlets or irrigation drains coming from the farms established in the shoreline of the northwest side of the lake growing flowers, wheat, vegetables and fodder.

**Zone 3: Central and southern part of the lake**

These portions are quite homogenous and mean concentration values of conductivity, pH and dissolved oxygen prevail. Because the largest horticulture industries are located along the shore in the south, for instance, Sulmac, Longonot, Safari, among others; the chloride and organic matter, indicators of wastewater contamination, are often high and, low concentrations of dissolved oxygen are detected near the farms discharge channel caused by decomposition processes. Iron and aluminum are presented in small quantities. The deepest part of the lake is located in the center (5 m.) and low values of turbidity contribute in the transparency of the water.

**Zone 4: Zone of influence to Naivasha town and Karati River**

The location of the Naivasha township plant outlet (<500 m) from the lake, the seasonal inflow of Karati River, the run-off coming from the town and the high permeability levels reported for the northeast area (Mbathi, 2001), have significant implications in the northeast water quality area, characterized mainly by high chloride and organic matter concentrations and low dissolved oxygen concentrations. This portion is normally shallow (0.8-0.9 m) where hippos like very much to live contributing as well to decrease the dissolved oxygen concentration and to increase the turbidity. The high conductivity values are related with the pollution discharges, the influence of run-off waters and amount of mineral salts dissolved, i.e. sodium and potassium.

**Zone 5: Crescent Island**

Crescent Island Bay is a typical crater lake. It is distinctive from the main lake because of its high pH and conductivity values. The high dissolved oxygen levels allow preserving clear and well-oxygenated water reflected in its remarkably blue intense color caused by its depth and green algae colonies. Nevertheless, high organic matter and chloride levels reflects the presence of pollution probably transported by water movements and wind direction from the Naivasha township sewage plant located at 3 km to the North. Bicarbonate and sodium prevail between the major ions with high concentrations. Low concentrations of aluminium and iron are common in this area.

### 5.3.3 Zone of inflowing rivers influence: spatio - temporal water quality changes

Comparisons between the spatial data from the first survey (Sept. 24-29$^{th}$) and the second (Sept. 30$^{th}$) revealed changes in the water quality concentrations for the immediate zone influenced by the rivers (northern part of the lake).

From the Table 5.4, it is shown that the major ions concentrations decrease during the second survey compared to the first survey. The reason is the effect of rainfall-based run off.

Looking at the Table 5.5, it is noticed that the opposite occurred for the nutrients, except for the ammonia, because the run-off water coming from the urban and agricultural areas is rich in phosphate and nitrate, contributing to increase the levels of concentration in the lake therefore the differential concentration between the two periods became positive (see Fig. 5.27). This case depicts the typical contamination of the lake by non point sources (i.e. animal waste, fertiliser run-off).

**Table 5.4.** Differences in concentration of major ions between the two survey datasets, 2001 (northern part of the lake).

| Constituent | First survey | Second survey |
|---|---|---|
| | Mean concentration (ppm) | Mean concentration (ppm) |
| $SO_4^{2-}$ | 1 | 0.67 |
| $Cl^-$ | 14.41 | 9.43 |
| $HCO_3^*$ | 187.10 | 73.22 |
| $Na^+$ | 26.77 | 12.83 |
| $K^+$ | 16.30 | 6.44 |
| $Ca^{2+}$ | 15.07 | 9.45 |
| $Mg^{2+}$ | 6.42 | 3.01 |

**Table 5.5.** Differences in concentration of nutrients between the two survey datasets, 2001 (northern part of the lake).

| Nutrients | First survey | Second survey |
|---|---|---|
| | Mean concentration (ppm) | Mean concentration (ppm) |
| $PO_4^{3-}$ | 0.31 | 0.54 |
| $NO_3^-$ | 0.74 | 1 |
| $NH_4^+$ | 1.81 | 0.73 |

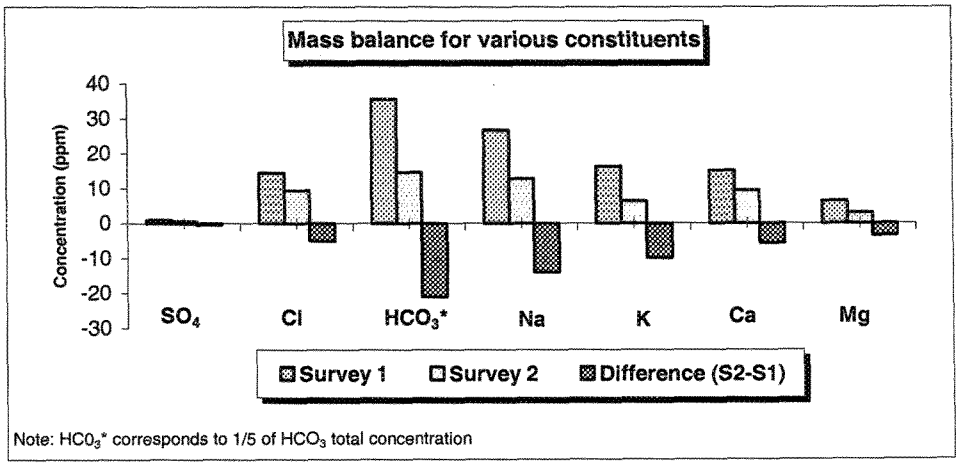


**Fig. 5.26.** Mean concentration of major cations and anions for the first and second survey, and differential concentrations between the two dataset periods (inflowing rivers zone).

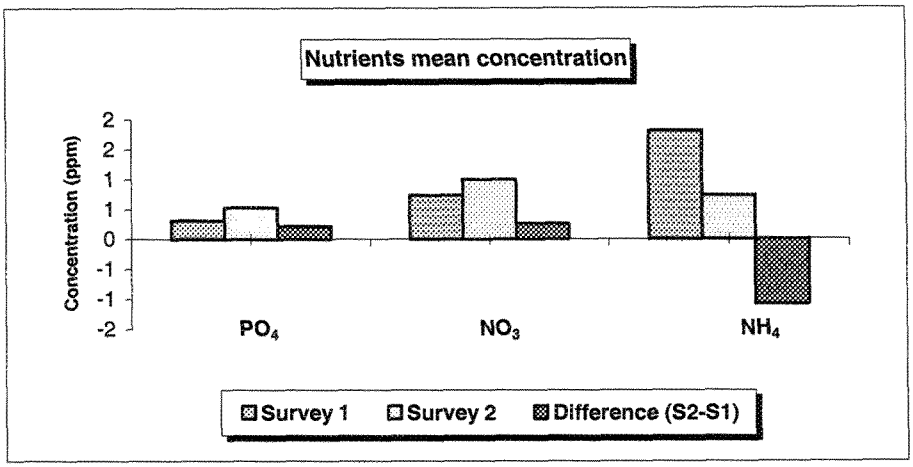


**Fig. 5.27.** Mean concentration of nutrients for the first and second survey, and differential concentrations between the two dataset periods (inflowing rivers zone).

## 5.4 Compliance with water quality guidelines and standards

Pollution and water quality degradation interfere with vital and legitimate water uses at any scale, i.e. local, regional or international (Meybeck *et al.*, 1989).

Water quality criteria, standards and the related legislation are used as the main administrative means to manage water quality in order to achieve user requirements.

The water quality evaluation in the area of study was carried out to determine their suitability for drinking water based on the WHO (1993) guidelines for drinking water quality, based on the data collected from fieldwork. This section also presents an evaluation of the lake water for irrigation purposes using a chemical analysis given by Sulmac, Ltd., from a water sample collected nearby their meteorological sampling station on March 26$^{th}$, 2001.

In terms of the WHO (1993) standard, a look at the Tables 5.6 and 5.7 show that the Malewa and Gilgil Rivers, 10% of ammonia and 100% of turbidity, aluminum and iron are outside the WHO (1993) recommended maximum concentration values for drinking purposes. In the case of Lake Naivasha, 7% of manganese, 28% of ammonia, 81% of turbidity, 92% of iron, and 100% of aluminum and pH do not fulfill the requirements for drinking purposes.

Based on the water quality for agriculture guidelines of FAO[1] #29 (1985), the evaluation for irrigation purposes (Table 5.8) was performed finding that the lake is low sodium and salinity water, which can be used for irrigation with most crops on most soils. The pH of the lake water (>8.0) may cause nutritional imbalance due to decreases in micronutrients, for example, plant-available Mn is highly dependent on pH (Lindsay, 1972) therefore this compound decreases with increasing pH. High bicarbonate level in the water ($HCO_3$>2 me/l) can derived to zinc deficiency. Regarding to ion ratios, the approximate optimum range of Ca: Mg for most crops is 3:1 to 4:1. In this case the Ca: Mg ratio is low (<3.1), which may be inhibited the phosphate uptake (Yates, 1964).

Also a comparison was performed with the Kenyan guidelines of effluent discharges into public watercourse, finding that the Malewa samples went beyond the recommended maximum concentration in 50% of COD and together with Gilgil River, 100% of ammonia (see Table 5.9). Lake Naivasha exceeded the maximum concentration values in the next parameters: 6% of chloride, 7% of manganese, 20% of pH, 80% of ammonia and 86% of COD (see Table 5.10).

[1] Food and Agriculture Organization of United Nations

**Table 5.6.** Malewa and Gilgil rivers: compliance with water quality standards for drinking water uses

| Parameters/Sample locations | | M1 | M2 | M3 | M4 | G1 | G2 | G3 | WHO[1] 1993 |
|---|---|---|---|---|---|---|---|---|---|
| Temperature | °C | 16.1 | 17.4 | 17.8 | 17.0 | 18.9 | 17.5 | 17.7 | * |
| pH | | 7.5 | 7.6 | 8.0 | 7.6 | 7.7 | 7.4 | - | **< 8.0[2]** |
| Conductivity | µS | 71.0 | 80.7 | 81.0 | 80.0 | 88.0 | 92.1 | 91.0 | * |
| TDS | mg/L | 34.0 | 38.7 | 38.8 | 38.4 | 42.2 | 44.2 | - | **1000** |
| Turbidity | NTU | 197 | 131 | 191 | 215 | 60 | 78 | 107 | **5** |
| Dissolved oxygen | mg/L | 7.90 | 7.34 | 6.57 | 7.23 | - | 7.35 | - | * |
| Oxygen saturated | % | 99 | 88 | 85 | 94 | - | 93 | - | * |
| COD | mg/L | 36 | 53 | 53 | 49 | 24 | 31 | 35 | * |
| $K^+$ | mg/L | 3.69 | 3.94 | 3.34 | 3.36 | 4.65 | 4.70 | 5.25 | * |
| $Na^+$ | mg/L | 6.29 | 7.75 | 6.68 | 6.66 | 11.47 | 11.13 | 12.07 | **200** |
| $Ca^{2+}$ | mg/L | 5.22 | 5.80 | 6.03 | 6.05 | 4.04 | 5.39 | 4.44 | * |
| $Mg^{2+}$ | mg/L | 1.92 | 2.04 | 2.18 | 2.20 | 1.18 | 1.17 | 1.23 | * |
| $Al^{3+}$ | mg/L | 1.39 | 1.75 | 1.54 | 1.56 | 0.84 | 0.97 | 1.15 | **0.2** |
| $Fe^{3+}$ | mg/L | 1.92 | 2.32 | 1.97 | 1.93 | 1.71 | 2.16 | 1.68 | **0.3** |
| $Mn^{2+}$ | mg/L | 0.33 | 0.43 | 0.38 | 0.38 | 0.31 | 0.24 | 0.21 | **0.5(P)** |
| $Li^+$ | mg/L | < 0.05 | < 0.05 | < 0.05 | < 0.05 | < 0.05 | < 0.05 | < 0.05 | * |
| $Cl^-$ | mg/L | 21.2 | 12.9 | 14.6 | 17.5 | 7.5 | 2.2 | 6.3 | **250** |
| $NH_4^+$ | mg/L | 1 | 6.1 | 1.1 | 1 | 0.9 | 0.4 | 0.7 | **1.5** |
| $NO_3^-$ | mg/L | 1.0 | 0.8 | 1.0 | 1.1 | 0.8 | 0.9 | 0.8 | **50** |
| $SO_4^{2-}$ | mg/L | 1 | < LOD | 2 | 2 | < LOD | 2 | 2 | **250** |
| $PO_4^{3-}$ | mg/L | 0.27 | 0.40 | 0.41 | 0.28 | 0.49 | 0.60 | 0.76 | * |
| Total alkalinity | mg/L | 54.92 | 54.92 | 61.02 | 42.71 | 61.02 | 54.92 | 91.53 | * |
| Total hardness as $CaCO_3$ | mg/L | 30.03 | 25.02 | 28.03 | 28.03 | 22.02 | 250.23 | 220.20 | **500** |
| | | | | | | | | | |
| Σ Cations | meq/L | 1.24 | 1.26 | 1.11 | 1.41 | 1.20 | 1.16 | 1.26 | |
| Σ Anions | meq/L | 1.54 | 1.29 | 1.48 | 1.26 | 1.24 | 1.04 | 1.76 | |

Sources: WHO, 1993.

WHO World Health Organization
NTU Nephelometric turbidity units
COD Chemical oxygen demand
LOD Limit of detection
(P) Provisional value

[1] Guideline value
[2] For effective disinfection with chlorine

**Table 5.7.** Lake Naivasha: compliance with water quality standards for drinking water uses

| Parameters/Sample locations | | LA | LB | L1 | L2 | L3 | L4 | L5 | L6 |
|---|---|---|---|---|---|---|---|---|---|
| Temperature | °C | 25.0 | 20.6 | 23.9 | 26.6 | 24.1 | 25.2 | 21.4 | 21.0 |
| pH | | 8.1 | 9.0 | 8.7 | 8.8 | 8.1 | 8.6 | 9.0 | 9.0 |
| Conductivity | µS | 247.05 | 402.21 | 326.84 | 324.19 | 321.86 | 285.01 | 310.24 | 287.67 |
| TDS | mg/L | 131.4 | 192.8 | 156.7 | 155.4 | 154.3 | 136.6 | 148.7 | 137.9 |
| Turbidity | NTU | - | - | - | - | 27 | 36 | 42 | 50 |
| Dissolved oxygen | mg/L | - | - | 6.70 | 6.49 | 4.35 | 6.27 | 5.82 | 6.40 |
| Oxygen saturated | % | - | - | 95.0 | 100.0 | 68.0 | 95.0 | 80.0 | 88.0 |
| COD | mg/L | 70 | 66 | 54 | 59 | 64 | 48 | 61 | 60 |
| $K^+$ | mg/L | 15.83 | - | 16.90 | 17.37 | 16.96 | 15.56 | 16.09 | 15.40 |
| $Na^+$ | mg/L | 27.06 | - | 27.43 | 27.80 | 27.35 | 25.49 | 26.44 | 25.84 |
| $Ca^{2+}$ | mg/L | 13.79 | - | 14.29 | 20.10 | 14.94 | 13.76 | 14.07 | 14.54 |
| $Mg^{2+}$ | mg/L | 6.08 | - | 6.57 | 6.80 | 6.71 | 6.08 | 6.56 | 6.12 |
| $Al^{3+}$ | mg/L | 1.27 | - | 0.78 | 0.96 | 0.89 | 1.10 | 1.13 | 1.10 |
| $Fe^{3+}$ | mg/L | 1.44 | - | 1.30 | 1.00 | 0.81 | 1.06 | 0.95 | 0.93 |
| $Mn^{2+}$ | mg/L | 0.29 | - | 0.34 | 0.31 | 0.37 | 0.46 | 0.37 | 0.33 |
| $Li^+$ | mg/L | < 0.05 | - | < 0.05 | < 0.05 | < 0.05 | < 0.05 | < 0.05 | < 0.05 |
| $Cl^-$ | mg/L | 13.3 | 15.6 | 15.8 | 14.0 | 14.6 | < LOD | 13.0 | 13.0 |
| $NH_4^+$ | mg/L | 4.0 | 1.2 | < LOD | 5.3 | 2.1 | < LOD | 1.4 | 0.5 |
| $NO_3^-$ | mg/L | 0.8 | 0.6 | 0.8 | 0.5 | 0.7 | 0.6 | 0.8 | 0.9 |
| $SO_4^{2-}$ | mg/L | 1 | - | 1 | 1 | 1 | 1 | 1 | 1 |
| $PO_4^{3-}$ | mg/L | 0.28 | - | 0.18 | 0.19 | 0.26 | 0.34 | 0.22 | 0.73 |
| Total alkalinity | mg/L | 152.55 | 219.67 | 176.96 | 183.06 | 167.81 | 176.96 | 176.96 | 170.86 |
| Total hardness as $CaCO_3$ | mg/L | 60.5 | 90.08 | 70.06 | 75.07 | 75.07 | 70.06 | 78.07 | 70.06 |
| | | | | | | | | | |
| Σ Cations | meq/L | 3.20 | 0.07 | 3.02 | 3.66 | 3.18 | 2.87 | 3.05 | 2.94 |
| Σ Anions | meq/L | 2.92 | 4.05 | 3.39 | 3.43 | 3.20 | 3.39 | 3.31 | 3.23 |

**Table 5.7.** Continued

| Parameters/Sample locations | | L7 | L8 | L9 | L10 | L11 | L12 | L13 | **WHO[1] 1993** |
|---|---|---|---|---|---|---|---|---|---|
| Temperature | °C | 21.2 | 21.6 | 18.1 | 17.2 | 17.0 | 19.1 | 21.1 | * |
| pH | | 9.1 | 8.7 | 9.1 | 9.1 | - | 9.0 | 8.3 | **< 8.0[2]** |
| Conductivity | µS | 401.87 | 337.47 | 399.00 | 92.00 | 92.00 | 213.00 | 332.00 | * |
| TDS | mg/L | 192.7 | 161.8 | 191.3 | 44.1 | 44.1 | 102.1 | 159.1 | **1000** |
| Turbidity | NTU | 3 | 18 | - | - | - | - | - | **5** |
| Dissolved oxygen | mg/L | 7.07 | 4.13 | 7.40 | 7.05 | - | 6.0 | 6.03 | * |
| Oxygen saturated | % | 98.4 | 60.0 | 108.6 | 101.3 | - | 83.0 | 81.9- | * |
| COD | mg/L | 55 | 66 | 66 | 19 | 12 | 59 | 65 | **50** |
| $K^+$ | mg/L | 21.65 | 20.49 | 22.13 | 3.95 | 4.06 | 11.31 | 17.41 | * |
| $Na^+$ | mg/L | 32.02 | 32.83 | 32.02 | 8.22 | 8.51 | 21.76 | 27.82 | **200** |
| $Ca^{2+}$ | mg/L | 15.08 | 16.97 | 15.81 | 11.27 | 6.53 | 10.55 | 14.29 | * |
| $Mg^{2+}$ | mg/L | 8.51 | 8.17 | 8.86 | 2.31 | 2.31 | 4.40 | 6.70 | * |
| Al | mg/L | 0.25 | 0.53 | 1.57 | 1.33 | 1.35 | 1.53 | 0.58 | **0.2** |
| Fe | mg/L | 0.19 | 0.74 | 1.13 | 1.93 | 1.80 | 1.85 | 0.83 | **0.3** |
| Mn | mg/L | 0.07 | 0.45 | 0.43 | 0.35 | 0.32 | 1.23 | 0.35 | **0.5(P)** |
| Li | mg/L | < 0.05 | < 0.05 | < 0.05 | < 0.05 | < 0.05 | < 0.05 | < 0.05 | * |
| $Cl^-$ | mg/L | 15.3 | 15.2 | 19.6 | 8.3 | 7.2 | 12.8 | 20.7 | **250** |
| $NH_4^+$ | mg/L | < LOD | 1.1 | 1.3 | 0.9 | 0.4 | 0.9 | 3.2 | **1.5** |
| $NO3^+$ | mg/L | 0.9 | 0.6 | 0.6 | 1.1 | 1 | 0.8 | 0.8 | **50** |
| $SO_4^-$ | mg/L | 1 | 2 | < LOD | 1 | 1 | < LOD | < LOD | **250** |
| $PO_4^{3-}$ | mg/L | 0.09 | 0.16 | 0.26 | 0.59 | 0.58 | 0.44 | 0.50 | * |
| $HCO_3^-$ | mg/L | 234.93 | 200.15 | 231.88 | 67.12 | 48.82 | 103.73 | 259.34 | * |
| Total hardness | mg/L | 79.07 | 75.07 | 85.08 | 28.03 | 29.03 | 42.04 | 80.07 | **500** |
| | | | | | | | | | |
| Σ Cations | meq/L | 3.44 | 3.63 | 3.78 | 1.49 | 1.24 | 2.42 | 3.21 | |
| Σ Anions | meq/L | 4.32 | 3.77 | 4.37 | 1.39 | 1.06 | 2.09 | 4.86 | |

Sources: WHO, 1993.

WHO World Health Organization
NTU Nephelometric turbidity units
COD Chemical oxygen demand
LOD Limit of detection
(P) Provisional value

[1] Guideline value
[2] For effective disinfection with chlorine

## Table 5.8. Lake Naivasha: evaluation for irrigation water quality

Data

| | | |
|---|---|---|
| EC | 0.3 | dS/m |
| pH* | 7.7 | [-] |

* *field measured data*

| Ions | ppm | mmol/l | meq/l |
|---|---|---|---|
| Na | 35 | 1.52 | 1.52 |
| Ca | 12 | 0.30 | 0.60 |
| Mg | 4.9 | 0.20 | 0.40 |
| K | 20 | 0.51 | 0.51 |
| Cl | 14 | 0.39 | 0.39 |
| SO4 | 30 | 0.31 | 0.63 |
| HCO3 | 140 | 2.30 | 2.30 |

**Parameter evaluation**

| | | |
|---|---|---|
| pH | 7.7 | * *high (> 7.5); may restrict nutrient uptake;* |
| SAR | 2.15 | * *low* |
| pHc | 7.79 | * *S.I. = pHm-pHc = - 0.09 ; almost in equilibrium with calcite* |
| Adj.SAR | 3.46 | * *low to medium* |
| Ca(0) | 7.30E-04 | **See table 4.10 FAO #29 (after Suarez, 1981) in eq/l* |
| Ca(eq) | 6.00E-04 | **using Phreeqc in eq/l (with soil pCO2 = 0.001 atm)* |
| Adj.R_Na | 2.02 | * *using Ca(0)* |
| ESP% | 6.9 | **Exchangeable sodium % ; (equation for high HCO3 waters); ok* |
| RSC | 1.29 | * *Residual sodium (bi-)carbonate > 1.25 : medium restriction for riego* |

| | | |
|---|---|---|
| Salinity hazard class** | C2 | *Low to medium; but some leaching has to occur* |
| Sodium hazard class | S1 | *Low sodium hazard but relatively high Na content with low EC* |
| Infiltration SAR-EC(w) | Med | *Medium restriction for use* *table 8.9 FAO #29* |

** *USDA_Salinity Lab classes*

| Major ion problems | | meq/l | *(Irrigation water application problems)* |
|---|---|---|---|
| Sodium | | 1.52 | * *No restriction for overhead, drip,* |
| Chloride | | 0.4 | * *No restriction for overhead, sprinkler etc* |
| CaCO3 | | 0.6 | * *S.I. = -0.09, No salt precipitation likely to occur (e.g. drip irr.)* |

| Trace elements | | ppb | *(toxicity at high level; deficiency at very low..)* |
|---|---|---|---|
| B | | 54 | **FAO #29 Table 8.9&8.10; no problems* |
| Fe | *data->* | 117 | **FAO #29 Table 8.10; no toxicity problems,* |
| Mn | | 11 | * *Due to high pH, deficiency problems may occur for* |
| Zn | | 13 | *some trace elements* |
| Cu | | 13 | **idem* |
| Mo | | 9.6 | **idem* |

...

| Ion ratios | | * *(soil fertility, ion imbalances)* |
|---|---|---|
| HCO3:Ca | 3.83:1 | * *high* |
| Ca:Mg | 1.5:1 | * *Low* *(good = 3:1 to 4:1); Phosphate uptake maybe problem* |
| K:Mg | 1.2:1 | * *Ok* |
| Na:CEC | | * *needs estimate or value of soil CEC* |

**Table 5.9.** Malewa and Gilgil rivers: compliance with water quality standards of effluent discharges into public watercourse

| Parameters/Sample locations | | M1 | M2 | M3 | M4 | G1 | G2 | G3 | Kenya government guidelines |
|---|---|---|---|---|---|---|---|---|---|
| Temperature | | 16.1 | 17.4 | 17.8 | 17.0 | 18.9 | 17.5 | 17.7 | ± 2 °C[1] |
| pH | | 7.5 | 7.6 | 8.0 | 7.6 | 7.7 | 7.4 | - | **6.0 – 9.0** |
| Conductivity | µS | 71.0 | 80.7 | 81.0 | 80.0 | 88.0 | 92.1 | 91.0 | * |
| TDS | mg/L | 34.0 | 38.7 | 38.8 | 38.4 | 42.2 | 44.2 | - | **1200** |
| Turbidity | NTU | 197 | 131 | 191 | 215 | 60 | 78 | 107 | * |
| Dissolved oxygen | mg/L | 7.90 | 7.34 | 6.57 | 7.23 | - | 7.35 | - | * |
| Oxygen saturated | % | 99 | 88 | 85 | 94 | - | 93 | - | * |
| COD | mg/L | 36 | 53 | 53 | 49 | 24 | 31 | 35 | **50** |
| $K^+$ | mg/L | 3.69 | 3.94 | 3.34 | 3.36 | 4.65 | 4.70 | 5.25 | * |
| $Na^+$ | mg/L | 6.29 | 7.75 | 6.68 | 6.66 | 11.47 | 11.13 | 12.07 | * |
| $Ca^{2+}$ | mg/L | 5.22 | 5.80 | 6.03 | 6.05 | 4.04 | 5.39 | 4.44 | * |
| $Mg^{2+}$ | mg/L | 1.92 | 2.04 | 2.18 | 2.20 | 1.18 | 1.17 | 1.23 | * |
| $Al^{3+}$ | mg/L | 1.39 | 1.75 | 1.54 | 1.56 | 0.84 | 0.97 | 1.15 | * |
| $Fe^{3+}$ | mg/L | 1.92 | 2.32 | 1.97 | 1.93 | 1.71 | 2.16 | 1.68 | * |
| $Mn^{2+}$ | mg/L | 0.33 | 0.43 | 0.38 | 0.38 | 0.31 | 0.24 | 0.21 | **1.0** |
| $Li^+$ | mg/L | < 0.05 | < 0.05 | < 0.05 | < 0.05 | < 0.05 | < 0.05 | < 0.05 | * |
| $Cl^-$ | mg/L | 21.2 | 12.9 | 14.6 | 17.5 | 7.5 | 2.2 | 6.3 | **1000** |
| $NH_4^+$ | mg/L | 1 | 6.1 | 1.1 | 1 | 0.9 | 0.4 | 0.7 | **0.2** |
| $NO_3^-$ | mg/L | 1.0 | 0.8 | 1.0 | 1.1 | 0.8 | 0.9 | 0.8 | * |
| $SO_4^{2-}$ | mg/L | 1 | < LOD | 2 | 2 | < LOD | 2 | 2 | **500** |
| $PO_4^{3-}$ | mg/L | 0.27 | 0.40 | 0.41 | 0.28 | 0.49 | 0.60 | 0.76 | **1.0** |
| Total alkalinity | mg/L | 54.92 | 54.92 | 61.02 | 42.71 | 61.02 | 54.92 | 91.53 | * |
| Total hardness as $CaCO_3$ | mg/L | 30.03 | 25.02 | 28.03 | 28.03 | 22.02 | 250.23 | 220.20 | * |
| | | | | | | | | | |
| Σ Cations | meq/L | 1.24 | 1.26 | 1.11 | 1.41 | 1.20 | 1.16 | 1.26 | |
| Σ Anions | meq/L | 1.54 | 1.29 | 1.48 | 1.26 | 1.24 | 1.04 | 1.76 | |

NTU Nephelometric turbidity units
COD Chemical oxygen demand
LOD Limit of detection

Sources: Legislative environmental controls of Kenya expressed as Water Acts.

[1] Ambient temperature of the water body

**Table 5.10.** Lake Naivasha: compliance with water quality standards of effluent discharges into public watercourse

| Parameters/Sample locations | | LA | LB | L1 | L2 | L3 | L4 | L5 | L6 |
|---|---|---|---|---|---|---|---|---|---|
| Temperature | °C | 25.0 | 20.6 | 23.9 | 26.6 | 24.1 | 25.2 | 21.4 | 21.0 |
| pH | | 8.1 | 9.0 | 8.7 | 8.8 | 8.1 | 8.6 | 9.0 | 9.0 |
| Conductivity | µS | 247.05 | 402.21 | 326.84 | 324.19 | 321.86 | 285.01 | 310.24 | 287.67 |
| TDS | mg/L | 131.4 | 192.8 | 156.7 | 155.4 | 154.3 | 136.6 | 148.7 | 137.9 |
| Turbidity | NTU | - | - | - | - | 27.7 | 36.2 | 42.8 | 50.8 |
| Dissolved oxygen | mg/L | - | - | 6.70 | 6.49 | 4.35 | 6.27 | 5.82 | 6.40 |
| Oxygen saturated | % | - | - | 95.0 | 100.0 | 68.0 | 95.0 | 80.0 | 88.0 |
| COD | mg/L | 70 | 66 | 54 | 59 | 64 | 48 | 61 | 60 |
| $K^+$ | mg/L | 15.83 | - | 16.90 | 17.37 | 16.96 | 15.56 | 16.09 | 15.40 |
| $Na^+$ | mg/L | 27.06 | - | 27.43 | 27.80 | 27.35 | 25.49 | 26.44 | 25.84 |
| $Ca^{2+}$ | mg/L | 13.79 | - | 14.29 | 20.10 | 14.94 | 13.76 | 14.07 | 14.54 |
| $Mg^{2+}$ | mg/L | 6.08 | - | 6.57 | 6.80 | 6.71 | 6.08 | 6.56 | 6.12 |
| $Al^{3+}$ | mg/L | 1.27 | - | 0.78 | 0.96 | 0.89 | 1.10 | 1.13 | 1.10 |
| $Fe^{3+}$ | mg/L | 1.44 | - | 1.30 | 1.00 | 0.81 | 1.06 | 0.95 | 0.93 |
| $Mn^{2+}$ | mg/L | 0.29 | - | 0.34 | 0.31 | 0.37 | 0.46 | 0.37 | 0.33 |
| $Li^+$ | mg/L | < 0.05 | - | < 0.05 | < 0.05 | < 0.05 | < 0.05 | < 0.05 | < 0.05 |
| $Cl^-$ | mg/L | 13.3 | 15.6 | 15.8 | 14.0 | 14.6 | 16.0 | 13.0 | 13.0 |
| $NH_4^+$ | mg/L | 4.0 | 1.2 | 0.00 | 5.3 | 2.1 | < LOD | 1.4 | 0.5 |
| $NO_3^-$ | mg/L | 0.8 | 0.6 | 0.8 | 0.5 | 0.7 | 0.6 | 0.8 | 0.9 |
| $SO_4^{2-}$ | mg/L | 1 | - | 1 | 1 | 1 | 1 | 1 | 1 |
| $PO_4^{3-}$ | mg/L | 0.28 | - | 0.18 | 0.19 | 0.26 | 0.34 | 0.22 | 0.73 |
| Total alkalinity | mg/L | 152.55 | 219.67 | 176.96 | 183.06 | 167.81 | 176.96 | 176.96 | 170.86 |
| Total hardness as $CaCO_3$ | mg/L | 60.5 | 90.08 | 70.06 | 75.07 | 75.07 | 70.06 | 78.07 | 70.06 |
| | | | | | | | | | |
| Σ Cations | meq/L | 3.20 | 0.07 | 3.02 | 3.66 | 3.18 | 2.87 | 3.05 | 2.94 |
| Σ Anions | meq/L | 2.92 | 4.05 | 3.39 | 3.43 | 3.20 | 3.39 | 3.31 | 3.23 |

**Table 5.10.** Continued

| Parameters/Sample locations | | L7 | L8 | L9 | L10 | L11 | L12 | L13 | Kenya government guidelines |
|---|---|---|---|---|---|---|---|---|---|
| Temperature | °C | 21.2 | 21.6 | 18.1 | 17.2 | 17.0 | 19.1 | 21.1 | ± 2 °C[1] |
| pH | | 9.1 | 8.7 | 9.1 | 9.1 | - | 9.0 | 8.3 | **6.0 – 9.0** |
| Conductivity | µS | 401.87 | 337.47 | 399.00 | 92.00 | 92.00 | 213.00 | 332.00 | * |
| TDS | mg/L | 192.7 | 161.8 | 191.3 | 44.1 | 44.1 | 102.1 | 159.1 | **1200** |
| Turbidity | NTU | 3.81 | 18.7 | - | - | - | - | - | * |
| Dissolved oxygen | mg/L | 7.07 | 4.13 | 7.40 | 7.05 | - | 6.0 | 6.03 | * |
| Oxygen saturated | % | 98.4 | 60.0 | 108.6 | 101.3 | - | 83.0 | 81.9- | * |
| COD | mg/L | 55 | 66 | 66 | 19 | 12 | 59 | 65 | **50** |
| $K^+$ | mg/L | 21.65 | 20.49 | 22.13 | 3.95 | 4.06 | 11.31 | 17.41 | * |
| $Na^+$ | mg/L | 32.02 | 32.83 | 32.02 | 8.22 | 8.51 | 21.76 | 27.82 | * |
| $Ca^{2+}$ | mg/L | 15.08 | 16.97 | 15.81 | 11.27 | 6.53 | 10.55 | 14.29 | * |
| $Mg^{2+}$ | mg/L | 8.51 | 8.17 | 8.86 | 2.31 | 2.31 | 4.40 | 6.70 | * |
| $Al^{3+}$ | mg/L | 0.25 | 0.53 | 1.57 | 1.33 | 1.35 | 1.53 | 0.58 | * |
| $Fe^{3+}$ | mg/L | 0.19 | 0.74 | 1.13 | 1.93 | 1.80 | 1.85 | 0.83 | * |
| $Mn^{2+}$ | mg/L | 0.07 | 0.45 | 0.43 | 0.35 | 0.32 | 1.23 | 0.35 | **1.0** |
| $Li^+$ | mg/L | < 0.05 | < 0.05 | < 0.05 | < 0.05 | < 0.05 | < 0.05 | < 0.05 | * |
| $Cl^-$ | mg/L | 15.3 | 15.2 | 19.6 | 8.3 | 7.2 | 12.8 | 20.7 | **1000** |
| $NH_4^+$ | mg/L | < LOD | 1.1 | 1.3 | 0.9 | 0.4 | 0.9 | 3.2 | **0.2** |
| $NO_3^-$ | mg/L | 0.9 | 0.6 | 0.6 | 1.1 | 1 | 0.8 | 0.8 | * |
| $SO_4^{2-}$ | mg/L | 1 | 2 | < LOD | 1 | 1 | < LOD | < LOD | **500** |
| $PO_4^{3-}$ | mg/L | 0.09 | 0.16 | 0.26 | 0.59 | 0.58 | 0.44 | 0.50 | **1.0** |
| Total alkalinity | mg/L | 234.93 | 200.15 | 231.88 | 67.12 | 48.82 | 103.73 | 259.34 | * |
| Total hardness as $CaCO_3$ | mg/L | 79.07 | 75.07 | 85.08 | 28.03 | 29.03 | 42.04 | 80.07 | * |
| | | | | | | | | | |
| Σ Cations | meq/L | 3.44 | 3.63 | 3.78 | 1.49 | 1.24 | 2.42 | 3.21 | |
| Σ Anions | meq/L | 4.32 | 3.77 | 4.37 | 1.39 | 1.06 | 2.09 | 4.86 | |

NTU Nephelometric turbidity units
COD Chemical oxygen demand
LOD Limit of detection

Source: Legislative environmental controls of Kenya expressed as Water Acts

[1] Ambient temperature of the water body

# Chapter 6

# Conclusions and recommendations

The research examined the status of Lake Naivasha and main rivers inflow water quality and the effects of pollution sources derived from economic activities - mainly flower growing, diary farming and water supply. An evaluation of the rivers and lake for drinking water purposes, based on WHO (1993) guidelines for drinking water quality, was carried out along with the suitability of the lake water for irrigation purposes, based on the FAO #29 (1985) for agriculture guidelines.

The spatial assessment in Malewa River involved the analysis and interpretation of water quality concentration profiles.

Regarding to Lake Naivasha, geostatistical techniques were tested and applied for describing and estimating water quality issues over the lake. Moreover, the water quality data collected from the two different sampling surveys and climatic events in between, contributed substantially to analyze temporal variations of conductivity as well as to observe changes and trends on salts and nutrients concentration for the zone of inflowing rivers influence (northern part of the lake).

Next, a description of the research findings, conclusions and recommendations for further studies are present. The results obtained are not only quantitative, methodological issues were tested and are considered as contribution.

## 6.1 Conclusions

- **Water quality status and compliances**

  Based on the analyses indicate that the Lake Naivasha and Malewa and Gilgil river waters are alkaline (pH>7), moderate hard ($60<H_T<120$ mg/l as $CaCO_3$) and fresh ($80<EC<400$ µS/cm) with a predominance of sodium and bicarbonate among the major dissolved ions.

  In the Malewa and Gilgil rivers, with the exception of turbidity, ammonia and aluminium, the mean values of all parameters analysed are within the WHO (1993) international standard for drinking purposes. In the case of Lake Naivasha, turbidity, aluminium, iron and pH were the parameters outside of the standard.

Significant quantities of ammonia were detected in Gilgil River. Malewa River reported also concentrations of ammonia and COD above the Kenyan guidelines[1] set for effluent discharges into public watercourses. Both rivers are located on farmlands and settlements area, so these likely that sources of pollution are agricultural run-off and domestic wastewater discharges.

Regarding to Lake Naivasha, the point pollution sources (the Naivasha Township sewage outlet and drainage wastewater channels coming from farms) besides the non point contamination (urban and agricultural run-off and domestic wastewater) and the rivers inflows, are the responsible for the COD, ammonia and some chloride levels outside of the recommended maximum concentration according to the Kenya guidelines.

It is concluded that the degradation of the Lake Naivasha and its main rivers water quality arise from pollutants regarded to anthropogenic activities.

- **Water quality evaluation for irrigation**

Based on the water quality for agriculture guidelines of FAO #29 (1985), the evaluation for irrigation purposes in Lake Naivasha, indicated that the lake is low sodium and salinity water, which can be used for irrigation with most crops on most soils. The pH (>8.0) and bicarbonate ($HCO_3$>2 me/l) may cause nutritional imbalances due to decrease availability of micronutrients.

- **Spatial and temporal assessment**

Geostatistical tools were used to represent the spatial variability of pH, temperature, dissolved oxygen, conductivity and total dissolved solids based on a high dense distributed sampling scheme (First survey) in Lake Naivasha. The spatial variability of the parameters could be described by spherical and linear semivariograms.

Data values collected from a line transect survey (Second survey), did not permit a full spatial assessment of the lake water quality, but only the correlation with data from the first survey made it possible.

Among the estimated parameters derived from kriging techniques in the two datasets, the conductivity showed a pattern permitting to observe the rivers inflow mixed with the lake water (plumes) and quantify the effects of the inflowing rivers.

Considering the conductivity as a parameter that can be easily measured in the field, relevant information can be deducted from its correlation with the major ions leading to estimate parameters, which are normally difficult or expensive to measure (i.e. sodium, potassium, calcium, bicarbonate, among others).

[1] Legislative environmental controls of Kenya expressed as Water Acts

The above mentioned lead to the conclusion that the EC came up to be an interesting water quality parameter, because could detect the response of the lake at rivers inflow and depicted the refreshening process by rainfall-based runoff due to its main rivers.

Finally, a spatio-temporal assessment was attempted in the inflowing rivers zone for detecting changes and trends in major ions and nutrients concentration, between the two sampling dates. The findings were that major ions (sulphate, chloride, sodium, potassium, calcium and magnesium) tended to dilute caused by the influence of rainfall and rainfall-based runoff in the lake. Conversely, the nitrate and phosphate concentrations increased as run off waters rich of nutrients from the surrounded lake farmlands, enters the lake.

## 6.2 Recommendations

Monitoring and analysis of the run off water coming to lake and main rivers should be done to qualify and quantify the contribution of the non-point pollution derived by the intensive agricultural activities and urban growth.

To study the temporal variation of the chemical quality of the lake and rivers, it is important to define previously a limited number of locations and frequency of sampling. For example, day-to-day variability resulting from water mixing, fluctuations in inputs, etc., mostly linked to meteorological conductions; diurnal variability is limited to biological cycles, light/dark cycles, etc.

## 6.3 Future research

Groundwater studies on water quality issues nearby Naivasha town should be carried out to assess the impacts of possible urban contamination into the lake, since that zone has been reported to have high permeability levels (Mbathi, 2001).

Depending on the continuity and reliability of the times series data, it is possible to develop a model for simulating the chemical balance of the Lake Naivasha or Malewa River for long and short time periods.

# References

Abiya, I.O., 1996. Towards sustainable utilization of Lake Naivasha, Kenya, *Lakes & Reservoirs: Research and Management, 2:* 231-242.

Ase, L.E., Sernbo, K. and Syren, P. 1986. Studies of Lake Naivasha, Kenya, and its drainage area. *Forsk. Naturgeogr. Inst. Stockholms Univ.,* 63: 1-75.

Ayers, R.S. and Westcot, D.W., 1985. Water quality for agriculture, *Food and Agriculture Organization of the United Nations (FAO)* 29:1

Beltran, F.J., 2001. Building a dynamic water quality evaluation system for Lake Naivasha (Kenya): exploration in the use of DMS. International Institute for Aerospace Survey and Earth Sciences (ITC): Enschede.

Chapman, D., 1992. *Water quality assessments, a guide to use of biota, sediments and water in environmental monitoring.* E & FN SPON, London and New York

Clesceri, L.S., Greenberg, A.E. and Eaton, A.D., 1998. *Standard methods for the examination of water and wastewater,* APHA, AWWA, WEF, Washington, D.C.

Donia, N.S., 1998. Integration of GIS and computer modeling to study the water quality of lake Naivasha, Central Rift valley, Kenya. International Institute for Aerospace Survey and Earth Sciences (ITC): Enschede.

Gaudet, J.J. and Melack, J.M., 1981. Major ion chemistry in a tropical African lake basin. *Freshwater Biology* 11: 309-333.

Gaudet, J.J. and Muthuri F.M., 1981. Nutrient regeneration in shallow tropical lake water. *Verh. Internat. Verein. Limnol.* 21: 725-729.

Harper, D.M., Phillips, G., Chilvers, A., Kitaka, N. and Mavuti, K., 1993. Eutrophication prognosis for Lake Naivasha, Kenya. *Verh. Internat. Verein. Limnol.* 25: 861-865.

Harper, D.M.,1996. The ecology of Lake Naivasha and Hell's Gate National Park, Kenya, Field report.

Herschy, R.W., 1995. *Streamflow measurement.* E&FN SPON, London.

Jain, C.K., Bathia, K.K.S. and Seth, S.M., 1998. Assessment of point and non-point sources of pollution using a chemical mass balance approach. *Hydrological Sciences,* 43(3): 379 – 390.

Kitanidis, P.K., 1997. *Introduction to geostatistics: application in hydrogeology*. Press syndicate of the University of Cambridge, New York.

Landon, J.R., 1991. *Booker tropical soil manual.* Longman Group (FE), Hong Kong.

Litterick, M.R., Gaudet, J.J., Kalff, J. and Melack, J.M. 1979. The limnology of an African Lake, Lake Naivasha, Kenya.

Mbathi, M.M., 2001. Impact of Urban Land Use in Naivasha, Kenya. International Institute for Aerospace Survey and Earth Sciences (ITC): Enschede.

Mclean P., 2001. Spatial Analysis of Water Quality and Eutrophication controls in Lake Naivasha Kenya. International Institute for Aerospace Survey and Earth Sciences (ITC): Enschede.

Melack, J.M., 1979. Photosynthetic rates in four tropical African fresh waters. *Freshwater Biology* 9: 555-571.

Mulla, D.J., 1988. Estimating spatial patterns in water content, matric suction and hydraulic conductivity. *Soil Sci. Soc. Am. Journal* 52:1547-1553.

Myers, J.C., 1997. *Geostatistical error management: quantifying uncertainty for environmental sampling and mapping*, ITP, New York.

Offiong, O.E. and Edet, A.E., 1998. Water quality assessment in Akpabuyo, Cross River basin, South-Eastern Nigeria. *Environmental Geology* 34 (2/3): 167-174 p.

Siderius, W., 1998. Background information on the soils, geology and landscapes of the Lake Naivasha area (compilation).

Thomann, R.V. and Mueller, J.A., 1987. *Principles of surface water quality modeling and control,* Harper Collins, New York.

Thompson, A.O., Dodson R.G., 1958. Geology of the Naivasha area, International Institute for Aerospace Survey and Earth Sciences (ITC): Enschede.

Verschuren, D., Tibby, J., Leavitt, P.R. and Roberts, C.N., 1999. The Environmental History of a Climate-Sensitive Lake in the Former 'White Highlands' of Central Kenya, *Ambio,* 28(6): 494-501.

World Health Organization (WHO), 1993. Guidelines for drinking water quality. Vol. 1, Recommendations. Geneva.

# APPENDIX

# APPENDIX A

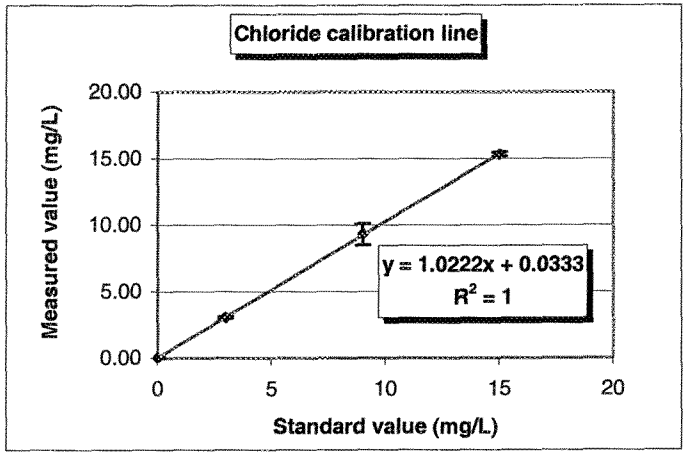


**Chloride analysis/HACH 2010 Spectrophotometer**

**0 - 20 mg/L, Mercuric thiocyanate method**

| Standard solution (mg/L) | Measured (1) (mg/L) | Measured (1) (mg/L) | Measured (1) (mg/L) | Mean (mg/L) | STD (mg/L) | Relative error (%) |
|---|---|---|---|---|---|---|
| 0 | 0 | 0 | 0.1 | 0.03 | 0.06 | - |
| 3 | 3 | 3.1 | 3.1 | 3.07 | 0.06 | 1.9 |
| 9 | 9.9 | 9.6 | 8.4 | 9.30 | 0.79 | 8.5 |
| 15 | 15.3 | 15.5 | 15.2 | 15.33 | 0.15 | 1.0 |

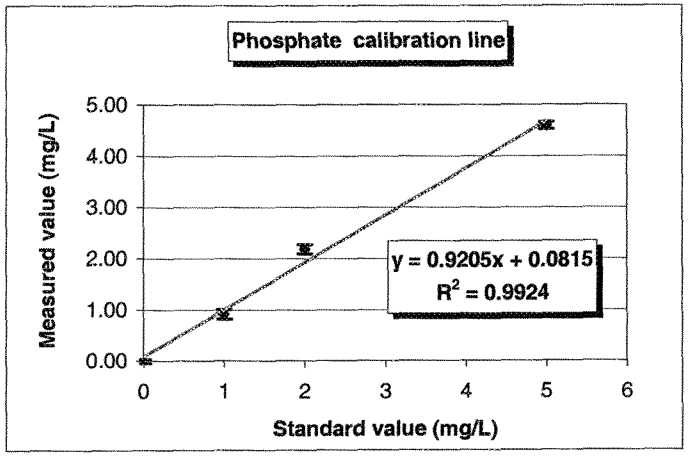


**Phosphate analysis/HACH 2010 Spectrophotometer**

**0 - 5 mg/L, Test 'N tube method**

| Standard solution (mg/L) | Measured (1) (mg/L) | Measured (1) (mg/L) | Measured (1) (mg/L) | Mean (mg/L) | STD (mg/L) | Relative error (%) |
|---|---|---|---|---|---|---|
| 0 | 0.04 | 0 | -0.06 | -0.01 | 0.04 | - |
| 1 | 0.98 | 0.88 | 0.89 | 0.92 | 0.09 | 10.2 |
| 2 | 2.23 | 2.19 | 2.13 | 2.18 | 0.09 | 4.2 |
| 5 | 4.66 | 4.56 | 4.57 | 4.60 | 0.07 | 1.5 |

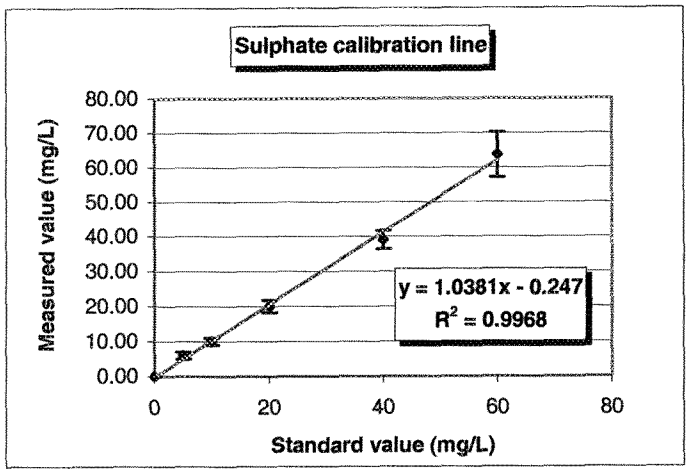


**Sulfate analysis/HACH 2010 Spectrophotometer**

**0 - 70 mg/L, Test 'N tube method**

| Standard solution (mg/L) | Measured (1) (mg/L) | Measured (1) (mg/L) | Measured (1) (mg/L) | Mean (mg/L) | STD (mg/L) | Relative error (%) |
|---|---|---|---|---|---|---|
| 0 | 0 | 0 | 0 | 0.00 | 0.00 | - |
| 5 | 5 | 6 | 7 | 6.00 | 1.00 | 16.7 |
| 10 | 9 | 10 | 11 | 10.00 | 1.00 | 10.0 |
| 20 | 19 | 19 | 22 | 20.00 | 1.73 | 8.7 |
| 40 | 38 | 37 | 42 | 39.00 | 2.65 | 6.8 |
| 60 | 64 | 57 | 70 | 63.67 | 6.51 | 10.2 |

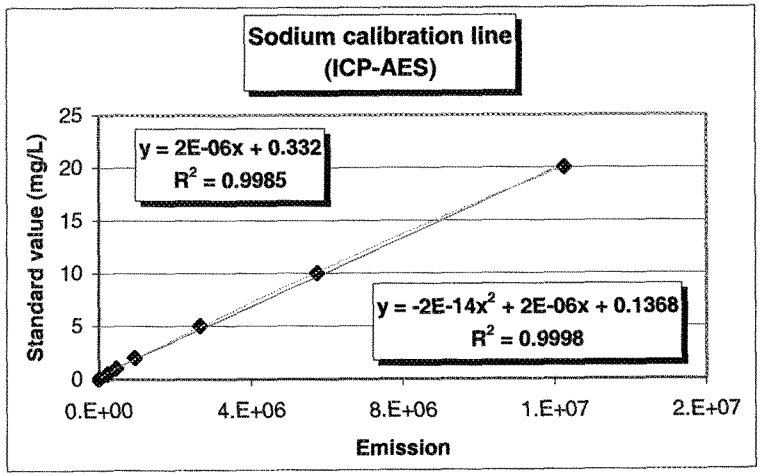


**Sodium analysis**
**ICP-AES/589.592 nm**

| Standard solution (mg/L) | Emission |
|---|---|
| 0 | 1382 |
| 0.5 | 223123 |
| 1 | 442853 |
| 2 | 952128 |
| 5 | 2658739 |
| 10 | 5739732 |
| 20 | 12264707 |

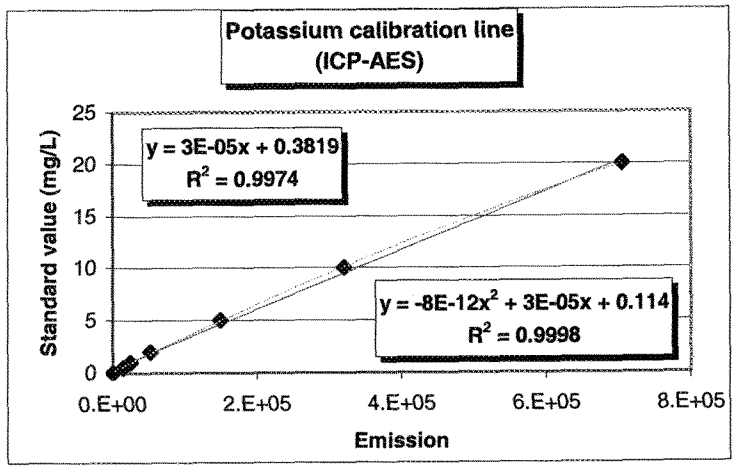


**Potassium analysis ICP-AES/769.896 nm**

| Standard solution (mg/L) | Emission |
|---|---|
| 0 | 221 |
| 0.5 | 14593 |
| 1 | 24287 |
| 2 | 52202 |
| 5 | 148999 |
| 10 | 320810 |
| 20 | 705190 |

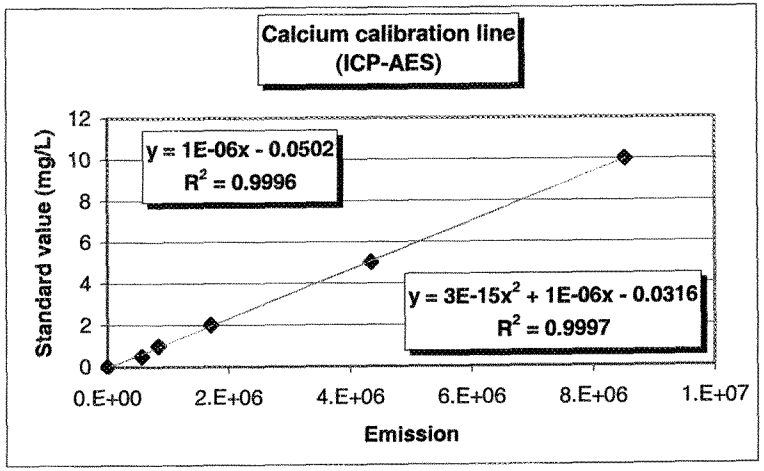


**Calcium analysis ICP-AES/422.673 nm**

| Standard solution (mg/L) | Emission |
|---|---|
| 0 | 4358 |
| 0.5 | 569273 |
| 1 | 839334 |
| 2 | 1702193 |
| 5 | 4347021 |
| 10 | 8527535 |
| 20 | 13542063 |

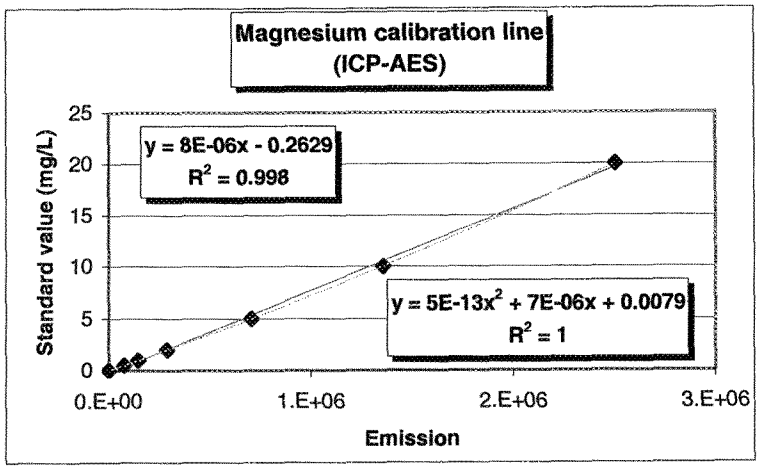


**Magnesium analysis ICP-AES/285.213 nm**

| Standard solution (mg/L) | Emission |
|---|---|
| 0 | 268 |
| 0.5 | 76239 |
| 1 | 145614 |
| 2 | 289341 |
| 5 | 705455 |
| 10 | 1357052 |
| 20 | 2504298 |

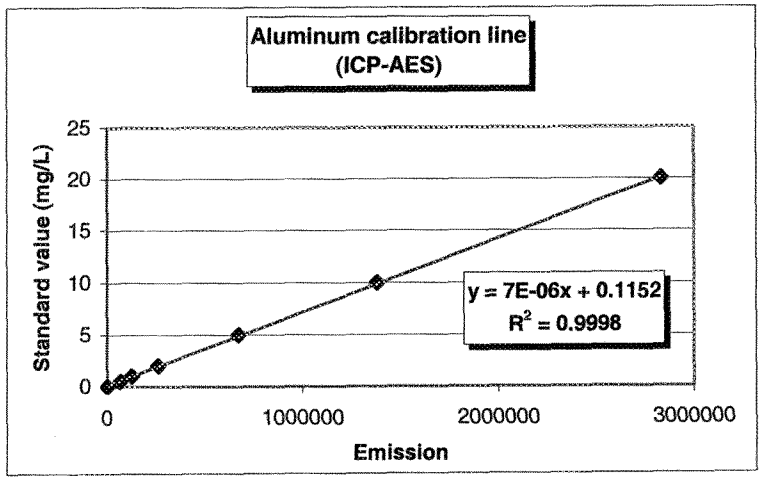


**Aluminum analysis ICP-AES/396.152 nm**

| Standard solution (mg/L) | Emission |
|---|---|
| 0 | 1145 |
| 0.5 | 67139 |
| 1 | 125832 |
| 2 | 262569 |
| 5 | 671130 |
| 10 | 1380766 |
| 20 | 2832211 |

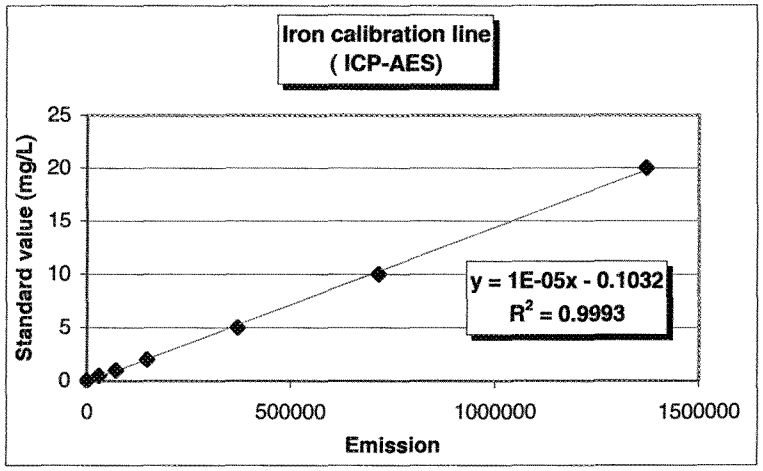


**Iron analysis ICP-AES/259.940 nm**

| Standard solution (mg/L) | Emission |
|---|---|
| 0 | 352 |
| 0.5 | 29855 |
| 1 | 70788 |
| 2 | 146648 |
| 5 | 369179 |
| 10 | 715558 |
| 20 | 1371751 |

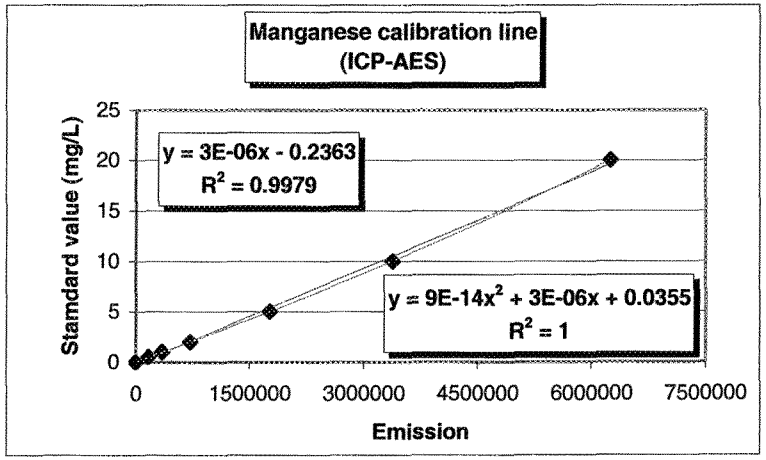


**Manganese analysis ICP-AES/257.610 nm**

| Standard solution (mg/L) | Emission |
|---|---|
| 0 | 1750 |
| 0.5 | 168315 |
| 1 | 350909 |
| 2 | 716868 |
| 5 | 1765866 |
| 10 | 3382781 |
| 20 | 6250130 |

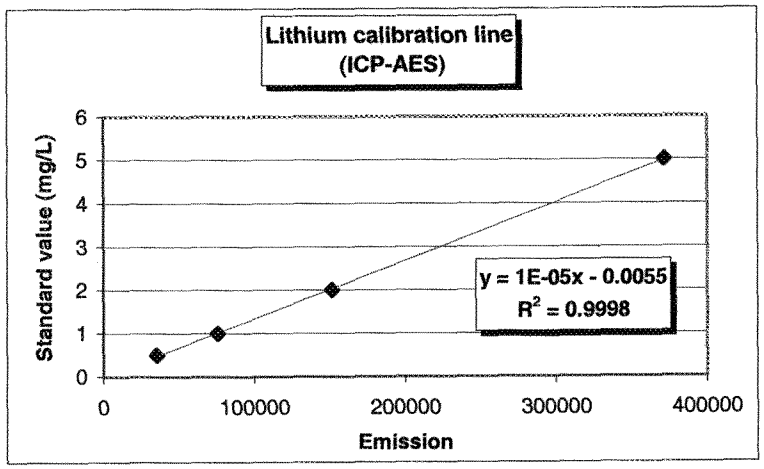


**Lithium analysis ICP-AES/670.784 nm**

| Standard solution (mg/L) | Emission |
|---|---|
| 0.5 | 35330 |
| 1 | 75732 |
| 2 | 151307 |
| 5 | 371372 |